Universitetet i Stavanger

FACULTY OF SCIENCE AND TECHNOLOGY

MASTER'S THESIS

Study programme / specialisation: Petroleum Engineering / Drilling Technology	Spring semester, 2017 Open
Author: Fridrik Hilmar Zimsen Fridriksson	…………………………………………… (signature of author)
Faculty supervisor: Mesfin Belayneh	

Title of master's thesis:

An improved cement slurry formulation for oil and geothermal wells

Credits: 30 ECTS

Keywords:		
Portland cement,	Geothermal well,	Number of pages: 104
High temperature,	Rubber,	
Silicone,	Nanoparticles,	+ supplemental material/other: 48
Micro particles,	Carbon fibre,	
Bond strength,	Leakage,	
Resilience,	Compressive strength	Stavanger, 15. June / 2017 date / year

Acknowledgment

First of all I want to give special thanks to my supervisor, Mesfin Belayneh, for helping and guiding me with this thesis. He gave me great advices, support and encouragements over the past months and was always ready to help. I want to thank Reidar Korsnes, who helped me to perform a shear bond strength test and to prepare holes in concreate blocks. I would also like to thank Samdar Kakay, he gave me the opportunity to run uniaxial compressive test on the cement core plugs, which tested the compressive strength of the plugs. I also want to express my gratitude to Mona Minde and Wakshum Mekonnen for giving me the opportunity and helping me performing EDC analysis and take SEM images. Last but not least I want to thank my fiancée, Herbjörg Andrésdóttir, for great support and motivation while I was working on this thesis.

The years I have been studying at the University of Stavanger have been enlightening and educational. This semester in particular has been exciting and informative as I have been working on this thesis. I have learned a lot about the different machines and technologies used for testing of cement and other materials, and how various additives effect the properties of cement.

Stavanger, June 2017

Fridrik Hilmar Zimsen Fridriksson

Abstract

Properly designed cement slurry and good cement job are crucial factors for integrity during a well's life cycle. For this, cement must be able to prevent migration of formation fluids, support the well construction and withstand high pressure and temperature. A survey on the Norwegian continental shelf showed that 11% of well integrity issues were due to cement related problems [1]. Another integrity survey in Pennsylvania showed that 2.41% of over 3,500 wells had casing or cementing related failures in 2011 and 2012 [2]. It has been reported that the primary reasons for gas leakage in a well are casing and cementing integrity issues [3]. This shows that the conventional cement has problems and to prevent future integrity problems the cement technology must be improved.

Drilling a geothermal well is in many way similar to drilling a hydrocarbon well. The main differences are the high temperature, generally from 160°C to above 300°C, the presence of highly corrosive gasses and often highly fractured formation [4]. This harsh environment demands even more need for cement with improved properties to withstand the geothermal environment.

In this thesis, new cement slurry additives have been studied and tested. G class Portland cement was mixed with various additives and exposed to temperature cycling to study its ability to withstand high temperature. Then the cement was tested for leakage, bond strength, compressive strength and resilience. The experiments showed the following results:

- The addition of acid treated silicone rubber to cement increased its compressive strength, resilience and bond strength with steel pipe by 26%, 34% and 1,435%, respectively. Also, it decreased the average leakage after number of temperature cycles by 30%.
- The addition of acid treated silicone debris to cement increased its compressive strength, resilience and bond strength with steel pipe by 63%, 107% and 727%, respectively.
- The addition of acid treated silicone rubber along with other additives to cement increased its compressive strength, resilience and bond strength with steel pipe by 29%, 72% and 1,738%, respectively. Also, it decreased the average leakage after number of temperature cycles by 42%.

This study showed that a new material, acid treated silicone rubber, both as the only additive and in mixture with others, can increased the strength of the cement significantly and showed improved resistance against temperature cycling.

Table of Contents

List of Figures

List of Tables

List of Abbreviations

API	American Petroleum Institute
ASV	Annulus safety valve
AT	Acid treated
Bwoc	By weight of cement
CC	Casing – Cement
CCP	Cement core plug
CF	Carbon fibre
CNT	Carbon Nano Tubes
C-S-H	Calcium Silicate Hydrate
E	Modulus of elasticity (Young's modulus)
E*	Dynamic elastic modulus
EDC	Elemental Dispersive Spectroscopy
FCC	Formation – Cement – Casing
ID	Inner diameter
NCS	Norwegian continental shelf
NORSOK	Norsk Sokkels Konkurranseposisjon (Competitive Standing of the Norwegian Offshore Sector)
OBM	Oil based mud
OD	Outer diameter
PSA	Petroleum Safety Authority
P&A	Plug and abandonment
R	Modulus of Resilience
ROP	Rate of penetration
SEM	Scanning electron microscope
SG	Specific gravity
UCS	Uniaxial compressive strength
UT	Untreated
WBE	Well barrier element
WBM	Water based mud
WCR	Water-to-Cement ratio
Wt%	Weight percent

1   Introduction

Appropriate well cementing is crucial to establish good well integrity during the life cycle of a well. The cement must be designed with the right attributes to withstand the harsh environment of a well and to provide an impermeable seal between the formation and the well. Cement slurry additives are continuously being developed by companies involved in the oil industry to improve the properties of cement. Nevertheless, due to high temperature, high pressure and corrosive environment the set cement can shrink, crack or lose its bonding with the formation or the casing. This will allow formation fluid to come in contact with the casing and consequently corroding the casing.

This thesis presents an experimental study of the effect of various additives in cement when exposed to high temperature cycling. Various cement slurry additives were designed to test its properties through both non-destructive and destructive test methods. The ability to bond with steel and formation was studied, and how well it can resist a flow of fluid after exposure to high temperature.

1.1   Background and research motivation

Cement used in the petroleum industry is hydraulic cement called Portland cement. When mixed with water a chemical reaction begins between the water and the compound present in the dry cement. The strength development and setting time is predictable, reliable and relatively rapid. After the cement is set, it has low permeability and sufficient strength, which are crucial attributes to provide zonal isolation. [5, pp. 23]

NORSOK D-010 defines well integrity as *"application of technical, operational and organizational solutions to reduce risk of uncontrolled release of formation fluids throughout the life cycle of a well."* [6] This means that barriers must be in place and understood, they must be tested and verified, monitored and maintained and have contingency plans if they would fail throughout the lifecycle of a well [1].

A well integrity survey was performed by the Petroleum Safety Authority (PSA) in 2006. It was based on 406 active wells (production and injection wells) on the Norwegian continental shelf (NCS). Out of these wells 75 (18%) had well integrity uncertainties or failures, and 7% of these were shut-in. Figure 1.1 shows which well barrier element (WBE) had problem of the 75 wells

that had integrity issues, and Figure 1.2 shows the percentage of these WBE problem. As shown on these figures the most common problem was related to tubing (39%), after tubing were annulus safety valve (ASV) (12%), cement (11%) and casing (11). These indicate the need to give special attention when designing and constructing a well. [1]
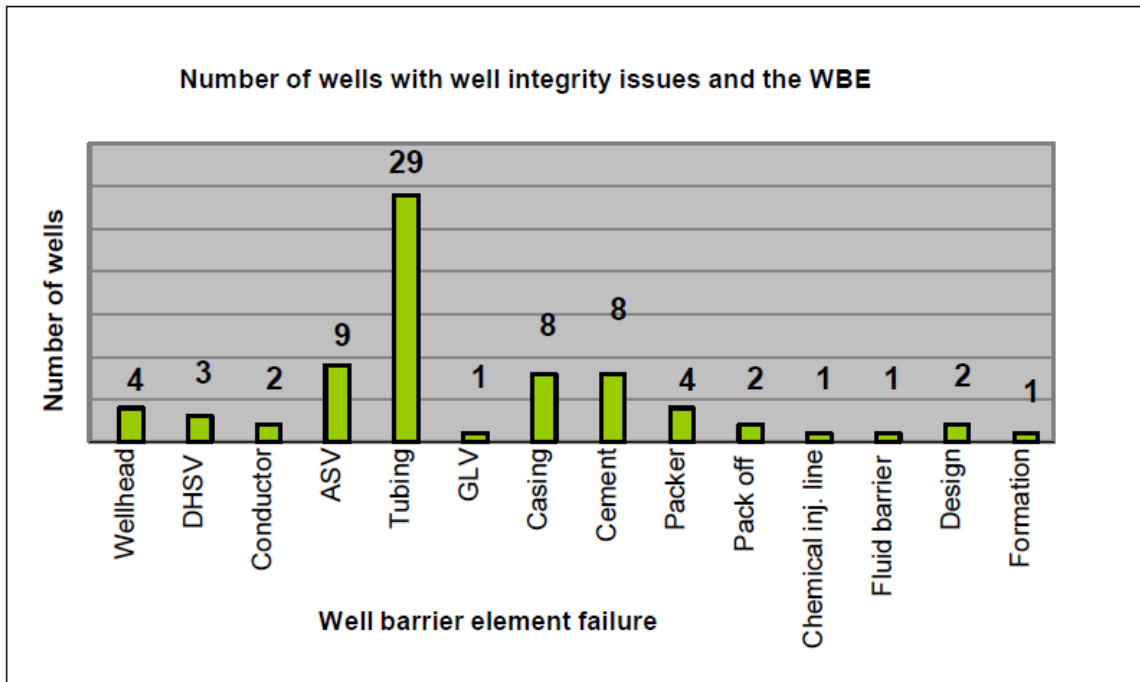
Figure 1.1: Illustration of which WBE had integrity problem from 75 wells with integrity issues. [1]
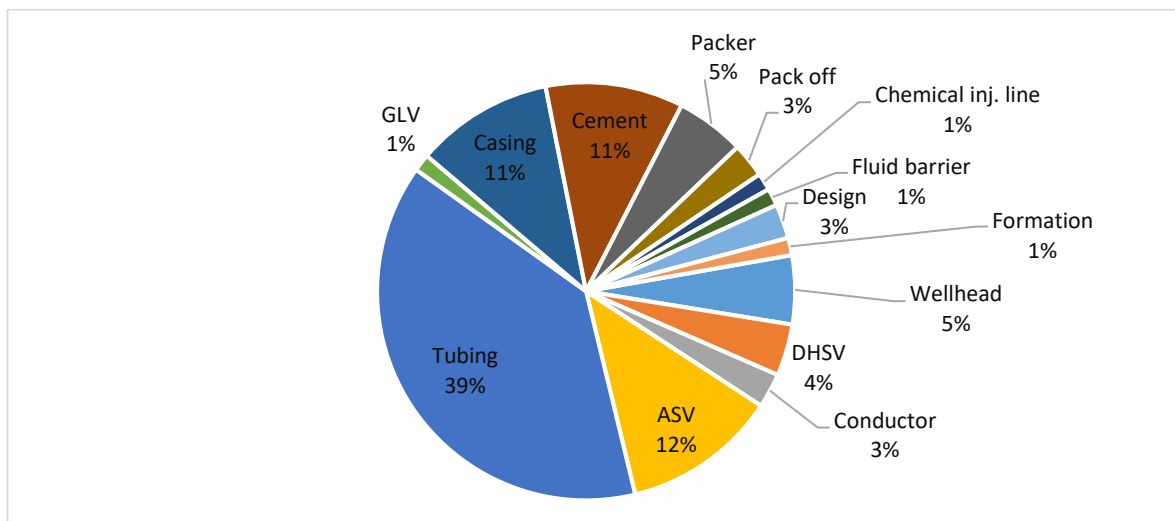
Figure 1.2: Percentage of how often a WBE had integrity problem from 75 wells that had integrity issues. [1]

The department of Environmental Protection in USA collated a database about oil and gas well records. It showed that 3.4% of shale gas production in Pennsylvania between 2008 and 2013 had well barrier leakage, i.e. 219 barrier problems out of 6,466 wells. Also, in 2011 and 2012 in Pennsylvania 2.58% of 3,533 wells had some form of barrier or integrity failure, and of which 2.41% had experienced cementing or casing failure. [2]

A survey based on 18 operators on the UK continental shelf showed that 10% of 6,137 wells had been shut-in due to structural integrity issues from 1999 to 2004 [2]. Another study carried out by Mineral Management Service concluded that 8,000 wells on the outer continental shelf on the United States Gulf of Mexico had experienced well completion leaks [7].

Bachu and Watson [3] did an analysis on over 300,000 wells in Alberta, Canada to evaluate the potential for gas leakage through or along wells. 4.6% of the wells in Alberta have been recorded to have either gas migration or surface casing vent flow between casing strings since 1995. They concluded that casing and cementing integrity issues are the primary reasons for gas leakage. [3]

From these surveys it can be concluded that conventional cement technology in oil and gas wells has integrity problems and to prevent future integrity problems its properties must be improved and properly designed.

In geothermal wells the high temperature and presence of corrosive gases are a major concern. It can be difficult to achieve effective zonal isolation, and a common problem during cementing is gas invasion into the cement before it hardens. This can form channels in the cement weakening its structure. After the cement is set an exposure to extreme temperature or changes in temperature and pressure can lead to lost bond at cement – casing interface. The set Portland cement is brittle and vulnerable temperature induced stresses, which can lead to cracking. Consequently, a flexible cement with high tensile strength is needed in a geothermal well. [8] Environmental concerns related to well integrity problems in geothermal wells are, among others, contamination of groundwater by mixing it with deep geothermal fluids. [2]

In general a geothermal well have a reservoir temperature at intervals from 160°C to above 300°C, and in extreme cases it can go up to 500°C [4]. The reservoir fluid usually consists of

brines and non-condensable gasses, such as CO_2 and H_2S. These gasses are very corrosive to both steel and cement [9]. The well is subjected to both temperature and pressure cycling, which can lead to reduced cement bond over the lifecycle of a well [10].

Based on the reviewed survey, the presented facts indicates the need to improve the performance of the current conventional technologies. Therefore, this thesis is motivated to develop a new system, with the idea of improving cement related properties.

1.2 Objective and problem formulation

As mentioned above, well integrity issues are a big concern and poorly designed cement and poor cementation, among others, are driving factors for integrity problems. In both geothermal and hydrocarbon wells desired attributes of cement are high strength, flexible, impermeable, among others. This thesis will address issues such as:

- How will high temperature and dryness affect the physical properties of cement?
- What additives can be used to improve high temperature tolerance of cement?
- How will various additives effect the bond strength at cement – casing and cement – formation interface?
- How will various additives effect leakage through cement plug and at the cement – casing interface?

The objective of this thesis is limited to experimental work. The primary objective of this thesis is to answer the research questions addressed. For this, the activities are:

- Review conventional cement.
- Review typical geothermal wells.
- Review various additives in cements and their effects.
- Experimental study on cement with old and new additives.
- Develop a new cement slurry additive that has improved physical properties compared with conventional cement when exposed to high temperature.

1.3 Research methodology

To improve properties of conventional cement such as permeability, bond strength and non-shrinkage when exposed to high temperature (200°C), a new cement slurry additives have been developed and studied through experimental methods. The bonding at cement – casing

interface and cement – formation interface was tested by means of leakage and shear bond strength. Cement core plugs were tested for non-destructive elastic property and destructive uniaxial strength. The summary of the experimental research method is illustrated in Figure 1.3.
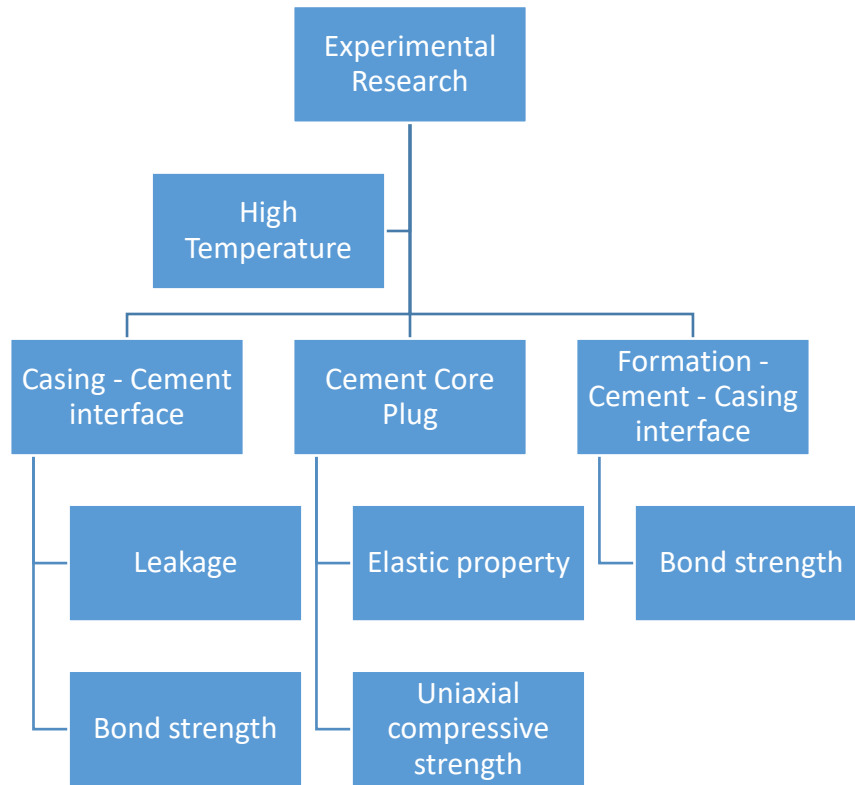
Figure 1.3: Research methodology.

2   Literature review

This chapter presents the literature review of standards and properties of conventional cement with and without various additives.

2.1 NORSOK Standard D-010

NORSOK Standard D-010 [6] describes both guidelines and requirements for well integrity in drilling and well operations. The main focus of this standard is to describe the minimum requirement and guidelines to establish well barriers and monitoring the well integrity.

2.1.1 Well barrier

A well barrier is defined in the standard as *"envelope of one or several well barrier elements preventing fluids from flowing unintentionally from the formation into the wellbore, into another formation or the external environment."* [6] Where well barrier element (WBE) is defined as *"a physical element which in itself does not prevent flow but in combination with other WBEs form a well barrier."* [6]

According to the standard [6], it shall have the capability to:

a) Withstand the maximum differential pressure and temperature it may become exposed to.
b) Be pressure tested, function tested or verified by other methods.
c) Ensure that no single failure of a well barrier or WBE can lead to uncontrolled flow of wellbore fluids or gases to the external environment.
d) Operate completely and withstand the environment for which it may be exposed over time.
e) Be independent of each other and avoid having common WBEs to the extent possible.

During drilling and production there are two main well barriers for every potential of inflow of formation fluid in a well, primary and secondary well barriers. The function of the primary barrier is *"to isolate a source of inflow, formation with normal pressure or over-pressured/impermeable formation from surface/seabed"* [6], and the secondary barrier is a *"back-up to the primary well barrier, against a source of inflow"* [6]. If a well is planned to be plugged and abandoned (P&A) a third well barrier must be installed, open hole to surface well barrier, which has the function *"to permanently isolate flow conduits from exposed*

formation(s) to surface after casing(s) are cut and retrieved and contain environmentally harmful fluids" [6]. Figure 2.1 is a schematic of a simple P&A of a well, where cement plugs are used as well barriers along with casing and in-situ formation.

Well barrier elements	EAC table	Verification/monitoring
Primary well barrier		
In-situ formation	51	
Cement plug	24	
Secondary well barrier		
Formation in-situ	51	
Casing cement	22	
Casing	2	
Cement plug	24	
Open hole to surface well barrier		
Casing cement	22	
Casing	2	
Cement plug	24	
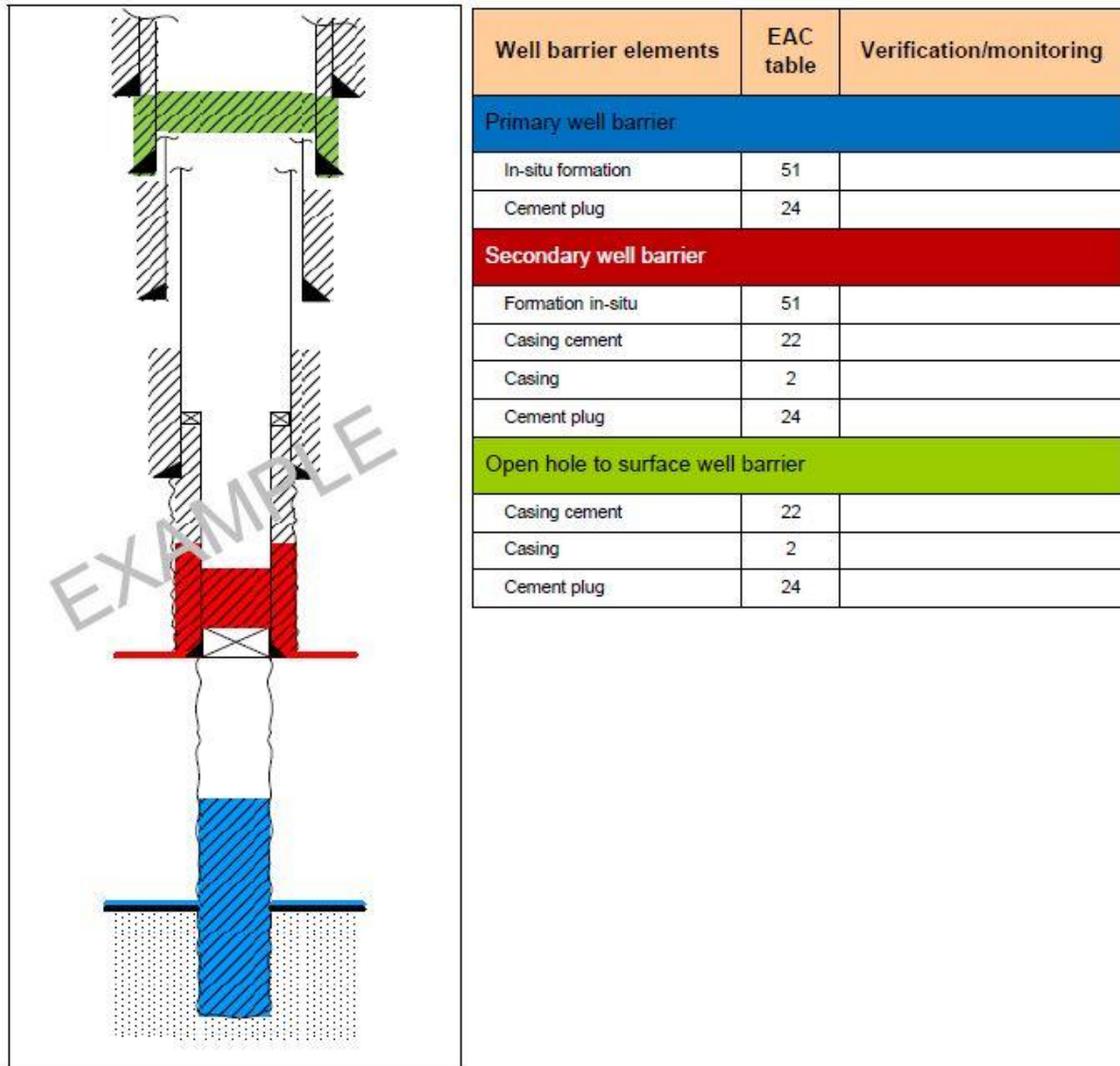
Figure 2.1: Simple example of a P&A of a well. [6, pp.100]

2.1.2 NORSOK D-010 cement property requirements

The purpose of a casing cement is to provide continuous impermeable hydraulic seal between the casing and the borehole wall, or between two casing strings. It should prevent flow of formation fluid, withstand pressure from all directions, and provide mechanical support to the casing or liner. Before use, the cement slurry must be laboratory tested with the right

additives and the expected well conditions, i.e. temperature, pressure, and possible exposure to gases (H_2S, CO_2). [6]

According to NORSOK D-010 [6], cement plug acting as a well barrier or WBE, in both well constructions and for plug and abandonment (P&A), must have the following attributes:

a) Provide long term integrity

b) Impermeable

c) Non-shrinking

d) Able to withstand mechanical loads/impact

e) Resistant to chemicals/substances (H_2S, CO_2 and hydrocarbons)

f) Ensure bonding to steel

g) Not harmful to the steel tubulars integrity

Figure 2.2 illustrates casing cement that is a part of both primary and secondary well barrier, and possible leak paths where some of the required attributes have failed.
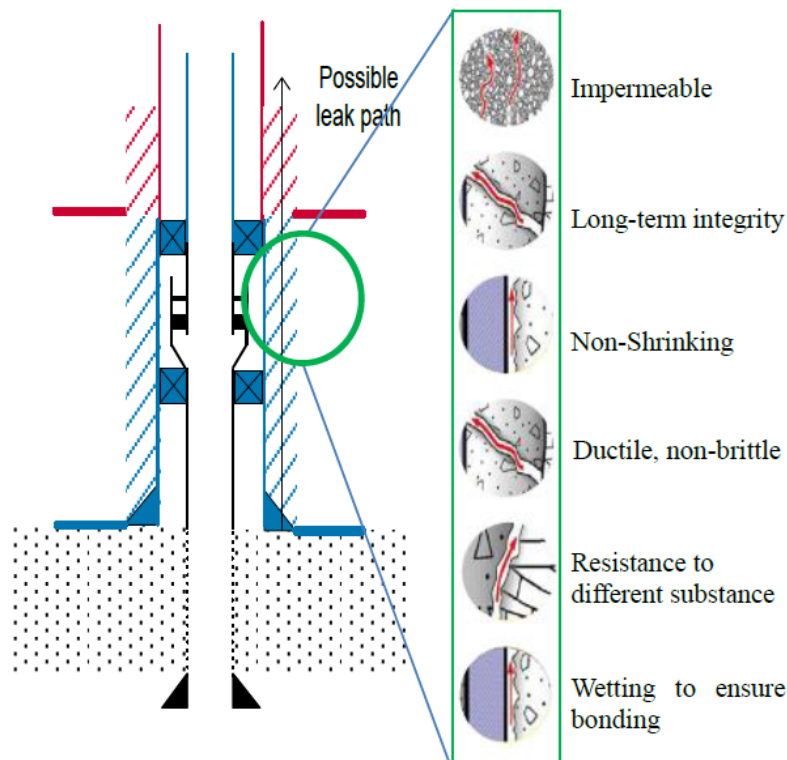
Figure 2.2: Possible leak paths because of failure in the casing cement. [6]

This thesis was designed to try to qualify the cement properties requirements demanded by NORSOK, such as ductility and good bonding.

2.2 Conventional cement

The cement used in the Petroleum industry is Portland cement, also called a hydraulic cement. Hydraulic cement hardens and develop its strength under a process called hydration, where it undergoes a chemical reaction between water and the compounds presented in the cement. To prepare Portland cement clinger, the burned material that exits the kiln, two types of materials are needed: (1) calcareous materials, containing lime, and (2) argillaceous materials, containing alumina, iron oxide, and silica. First, the raw material is finely crushed into desired size and uniformly blended. Then the material is heat treated in a rotary kiln, the kiln is slightly inclined and when rotated the material slowly move through the kiln while being heated (burned) in the process, creating cement clinker. The cement clinker is then cooled and grinded to a desired size. The composition of conventional Portland cement is given in Table 2.1 and the abbreviation of most oxides in cement is given in Table 2.2. The content of C_3A and C_4AF can differ significantly for special cements. [5, pp. 23-30]

Table 2.2: Abbreviation of most oxides in cement. [5, pp. 23]

Table 2.1: Composition of classic Portland cement clinker. [5, pp. 24]

Oxide Composition	Cement Notation	Common Name	Concentration (wt%)
$3CaO \cdot SiO_2$	C_3S	Alite	55–65
$2CaO \cdot SiO_2$	C_2S	Belite	15–25
$3CaO \cdot Al_2O_3$	C_3A	Aluminate	8–14
$4CaO \cdot Al_2O_3 \cdot Fe_2O_3$	C_4AF	Ferrite phase	8–12

C = CaO	A = Al_2O_3
S = SiO_2	F = Fe_2O_3
M = MgO	H = H_2O
N = Na_2O	K = K_2O
L = Li_2O	P = P_2O_5
f = FeO	T = TiO_2

2.2.1 API classification of Portland cement

API classifies Portland cement into eight classes, indicated with letters from A to H. The arrangement is according to the temperature and pressure the set cement is expected to be exposed to [5, pp. 45]. The typical composition of the principal elements and their fineness are illustrated in Table 2.3 for the different classes. In Table 2.4 a description of intended use of the different API classes is illustrated.

Table 2.3: Typical composition and fineness of API classified Portland cement [5, pp. 47]

API Class	ASTM Type	Typical Potential Phase Composition (wt%)				Typical Blaine Fineness (cm²/g)
		C_3S	β-C_2S	C_3A	C_4AF	
A	I	45	27	11	8	1,600
B	II	44	31	5	13	1,600
C	III	53	19	11	9	2,200
D	–‡	28	49	4	12	1,500
E	–	38	43	4	9	1,500
G	Nominal II	50	30	5	12	1,800
H	Nominal II	50	30	5	12	1,600

Table 2.4: Description of intended use of the API classes of Portland cement [5, pp. 45, 48], [11]

Class A	Intended for situations when no special properties are required.
Class B	Intended for situations when a moderate or high sulphate resistance is required.
Class C	Intended for situations when high early strength is required.
Class D, E and F	Intended for situations when moderately high temperature and pressure are expected. These classes are also called retarded cement, and are designed for deeper wells. The retardation is achieved by removing some of the fast hydrating elements and increasing the particles size. However, the technology of retarders have greatly improved since these classes were first manufactured, therefore are these classes rarely used today.
Class G and H	Intended as a basic well cement. These classes were developed after improvement of accelerators and retarders.

2.2.2 Hydration process of cement

As soon as the dry cement comes in contact with water the hydration process begins and hydrated compounds are formed. It begins with a step called dissolution, where the cement dissolves and releases ions into the water. This happens rapidly until the solution is supersaturated, i.e. the solution has enough energy to transform the ions from being dissolved in the solution to combine into new solids. This solidification is called precipitation, and these solid products are called hydration products and are different from the starting

cement minerals, but will still let the minerals dissolve. The water in the system have two purposes: (1) to enable the hydration process by dissolving the cement minerals, and (2) to provide ions, hydroxyl group (OH-), to the system. [12]

The most common material in cement is the silicate phase, and the C_3S is the main component. The chemical equation for the hydration of C_3S and C_2S (silicate phase) is given below, and shows that for both phases, calcium silicate hydrate and calcium hydroxide is formed. The compound $C_3S_2H_3$ is commonly called C-S-H (Calcium Silicate Hydrate) gel and is considered the primary binder in hardened cement. [5, pp. 30]

$$2C_3S \rightarrow C_3S_2H_3 + 3CH$$
$$2C_2S + 4H \rightarrow C_3S_2H_3 + CH$$
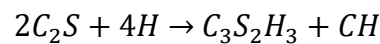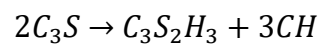
The hydration of C_3S is an exothermic process, i.e. the system releases energy in form of heat to the surroundings, and can be divided into five stages [5, pp. 31-34]:

1. **Pre-induction period** begins as soon as the cement comes in contact with water and will only last for a few minutes. Here the C-S-H gel will start to form as mentioned above.

2. **Induction period** is when the rate of heat liberation falls dramatically and very little hydration is observed, consequently will C-S-H gel form very slowly. The concentration of OH- and Ca^{2+} will continue to rise until critical supersaturation is reached, initiating precipitation of calcium hydroxide, $Ca(OH)_2$. Hydration will resume at a high rate marking the end of the period. The period will last for a few hours, and only a small portion of C_3S will have hydrated at its end.

3. **Acceleration period** is the period where the most rapid hydration occur. The rate of hydration accelerates and the cement begins to set and develop its strength.

4. **Deceleration period** is when the hydration rate will decelerate, but will still develop its strength. The acceleration and deceleration periods, together known as the setting period, will take several days.

5. **Diffusion period** is after the cement is set, and its structure will not change significantly. However, the hydration will still continue, developing strength and increasing its density by the growing C-S-H gel, reducing its porosity. The length of the period is unknown, it can be weeks, months, or even years.

A schematic of the rate of heat evolution during hydration of Portland cement is shown in Figure 2.3, including various events mentioned above. Although C_3S is often used as a model for hydration it must be noted that many other factors are involved in the process. It
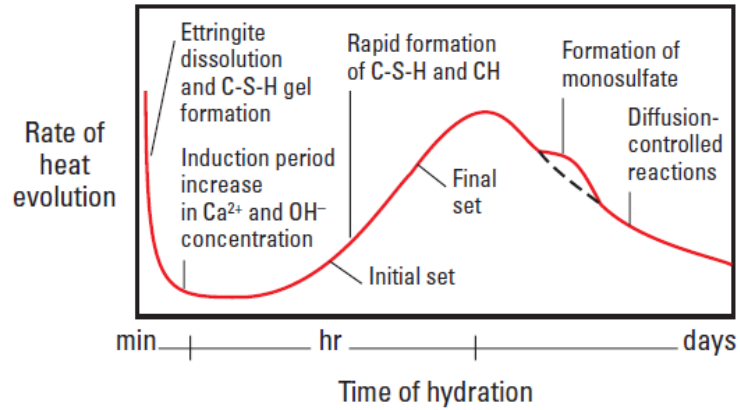
Figure 2.3: Schematic graph of the hydration of Portland cement. [5, pp. 37]

does not form from pure C_3S and C_2S but also from aluminium, sulphur, and iron. Furthermore, the cement is never perfectly pure, it will always contain some particles in addition to what was originally mixed together, which will affect the reaction. [5, pp. 36-37]

2.2.3 Temperature effect

During the first hours of hydration, the temperature is one of the main parameters for the rate of hydration, the structure, and the quality of the set cement. Increased hydration temperature gives increment in the rate of hydration, but often results in decreased strength. As shown in Figure 2.4, with increased temperature, the induction period and the setting period are reduced, and during the setting period the peak of hydration is much higher. When curing temperature is greater than 110°C the C-S-H gel is not
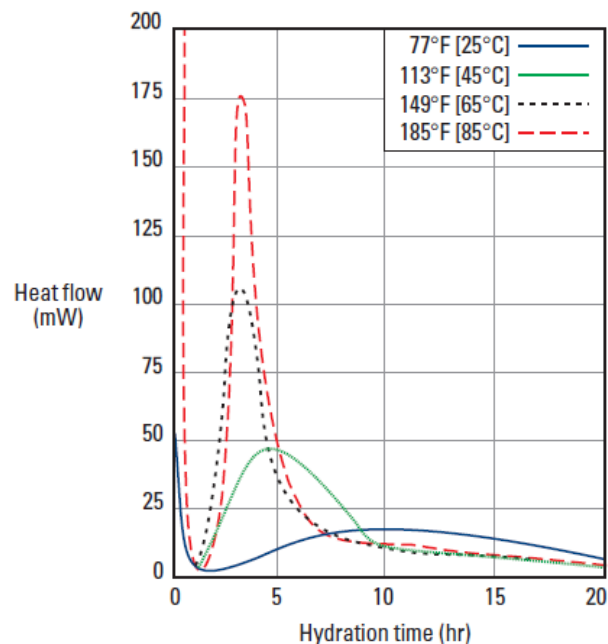
Figure 2.4: Effect of temperature on Portland cement. [5, pp. 37]

stable and crystalline calcium silicate is formed, which is much denser than C-S-H gel, and leads to shrinkage. As a result, the set cement has decreased compressive strength and increased permeability. To reduce the strength loss at high temperature, a form of silica can partially replace the cement, e.g. ground quartz, fine silica sand, or silica flour. [5, pp. 37-38, 319-321]

Ashok Santra et al. [13] studied the relation between heat of hydration and compressive strength at two curing temperatures, 30°C and 60°C. Over the period of 20 hours the heat of hydration and the compressive strength (from sonic measurements) was measured and the results are illustrated in Figure 2.5. Firstly, it shows, as mentioned above, that with increased temperature the peak of hydration is higher and occurs earlier than for lower temperature. Secondly, it shows that the strength development is highly related to the heat of hydration, thus also to the temperature. Higher temperature has earlier compressive strength development. [13]
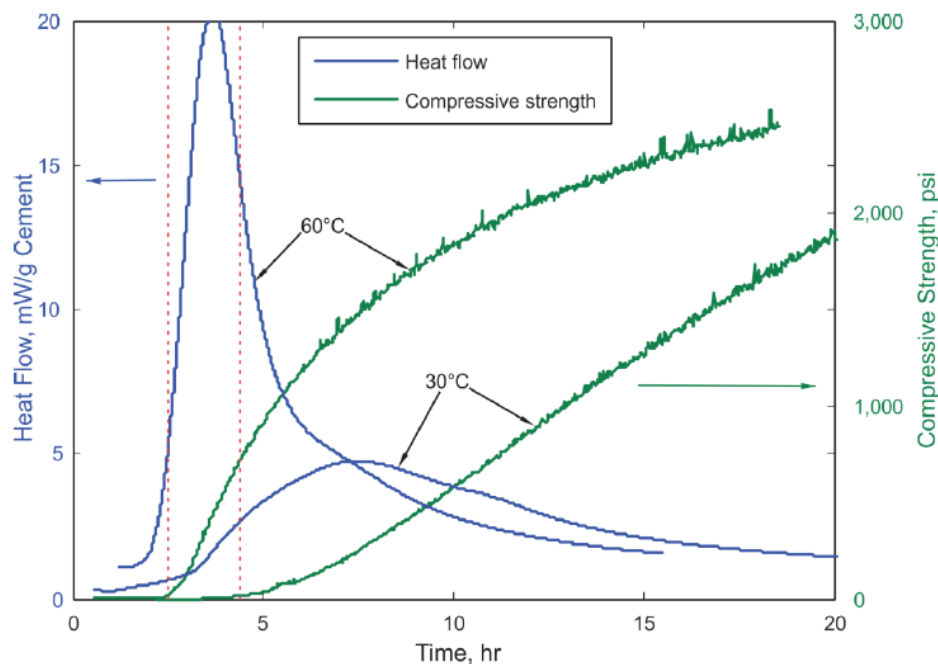
Figure 2.5: The development of heat of hydration and compressive strength of cement slurry for two different temperatures. [13]

2.3 Nanotechnology

Nanotechnology is the use of extremely small particles in any field of science that are 1-100 nanometres (nm) in diameter, where one nanometre is one billionth of a metre, or equal to 1×10^{-9} m. Due to their small size, they have much higher surface area to volume ratio compared to other materials, for instance micro and macro materials. Therefore nanoparticles have different physical and chemical properties than other materials [14].

This technology is still under development in the petroleum industry. In recent years, studies have shown that nanoparticles can improve the properties of Portland cement, among others, early strength development, increased compressive and tensile strength. Nanoparticles

creates good packing by filling out the pore spaces between micro and macro particles. Consequently, reducing the porosity and permeability, and increasing the density and strength. [13]

2.3.1 Application of nanoparticles in cement

Today there is a large variety of nanoparticles that vary in size, chemical composition, structure, etc. Depending on the nanoparticles used in cement, it will affect its properties differently. The following presents various studies on nanoparticles and how they affect the cement.

2.3.1.1 Nano silica

Patil and Deshpande [14] studied the effect of Nano silica (SiO_2) on compressive strength of Portland cement treated with latex. The particle size of silica was 5-7 nm. Micron sized silica was also studied for comparison. In Figure 2.6 the results are shown for the compressive strength and its development, it shows how Nano silica will work as an accelerator, increasing the early strength significantly. Also, it had threefold the compressive strength after 24 hours, compared with specimens without Nano silica. The temperature effect on Nano silica was also tested. Compressive strength of specimens with equal amount of Nano silica were tested in 27°C, 88°C and 166°C. It showed that the early strength development of the Nano silica was not affected. [14]

Latex (gal/sk)	Silica	Retarder (gal/sk)	Time to 500 psi (hr:min)	UCA Strength Rate of Strength Development (psi/hr)	24-hr Strength (psi)
1.5	0	0.05	23:05	172	690
1.5	Micron sized silica	0.05	21:45	160	610
1.5	Nanosilica	0.05	13:29	460	2203

[a]Premium Class H cement, defoamer 0.05 gal/sk, stabilizer 0.2 gal/sk, dispersant 0.143 gal/sk, density 16.4 lbm/gal, Yield 1.1 ft^3/sk.

Figure 2.6: Effect of Nano silica on compressive strength of cement. [14]

A study conducted by E. Ghafari et al. [15] showed that by adding Nano silica to the cement slurry the cement became denser and more homogeneous. This increases the strength of the cement but at the same time reduces the flowability. The microstructure showed that Nano silica reacts with $Ca(OH)_2$ crystals, improving the microstructure between the aggregates and the binding paste.

2.3.1.2 Carbon nanotubes

Carbon nanotubes (CNT) are made of graphene sheets that have been rolled up to form a tube-shaped structure; where graphene is a hexagonal structure made out of carbon atoms. It can be up to a few μm in length and can either be single wall or multiwall, where single wall CNT have a diameter of 1-2 nm and multiwall CNT have a diameter ranging from 2 to 25 nm [16].

Rahimirad and Baghbadorani [17] conducted an experiment to study the effect of CNT on foam concrete. It showed that by adding 0.05% CNT by weight decreased the conductivity of concrete and increased its compressive strength by up to 70%. It also showed more homogeneous microstructure and less porous. However, a study performed by Santa et al. [13] showed that if too much of CNT is added to cement it can decrease its strength. 0.1% and 0.2% bwoc CNT was added to cement, which decreased the compressive strength.

To improve the dispersion of CNT in concrete Kazi Fattah et al. [18] studied the effect of adding polar impurities on CNT. Four multiwall CNT were tested, namely pure CNT, CNT-OH, CNT-COOH, and CNT-water. Specimens with 1% pure CNT weakened the compressive strength of the concrete. But 1% CNT with OH and CNT with COOH both increased the compressive strength, especially after long curing time.

2.4 Geothermal wells

Drilling a geothermal well can be similar to drilling an oil or gas well. The major differences are the high temperature, typically ranging from 160°C to above 300°C and underpressured formation [4]. The reservoir rocks are typically highly fractured metamorphic or igneous rocks and often contain corrosive non-condensable gases, such as CO_2 and H_2S [9]. These environments can lead to lost circulation, low rate of penetration (ROP) and corrosion. Cement have to be designed to withstand the high temperature cycling, and the casings are usually required to be cemented completely to the surface. To achieve better temperature resistance G class cement can be replaced with up to 40% silica flour. [4]

S. Aydin and B. Baradan [19] studied if replacing part of ordinary Portland cement with fly ash (type C) would increase the temperature resistance of cement. Samples were mixed with various amount of fly ash, replacing the cement with 0%, 20%, 40%, and 60% fly ash. After curing the samples were exposed to 300°C, 600°C and 900°C for three hours and then cooled,

some with rabid cooling (soaked in water at 20°C) and some with slow cooling (left at room temperature). The samples were then tested for flexural strength and compressive strength. All slowly cooled samples containing fly ash had increment in compressive strength when exposed to 300°C, 600°C and 900°C compared with the sample that was not exposed to high temperature. The samples with no fly ash had decreased compressive strength after exposure to high temperature. However, it still had the highest compressive strength of all other samples for all temperatures, except 900°C. The flexural strength of all samples was decreased after exposure to high temperature. The compressive and flexural strength of the samples are illustrated in Figure 2.7. [19] This shows that fly ash is good for temperature resistance of cement, but will at the same time decrease its strength.

Mixture	Compressive strength (MPa)								Flexural strength (MPa)							
	20 °C	300 °C		600 °C		900 °C			20 °C	300 °C		600 °C		900 °C	
		Air	Water	Air	Water	Air	Water			Air	Water	Air	Water	Air	Water
FA0	45.6	55.9	37.0	43.7	31.5	14.4	12.8		9.0	8.6	5.6	6.1	3.6	1.8	1.0
FA20	39.4	49.3	31.5	42.2	27.7	21.3	18.8		8.6	7.4	4.2	6.0	3.4	2.8	1.2
FA40	35.8	44.5	27.3	40.8	24.1	28.3	25.9		8.4	7.3	3.9	4.8	2.4	3.2	1.4
FA60	22.2	27.5	15.0	22.6	13.8	26.4	24.0		5.8	5.1	2.1	3.1	1.4	3.5	1.1

Figure 2.7: The compressive and flexural strength of cement partially replaced by fly ash when exposed to high temperatures. [19]

Li Li et al. [20] conducted an experimental study on how the different curing condition effects the tensile strength of cement. The cement was cured at various temperatures and pressures. By increasing the curing temperature from 32°C to 93°C, at a pressure of 3000 psi, the tensile strength decreased from 330 psi to 260 psi. They also tested the tensile strength at different pressures, where increasing the curing pressure from atmospheric pressure to 2000 psi and 3000 psi decreased the tensile strength with 20% and 30%, respectively. [20]

2.5 Bond strength of cement

Good cement bonding with casing and formation in a wellbore is important for it to be able to meet the requirements specified by NORSOK. Poor bonding creates a leak path at the cement – casing interface that allows formation fluids to migrate through and not be able to hold potential pressure.

Waqas Mushtaq [21] conducted an experiment to study the shear bond strength of cement with different types of formation rocks; sandstone, limestone, chalk and shale. When he tested the bond strength with dry rocks the failure did not occur at the cement – formation interface but rather in the rock itself, this was true for all rock types except the shale. This

indicates that the cement – formation bond strength was higher than the shear strength of the rock. Next he immersed the rock samples in drilling mud, two types of water based (WBM) and two types of oil based (OBM), then testing the bond strength of cement with formation with mud. Figure 2.8 shows the cement – formation bond strength treated with various mud systems. Firstly, this shows how the drilling mud has a huge impact on the bond strength, decreasing the bond strength significantly, and that the OBM is more damaging than the WBM. Secondly, it shows that shale seems to be least affected by the mud systems; especially in WBM. [21]
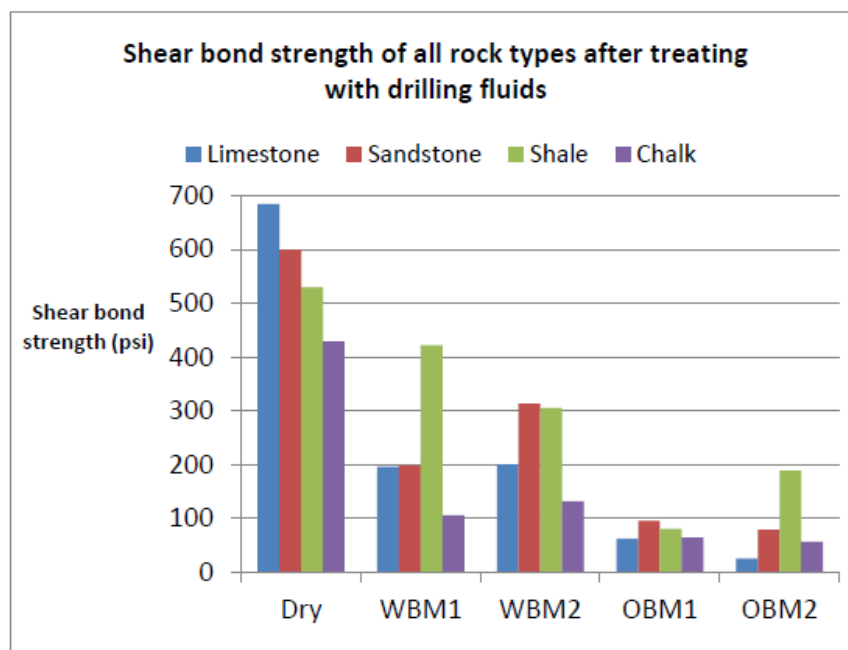
Figure 2.8: The shear bond strength of limestone, sandstone, shale and chalk treated with dry, WBM, and OBM. [21]

X Zhao et al. [22] conducted an experiment on cement bond with casing-sand adhesion. The outside of a casing was coated with bicomponent-epoxy adhesive and sand with various grain sizes. This study showed an increase in shear bond strength, which was obtained by coating the casing, and that the optimal grain size was 1.6-1.9 mm and coverage was 60-70%. The casing was also bathed in drilling mud, where the longer the casing was subjected to mud the weaker bond was measured.

2.6 Application of rubber in cement

S. Sgobba et al. [23] studied the effect of recycled car and truck tyres on Portland cement. The tyres were cut into various sizes, chipped rubber (25-30 mm), crumb rubber (3-10 mm), and ash rubber (<1 mm). The compressive strength decreased with increased amount of

crumb rubber, but decreased the density, and the rubber seem to have trapped air in the concrete structure. M. Yazdi et al. [24] also reported that tyre rubber has a significant effect on the strength of concrete. With increased rubber the strength decreases significantly, and the size of the rubber particles also effect the properties, the smaller the particles were the less decrement of the strength was reported. An untreated rubber is hydrophobic and will not bind well with the cement, but rather function as a pore due to its soft nature [24]. To create better bridging between the rubber particles and the cement gel X. Colom et al. [25] studied various acid treatments. Three types of acid solutions were tested, H_2SO_4, HNO_3, and $HClO_4$, and it showed that the sulphuric acid (H_2SO_4) proved to be the best choice. By pre-treating the rubber with sulphuric acid the rubber's surface was rougher and bonded better with the cement's particles, increasing the tensile strength.

Fung Xu et al. [26] reported that with increased amount of latex mixed with cement increased its thickness, making it more viscous. Also, if rubber powder or expandable perlite is added to the cement it will decrease the compressive and flexural strength with increased amount.

3 Theory

This chapter presents theories used to calculate parameters from the experimental measured data in chapter 4.

3.1 Mass and volume change

To study how much formation fluid could migrate through cement, one can measure how much water it absorbs. The more it absorbs the probability of migration is increased. To calculate the mass change one can use the following equation:

$$\Delta M = \frac{M_t - M_0}{M_0} * 100$$

<div align="right">(3.1)</div>

Where,

    ΔM is the change in mass (%);

    M_0 is the mass after setting;

    M_t is the mass at time t.

This equation can also be used to calculate the mass loss of cement, for instance if there is a pressure decrement in the surrounding environment allowing the cement fluid to escape its pores; this will give a negative value of ΔM.

The volume change can be calculated in a similar way, where M in eq. (3.1) is replaced with V:

$$\Delta V = \frac{V_t - V_0}{V_0} * 100$$

<div align="right">(3.2)</div>

Where,

    ΔV is the change in volume (%).

3.2 Sonic

The speed of sound through cement is related to its density and its strength. The traveling time of primary wave (P-wave) through a cement core was measured with Pundit 7 shown in Figure 3.1. A specimen is tightly place between two sensors, where one sends a P-wave signal and the other receives it, and the time is measured. The P-wave velocity is then calculated with the following equation:

$$v_p = \frac{l}{t}$$

Where,

v_p is the P-wave velocity (m/s);

l is the length of the specimen (l);

t is the P-wave's traveling time (sec).
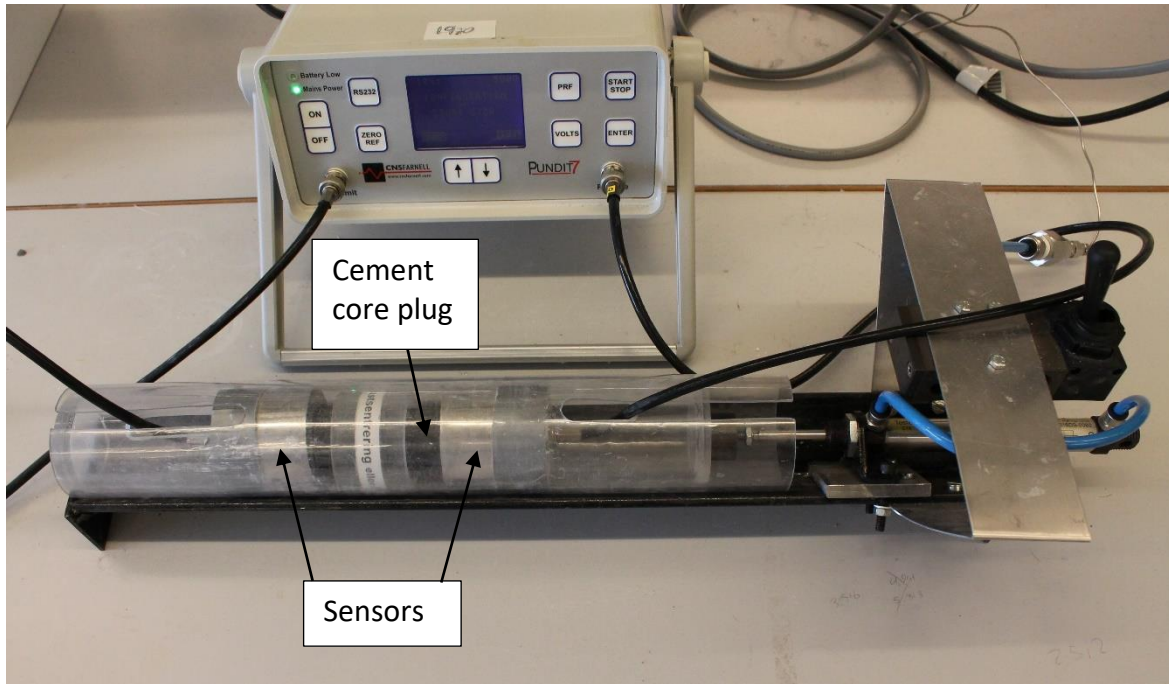
Figure 3.1: Pundit 7, an instrument used to measure the traveling time of P-wave through a cement core specimen.

The density of cement is given by:

$$\rho = \frac{M}{V}$$

(3.4)

Where,

ρ is the density (Kg/m^3);

M is the mass (Kg);

V is the volume (m^3).

From the P-wave velocity and the density the dynamic elastic modulus can be calculated with the following equation:

$$E^* = K + \frac{4}{3}G = v_p^2\,\rho * 10^{-9} \qquad (3.5)$$

Where,

E^* is the dynamic modulus of elasticity (GPa);

K is the bulk modulus, which measures the resistance to hydrostatic load (GPa);

G is the shear modulus, which measures the resistance to shear stress (GPa);

v_p is the P-wave's velocity (m/s);

ρ is the density (Kg/m^3).

3.3 Compressive strength

The uniaxial compressive strength (UCS) of cement is its maximum axial strength before failure. It can be measured with a destructive test where an axial force is applied to a cylindrical specimen and increased until failure. The UCS is calculated with the following equation:

$$\sigma_{UCS} = \frac{F_{max}}{A} \qquad (3.6)$$

Where,

σ_{UCS} is the stress at the time of failure, or the maximum stress, also called UCS (MPa);

F_{max} is the force at the time of failure (Pa);

A is the cross-sectional area of the specimen (mm^2).

Figure 3.2 shows the setup for the destructive test. Where a core plug is placed between parallel plates and the axial load is applied until the core plug fails.
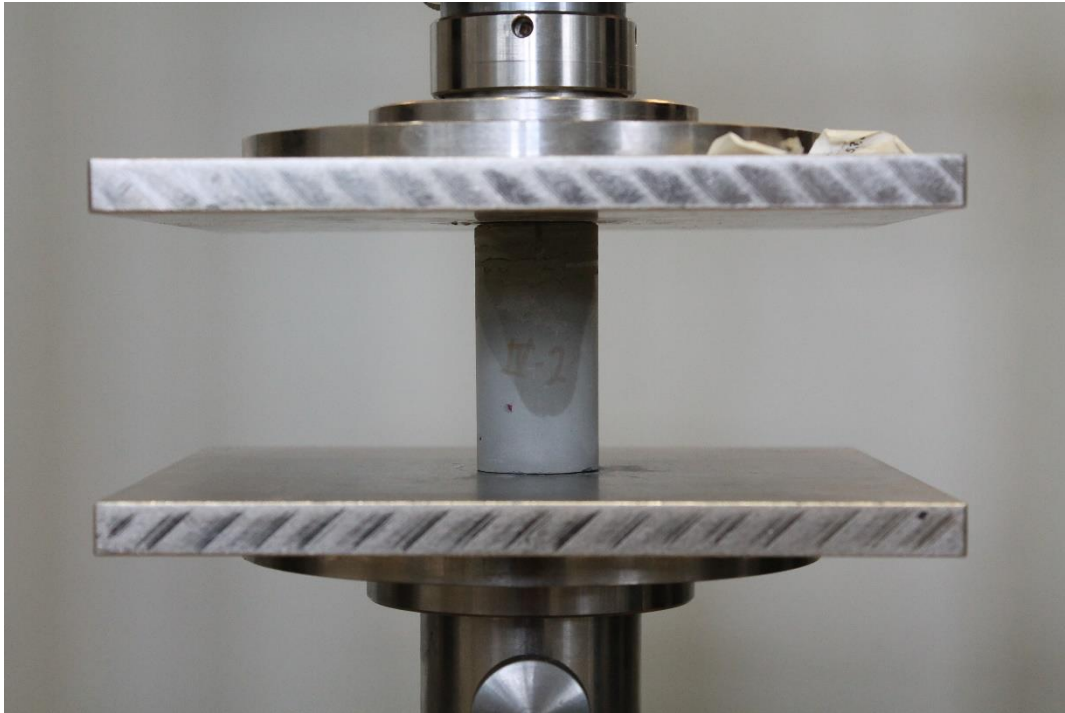
Figure 3.2: Setup for UCS destructive test, where force is applied from above until the specimen fails.

From the stress-strain curve (see Figure 3.3) obtained from the UCS test, the modulus of elasticity (E) and the modulus of resilience (R) of a specimen can be estimated. The modulus of elasticity describes a material's ability to resist deformation under pressure and is defined as the change of stress to the change in strain. It can be calculated as the slope of a stress-strain curve with the following equation:

$$E = \frac{\Delta\sigma}{\Delta\varepsilon}$$

(3.7)

Where,

E is the Young's modulus, also called modulus of elasticity (MPa);

$\Delta\sigma$ is the stress difference on the linear slope of a stress-strain curve (MPa);

$\Delta\varepsilon$ is the strain difference on the linear slope of a stress-strain curve (m/m).

The modulus of resilience describes a material's ability to absorb energy when it is subjected to deformation until yielding is reached. It can be calculated by integrating the stress-strain curve from zero to limit, i.e. the area under the stress-strain curve. An estimate of the modulus of resilience can also be found with the following equation:

$$R = \frac{\sigma_{UCS}^2}{2E} = \frac{\sigma_{UCS}\varepsilon_{max}}{2} \qquad (3.8)$$

Where,

R is the modulus of resilience (J/m^3);

σ_{UCS} is the uniaxial compressive strength (Pa);

ε_{max} is the strain at time of failure (m/m).

An example of a stress-strain curve is shown in Figure 3.3, it shows the modulus of elasticity and resilience as the slope of the curve and the area under the curve, respectively.
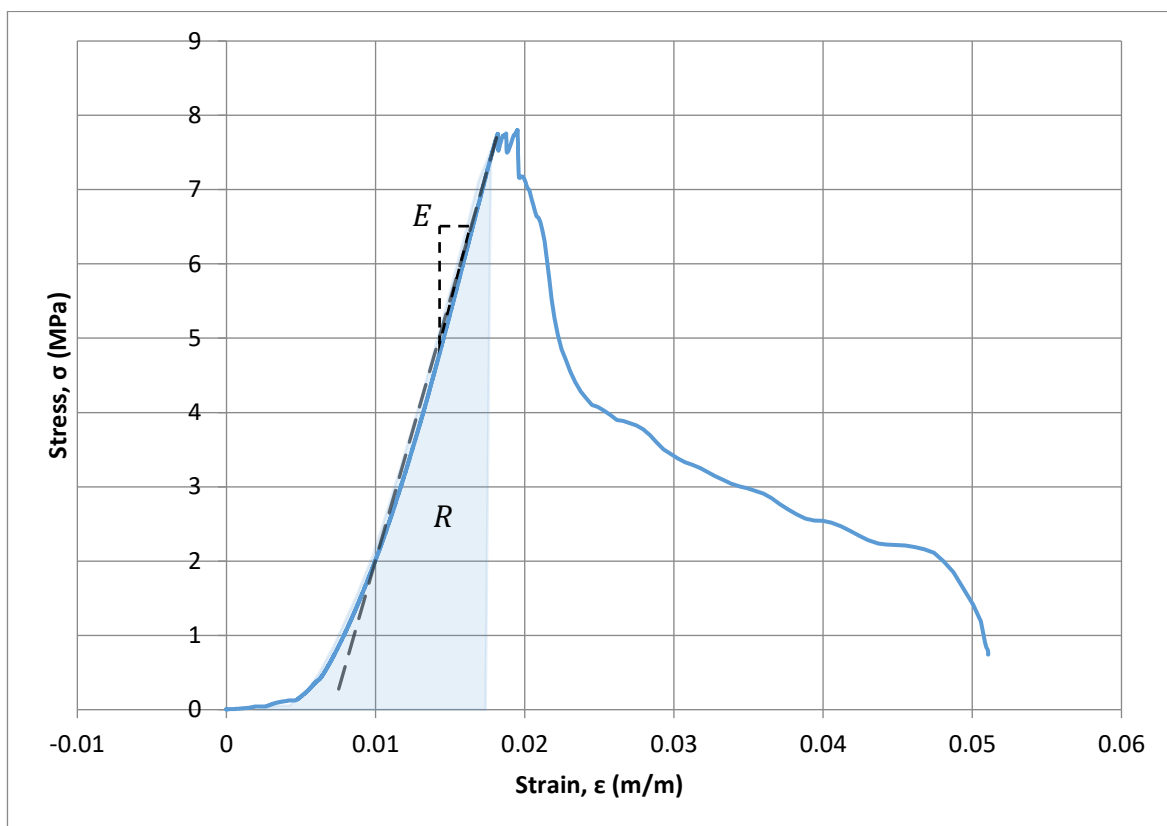
Figure 3.3: A stress-strain curve obtained from a UCS test, showing an estimated modulus of elasticity, E (the dashed line), and modulus of resilience, R (the shaded area under the curve).

3.4 Resistivity

Resistivity of cement describes its ability to resist a flow of electrons through its pores. A higher resistivity means that cement does not allow the electrons to travel through it easily and vice versa. The resistance of the cement core plugs was measured with LCR HiTester

shown in Figure 3.4. From the resistance, the resistivity of the core plug can be calculated from the following equation:

$$\rho_r = R\frac{A}{l}$$

Where,

ρ_r is the resistivity (Ωm);

R is the resistance (Ω);

A is the cross-section area of the core plug (m^2);

l is the length of the core plug (m).

(a)

(b)
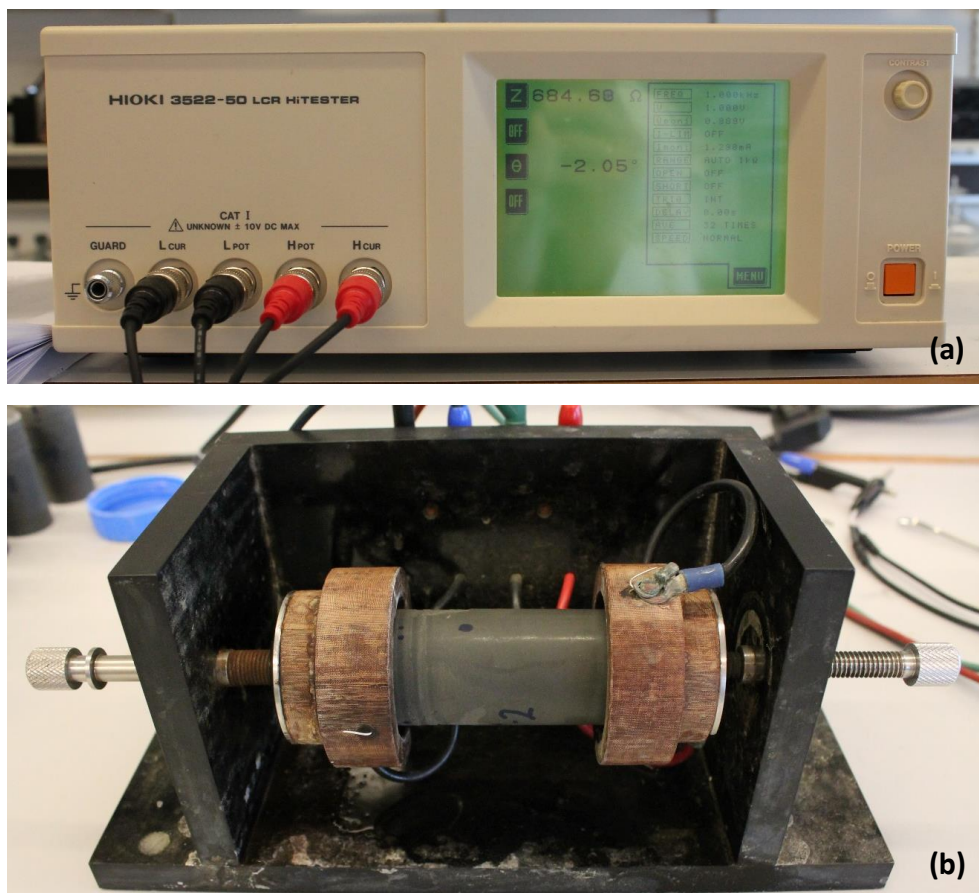
Figure 3.4: (a) HIOKI 3522-50 LCR HiTester, an instrument used to measure the resistance of a cement core specimen shown in (b).

3.5 Shear Bond strength

As force is applied on a core plug inside a casing, the reaction force at the cement – casing interface resist until the applied force overcome the interface bond strength. An illustration of the bond strength test is shown in Figure 3.5, including the variables used in eq. (3.10).
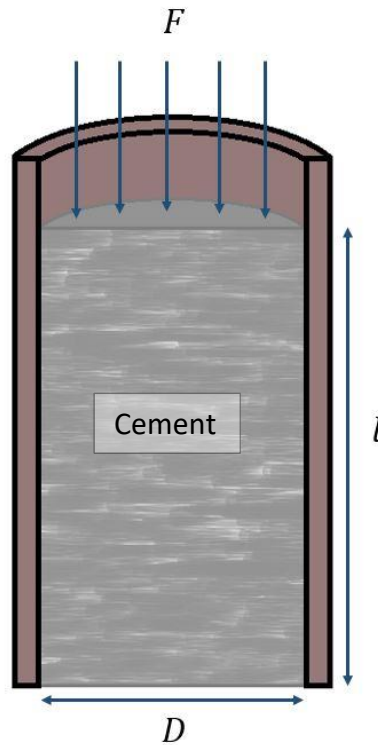
Figure 3.5: Illustration of cross-section of bond strength test

The shear bond strength of cement at the casing or formation interface can be calculated by the following equation:

$$\tau = \frac{F}{A} = \frac{F}{\pi D l} \qquad (3.10)$$

Where,

τ is the shear bond strength (Pa);

F is the maximum force (N);

A is the surface area in contact with cement (m^2);

D is the diameter of casing/formation in contact with cement (m);

l is the length of contact between cement and casing/formation (m).

3.6 Thermal expansion

Thermal expansion is the change of material's shape, length, area, and volume due to change in temperature. Most materials will expand when temperature increases. The expansion rate of a given material is given by the linear expansion coefficient, α. The following equations show the relation between the temperature change and the change in length, area, and volume, respectively:

$$\Delta L = L_f - L_0 = \alpha L_0 \Delta T \qquad (3.11)$$

$$\Delta A = A_f - A_0 = 2\alpha A_0 \Delta T \qquad (3.12)$$

$$\Delta V = V_f - V_0 = 3\alpha V_0 \Delta T \qquad (3.13)$$

Where,

α is the linear thermal expansion coefficient (K^{-1});

L is the length (m);

A is the area (m^2);

V the volume (m^3);

ΔT is the change in temperature (K);

Subscript 0 and f represents the original and the final value, respectively.

4   Experimental work

This chapter presents the description of the materials used in the experiments, cement slurry formulation and testing. The cement slurry was evaluated in terms of leakage, its bond strength, and its mechanical and elastic properties.

4.1 Description of material used

4.1.1 Cement

In the experiments class G Portland cement was used. It is one of the main oil well cement used in the industry. It consists mainly of hydraulic calcium silicates, and usually some form of calcium sulphate. It is used for instance in oil wells construction, gas wells, water wells, pipelines, and as a support for the base of offshore platforms. Due to its chemical composition it has predictable setting time, high sulphate resistance, high durability, low viscosity, great strength, fluid loss control, and low probability to segregate. This gives the cement the ideal properties for construction of oil wells and other similar activities; easily pumpable, low permeability, stable and with high corrosion resistance. [5, pp. 48], [27], [28] Figure 4.1 illustrates the composition, some of the physical properties and requirements of class G cement.

Oxide	Class G, wt%
Silicon dioxide, SiO_2	21.7
Calcium oxide, CaO	62.9
Aluminum oxide, Al_2O_3	3.2
Iron oxide, Fe_2O_3	3.7
Magnesium oxide, MgO	4.3
Sulfur trioxide, SO_3	2.2
Sodium oxide, Na_2O	
Potassium oxide, K_2O	
Total alkali as Na_2O	0.54
Loss on ignition	0.74
Insoluble residue	0.14

Phase Composition	
C_3S	58
C_2S	19
C_3A	2
C_4AF	11

Physical Properties	
% passing 325 mesh	87
Blaine fineness, cm^2/gm	3,470

Physical Requirements	
Thickening time, min, Sch 5	1:40
B_c at 30 min	14
8 hr compressive strength, 110°F (38°C)	928 psi (6.4 MPa)
8 hr compressive strength, 140°F (60°C)	2,247 psi (15.5 MPa)
Free fluid, mL[13]	4.4

Figure 4.1: Composition, physical properties, and requirements of class G and H cement. [11]

4.1.2 Casing

Two types of pipes were used to represent the casing: (1) a nickel based steel table leg (Figure 4.2 a), and (2) a steel pipe (Figure 4.2 b). Unfortunately, the exact composition of the material

was unknown. Along with the most important property for the experiments was the expansion coefficient, α. Therefore, during this research period the property was quantified and presented in the following.

The geometry of the casings; the length, the outer (OD) and inner diameter (ID), were measured with a digital calliper at room temperature (21°C) and then again after heating for 24 hours in 200°C. It was kept in the oven for a day to ensure that the material had time to expand to its maximum size at the given temperature. This was repeated three times to get an average value.

The α was calculated from the volume change with equation (3.13). However, a crucial factor in these experiments was the expansion of the ID because if the inside area of the casing expands more than the cement plug, the plug could lose its bonding with the casing wall. Hence, the α was also calculated from the inside circumference of the casing using equation (3.11) in a form of $\alpha = \frac{\pi(ID_f - ID_0)}{\pi ID_0 \Delta T}$, where πID is the inner circumference of the casing. Table 4.1 shows the original and the final ID and volume, and the linear expansion coefficient calculated from the volume, α_V, and the circumference, α_c, for both types of casings. As shown in Table 4.1 α_V and α_c are not the same, this could be because the material does not expand evenly in all directions, thus resulting in slightly different expansion coefficient. Another possible reason for this difference is inaccuracy in the measurements, the calliper used to measure the lengths had an error of 0.005 mm, and due to the very small values of α, only a small error in the measured value can significantly change the result.
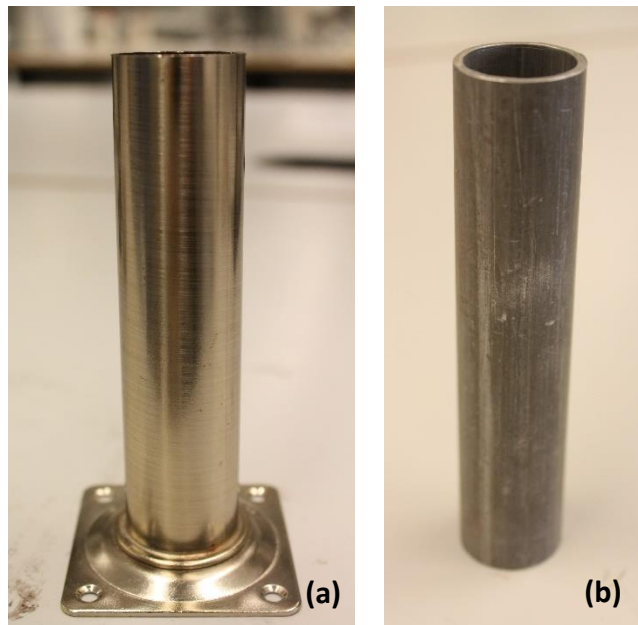
Figure 4.2: Casing pipes, (a) table leg casing and (b) steel pipe casing.

Table 4.1: Values from the thermal expansion measurements and calculations.

	Table leg casing	Steel pipe casing
ID_0 (mm)	28.14	21.35
ID_f (mm)	28.21	21.38
V_0 (mm^3)	6080.8	6202.5
V_f (mm^3)	6117.9	6237.0
α_V (K^{-1})	11.35 * 10^{-6}	10.36 * 10^{-6}
α_c (K^{-1})	13.90* 10^{-6}	9.55 * 10^{-6}

4.1.3 Nano particles

Two types of Nano sized particles used in the experiments were Nano silicon dioxide (SiO_2), also known as Nano silica, and Nano graphene.

4.1.3.1 Nano silica

A 15 nm sized Nano silica was used in the experiments. Elemental identification and structural analyses were performed to characterize the particles using Elemental Dispersive Spectroscopy (EDS) and Scanning Electron Microscopy (SEM). For the analyses to work the particles must be coated with palladium (Pd) beforehand. The elemental analysis is illustrated in Figure 4.3 and it shows how pure the Nano silica is, containing mainly silicon (Si) and oxygen (O) with a small amount of impurity in a form of carbon (C). Note that the Pd is not a part of the Nano particle, it was used as coating element for SEM analysis. A SEM image of the particles showing its microstructure is illustrated in Figure 4.4.
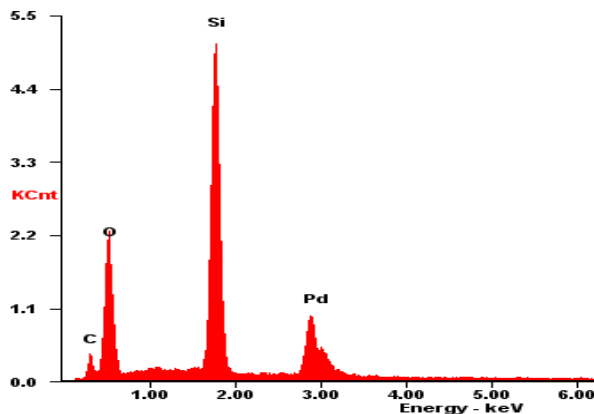
Figure 4.3: Elemental analysis of Nano SiO₂.   *Figure 4.4: A SEM image of Nano SiO₂.*
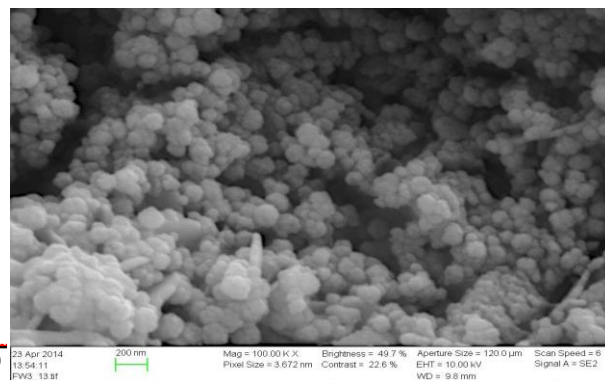
4.1.3.2 Graphene

Graphene is a pure thin layer of carbon, only one atom thick, and the carbon atoms are bonded together in a hexagonal lattice, similar to a honeycomb structure with 0.142 nm between each carbon atom. The structure is illustrated in Figure 4.5. Despite its small size it has very unique properties, it is stronger than steel, and the best known conductor of electricity and heat at room temperature. [29] A SEM analysis was executed to study the structure and is illustrated in Figure 4.6, it shows the thin layers of carbon, and how it can be many micrometres in length and width (2D), but its thickness is only one atom thick.
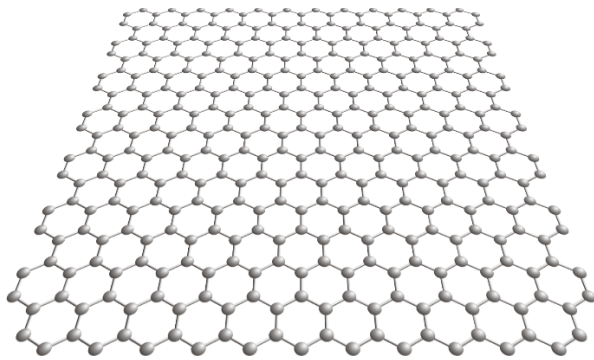
Figure 4.5: The structure of graphene at molecular scale. [30]
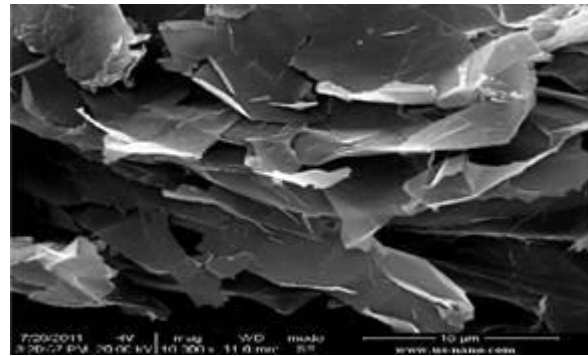
Figure 4.6: SEM image of graphene

4.1.4   Micro sized minerals

Three types of micro sized minerals were used in the experiments. They were all 100-150 μm in size. These were quartz, feldspar, and calcium carbonate ($CaCO_3$), and a short description of them is presented below.

4.1.4.1 Quartz

Quartz is one of the most common minerals found worldwide. Its chemical formula is SiO_2 and is in the trigonal and hexagonal crystal system, but its size, form and colour can vary significantly from one another. It has a density of 2.65 SG and a hardness of 7 on Mohs scale [31], [32]. At normal pressure it has a melting point between 1,550 – 1,705°C, depending on how fast the temperature changes, where the higher melting point is attained when the change in temperature occur very

Figure 4.7: Quartz, 100-150 μm

slowly [33]. A picture of the quartz used in the experiments is shown in Figure 4.7. To study the microstructure of the quartz grains a SEM analysis was executed and the images are illustrated in Figure 4.8 (a) and (b). These show how the grains have both sharp and wide angles.

(a)   (b)
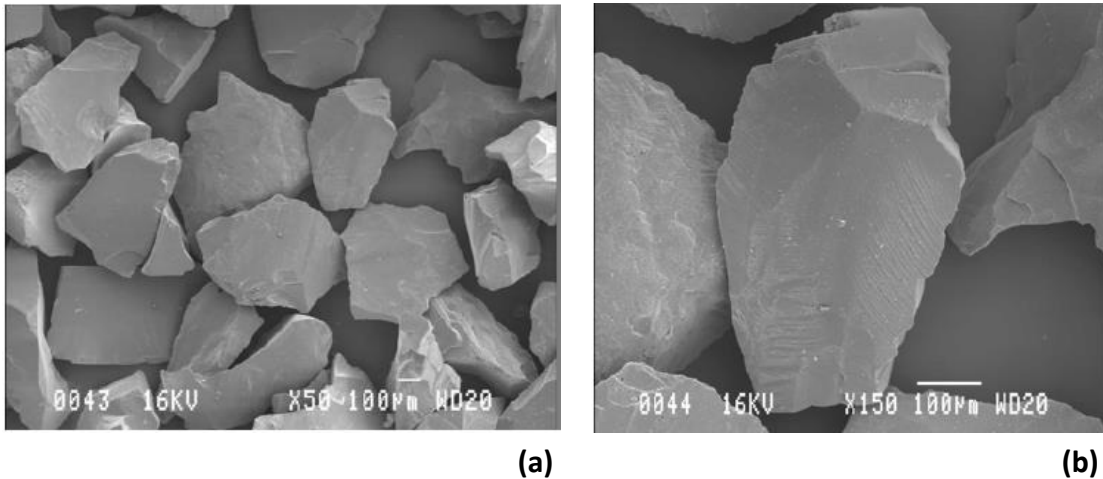
Figure 4.8: SEM images of 125-250µm quartz, (a) 50x and (b) 150x magnification.

4.1.4.2 Feldspar

Feldspar is a group of minerals that are the most frequent components in igneous rocks. The majority of this group can be classified chemically as a part of a ternary system of albite (Ab, $NaAlSi_3O_8$), K-feldspar (Or, $KAlSi_3O_8$) and anorthite (An, $CaAl_2Si_2O_8$), illustrated in Figure 4.10. Compositions of albite and K-feldspar are called alkali feldspars and compositions of albite and anorthite are called plagioclase feldspars [34, pp. 2]. In the experiments feldspar from a pulverised anorthosite (also called

Figure 4.9: Feldspar, 100-150 µm

labradorite [35]) was used, shown in Figure 4.9, which is a part of plagioclase feldspars. It is 40% albite and 60% anorthite, and has the chemical formula $Na_{0.4}Ca_{0.6}Al_{1.6}Si_{2.4}O_8$ $((Ca,Na)(Si,Al)_4O_8)$. It is in the triclinic crystal system and can be colourless, white, grey white, grey, or light green. It has a density of 2.69 SG and a hardness of 7 on mhos scale [36]. A SEM analysis was performed on the feldspar and is illustrated in Figure 4.11, it shows how the grains have 90° angles and can almost have a square form.

Figure 4.10: Feldspar ternary system. [37]

(a)   (b)
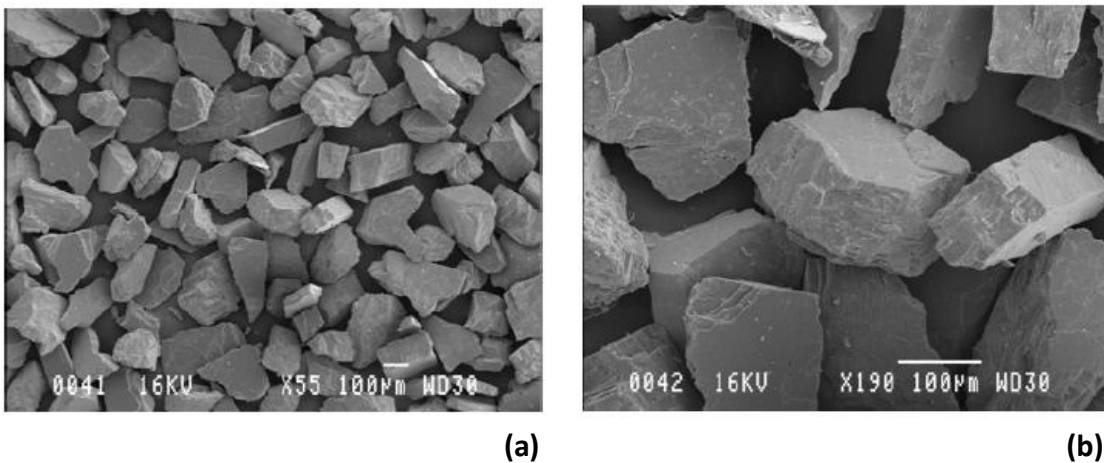
Figure 4.11: SEM images of 125-250μm feldspar, (a) 55x and (b) 100x magnification.

4.1.4.3 Calcium carbonate

Calcium carbonate, $CaCO_3$, is a common mineral found in rocks, for instance in limestone, chalk and marble. It is formed as a result of a sedimentation of the shells of small fossilized animals, and is usually white in colour [38]. There are two types of minerals, Calcite and aragonite, both primarily consists of $CaCO_3$ (often with some impurity), but have different crystal structures [39]. Calcite can be found in numerous colours and shapes, and
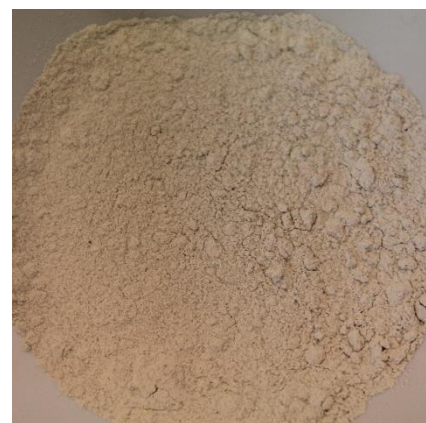
Figure 4.12: CaCO3, 100-150 μm

is in the trigonal and hexagonal crystal system. It has a density of 2.71 SG, a hardness of 3 on mhos scale [40], [41], and a melting point of 1,339°C [42]. Aragonite can be colourless, white, yellowish white or reddish white, or grey, and is in the orthorhombic crystal system. It has a density of 2.93 SG, a hardness of 3.5-4 on mhos scale [39], [43], and a melting point of 825°C [42]. The $CaCO_3$ used in the experiments was a white powder (see Figure 4.12) and a SEM analysis, illustrated in Figure 4.13 (a) and (b).

(a)   **(b)**
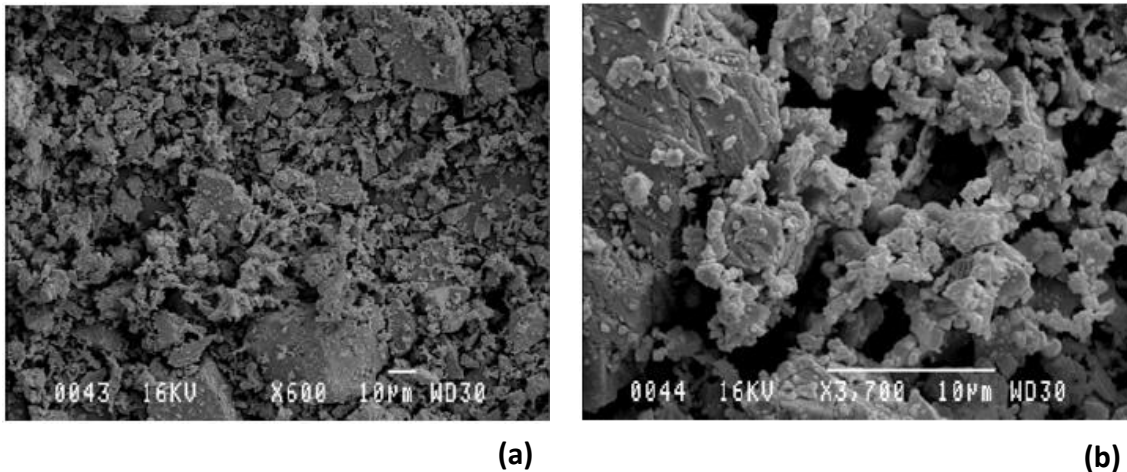
Figure 4.13: SEM images of medium sized $CaCO_3$, (a) 600x and (b) 700x magnification.

4.1.5 Rubber

Two types of rubber were used in the experiments, O-ring and silicone rubber. The rubber was cut down to <2 mm grain sizes and then treated with acid in a similar way to an experimental study performed by X. Colom, F. carrillo and J. Cañavate [25]. The specimen was treated with 95-97% sulphuric acid (H_2SO_4) according to the following steps: (1) immersion in acid for 1 min; (2) taken out of the acid bath and left in air to allow further reaction for 2 min; (3) washing with hot distilled water (~50°C) and ammonium hydroxide (NH_4OH) (15% ammonia) for neutralization; and (4) washing with distilled water at room temperature. Elemental identification and structural analyses were performed using EDS and SEM on both rubber types before and after the acid treatment.

4.1.5.1 O-ring rubber

An O-ring is shown in Figure 4.14, and Figure 4.15 (a) and (b) show the cut O-rings before and after the acid treatment. As can be seen on Figure 4.15 (b) a small amount of white residue from the acid treatment did not wash off. Furthermore, no other differences between these

two could be observed with the naked eye. However, when comparing the SEM images in Figure 4.16 (a) and (b) it showed that the acid treatment generated micro cracks on the rubber's surface. Figure 4.17 (a) shows the elemental composition of an untreated (UT) O-ring and how it consists primarily of carbon (C), with less than 10 wt% oxygen (O). Whereas, Figure 4.17 (b) shows the composition of an acid treated (AT) O-ring and how it has a small amount of acid still on its surface; with additional sulphur (S) and oxygen. This is also illustrated in Table 4.2, where the composition is given in weight percent (wt%). Note that the instrument used to do the EDS analysis cannot detect hydrogen (H) and is therefore not shown, and as mentioned earlier the Pd is not a part of the specimen.

Table 4.2: Elemental analysis (EDS) of O-ring rubber; untreated (UT) and acid treated (AT).

Element	UT (wt%)	AT (wt%)
C	91.85	82.15
O	8.15	9.97
S	-	7.88

Figure 4.14: O-ring before it was cut.

Figure 4.15: Cut O-rings (a) before acid treatment and (b) after acid treatment.

(a)

(b)
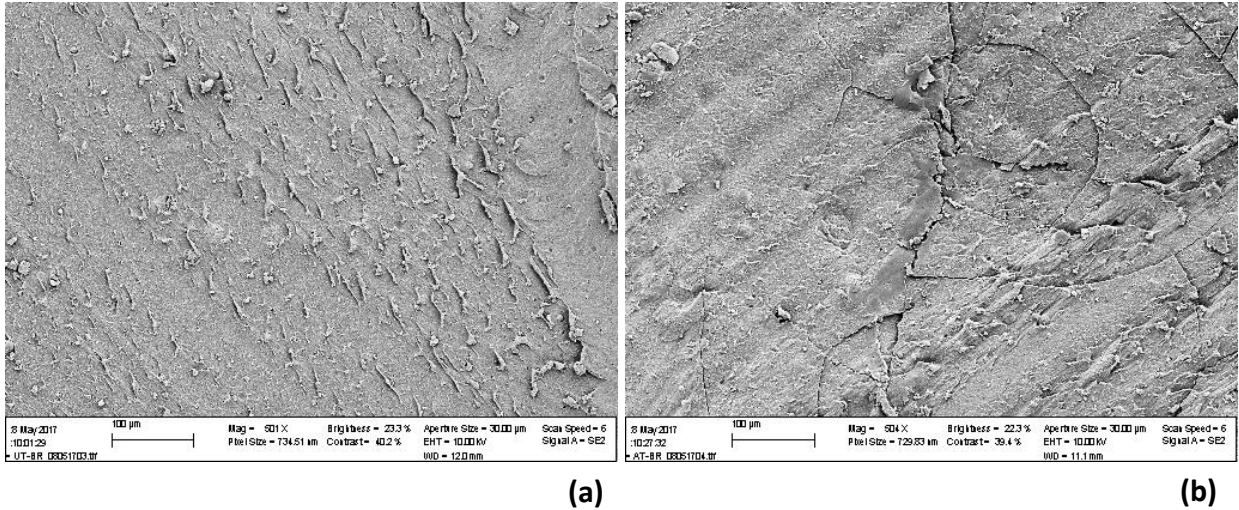
Figure 4.16: SEM images of O-ring rubber (a) before and (b) after acid treatment (500x magnification).

(a)

(b)
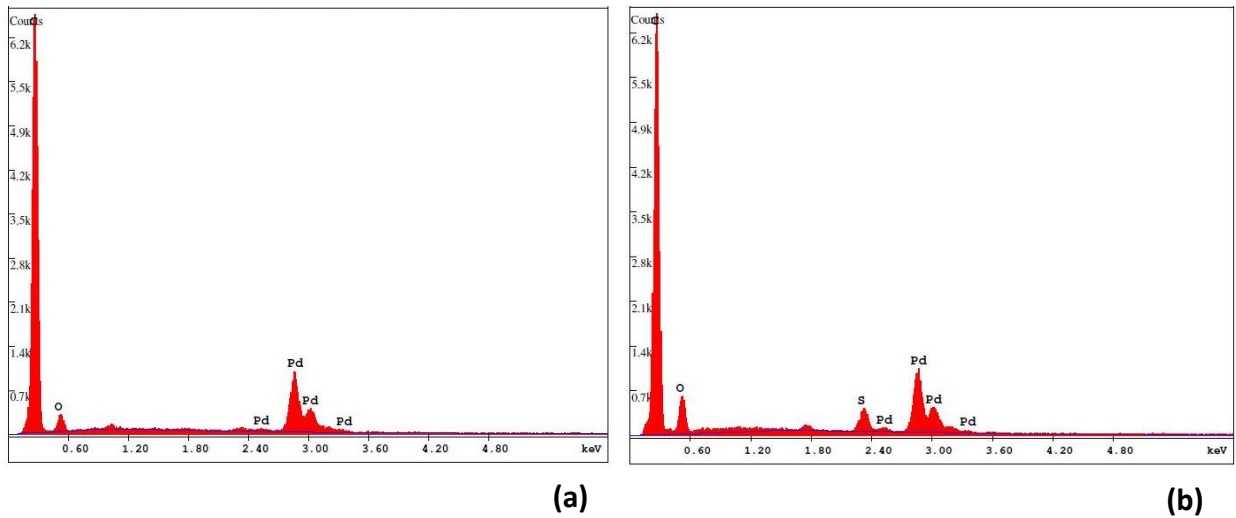
Figure 4.17: EDS of O-ring rubber (a) before and (b) after acid treatment. The peak to the far most left represents carbon.

4.1.5.2 Silicone rubber

Figure 4.18 shows a silicone cup that was cut down into smaller bits. Figure 4.19 shows the cut silicone before and after the acid treatment. As shown on Figure 4.19 (b) a lot of white residue from the treatment was glued to the surface and did not wash off. The SEM images in Figure 4.20 (a) and (b) show how the acid treatment completely changed the surface structure, creating many cracks and making it rougher. Figure 4.21 (a) shows the elemental composition of an UT silicone rubber and that it consists of silicon (Si), carbon, and oxygen. Whereas, Figure 4.21 (b) shows the composition of AT silicone and how some of the acid was

still on its surface; with additional sulphur and oxygen. The composition in wt% is illustrated in Table 4.3.

Table 4.3: Elemental analysis (EDS) of silicone rubber; untreated (UT) and acid treated (AT).

Element	UT (wt%)	AT (wt%)
C	50.51	36.75
O	18.18	23.02
Si	31.31	30.48
S	-	9.75

Figure 4.18: Silicone cup before it was cut.

Figure 4.19: Cut silicone rubber (a) before and (b) after acid treatment.
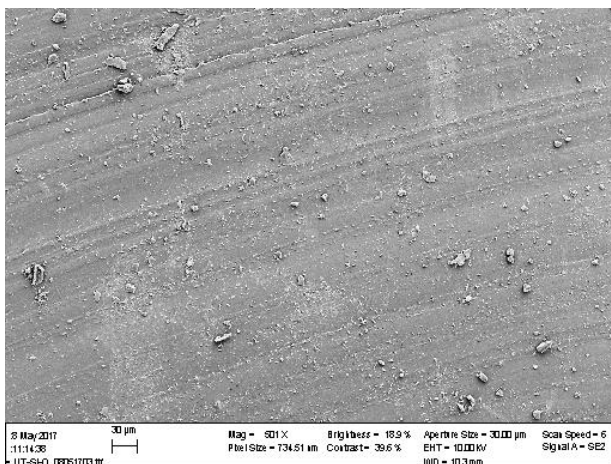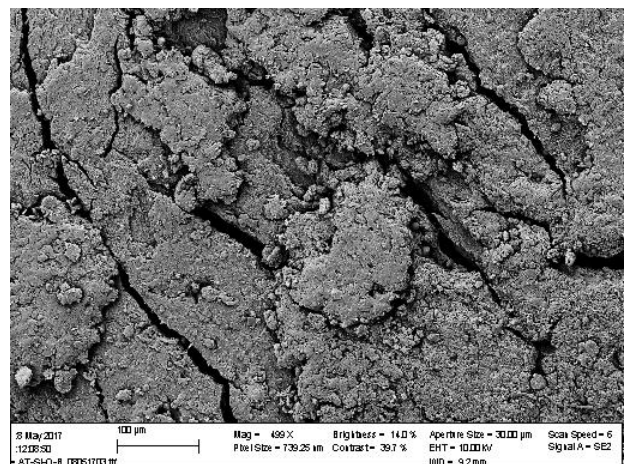
Figure 4.20: SEM images of silicone rubber (a) before and (b) after acid treatment (500x magnification).
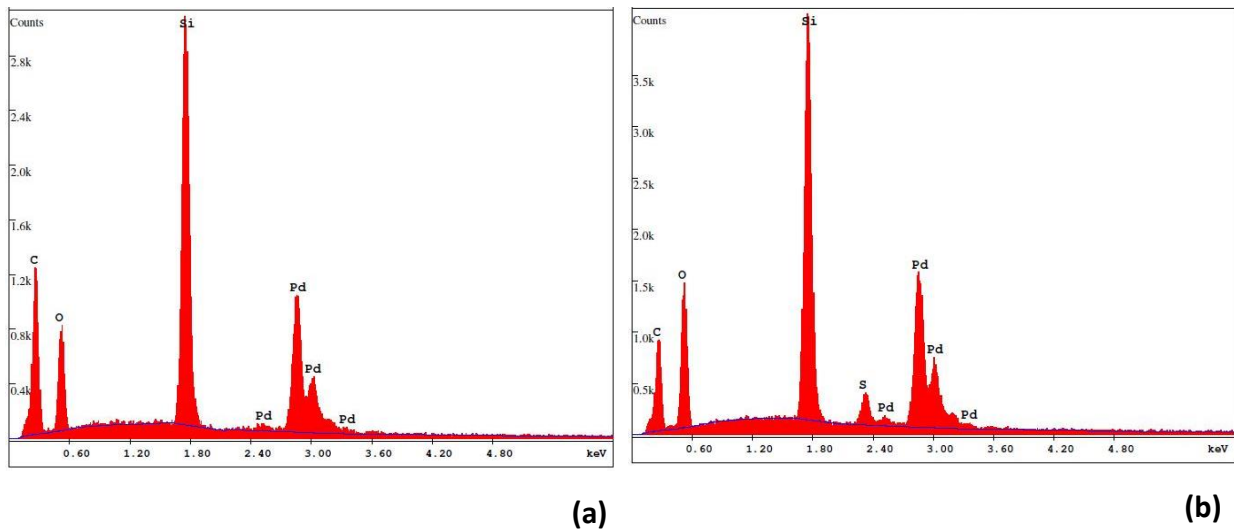
Figure 4.21: EDS of silicone rubber (a) before and (b) after acid treatment.

After the acid treatment of the silicone rubber it was noted that a silicone debris had formed. These particles are shown in Figure 4.22, they were very small and light, and it was decided to test these particles as an additive to the cement. As shown on Figure 4.22, the particles are clumped together, but they were easily taken apart by stirring before mixing it with the cement.
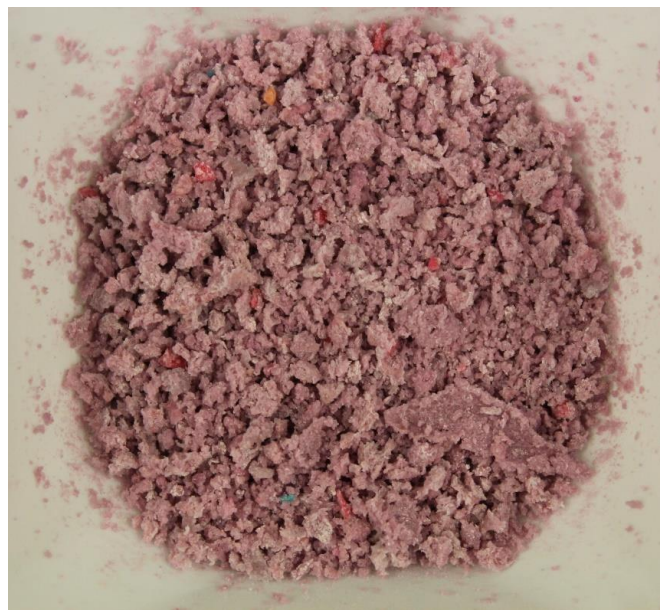
Figure 4.22: Silicone debris formed from the acid treatment of the silicone.

4.1.6 Carbon fibre

Carbon fibre (CF) consists mostly of carbon and is about 5-10 µm in diameter. The atoms are bonded together in tiny crystals grown more or less along its long axis instead of in a sheet [44]. The CF used in the experiments was cut down to <2 mm fibres. The cut fibres did cluster quite much and to be able to get a uniform distribution of the CF, it was first mixed with the water before mixing it with the dry cement. Figure 4.23 shows pictures of (a) CF before it was cut and (b) CF mixed with water.
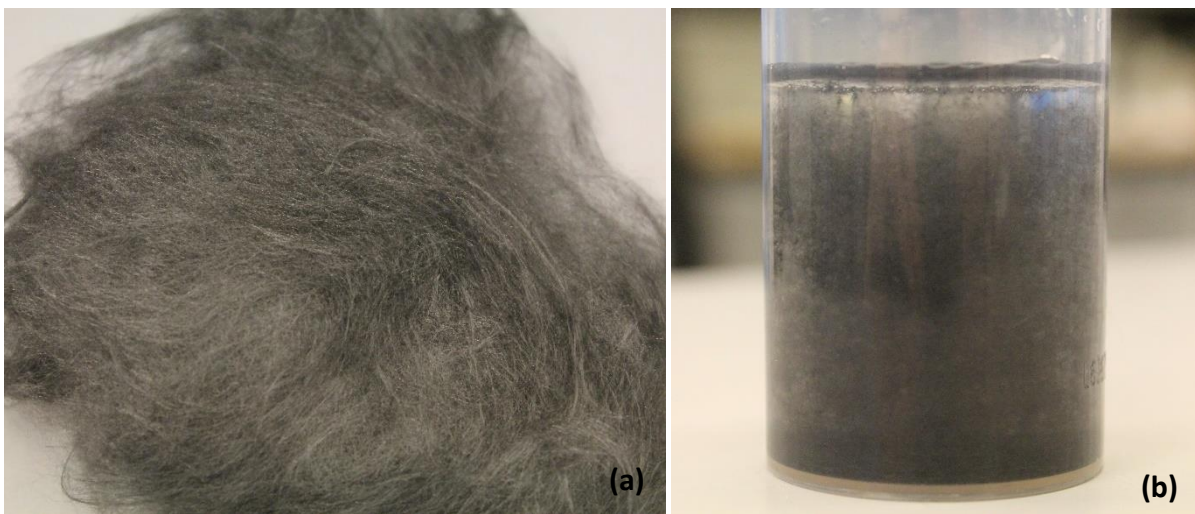
Figure 4.23: (a) Carbon fibre before it was cut. (b) The cut carbon fibre in water solution.

4.2 Experiments

A series of experiments were performed to study various properties of cement and how they are affected by high temperatures and additives. With the objective of having less viscous cement slurry to pump into a wellbore easily, water-to-cement ratio (WCR) of all specimens formulated in this thesis was 0.6. Tap water was used for the cement slurry. For all series of experiments, a specimen was created containing no additives for reference, containing only cement and water. This specimen is referred to as the control of the specific group in the following chapters, and is always a specimen number 1.

4.3 Casing – Cement interface

Three groups of specimens were created to exemplify a P&A scenario, where cement slurry is pumped down into the casing and left inside to establish a seal, plugging the casing. In these experiments a cement mixture was poured inside a casing and left to set. Experiments performed on the casing – cement were to study how various additives effects the sealing capability and the bond strength of cement when exposed to high temperatures. The casing

– cement will be referred to as CC for abbreviation and the different groups will be referred as CC-I, CC-II and CC-III.

4.3.1 Type 1 Casing – Cement bonding (CC-I)

4.3.1.1 Preparation of CC-I

Nine cement slurries were formulated with various additives listed in Table 4.4. The amount of every component added to the cement is listed by weight of cement in percent (% bwoc). CC-I-1 was mixed with no additives and was used as the control. When mixing specimens with carbon fibre (CF) or Nano silica, these additives were first mixed with the water with a mixer until homogeneous solution was obtained and then mixed with the cement powder. On the other hand, when mixing specimens with micro minerals (quartz, $CaCO_3$ or feldspar), these additives were first well mixed with the cement powder by hand, before mixing with the water. The cement powder (plus minerals) was then added to the water (plus CF or nanoparticle) and well mixed by hand until very well dispersed slurry was obtained.

Table 4.4: Composition of Casing – Cement-I

Specimen name	Water (% bwoc)	Cement (% bwoc)	Additive/-s	Amount additives (% bwoc)
CC-I-1	60	100	-	-
CC-I-2	60	100	Carbon fibre	0.10
CC-I-3	60	100	Nano silica	0.25
CC-I-4	60	100	Nano silica	0.50
CC-I-5	60	100	Micro quartz	2.00
CC-I-6	60	100	Micro $CaCO_3$	2.00
CC-I-7	60	100	Micro feldspar	2.00
CC-I-8	60	100	Carbon fibre Nano silica	0.03 0.25
CC-I-9	60	100	Micro quartz Micro $CaCO_3$ Micro feldspar	0.67 0.67 0.67

Table leg casings, described in section 4.1.2 (see Figure 4.2 (a)), were prepared with a plastic cap on bottom to prevent leakage of the cement allowing the cement to set inside the casing.

Cement slurry

Plastic cap

Possible leak path for water during setting of the cement.
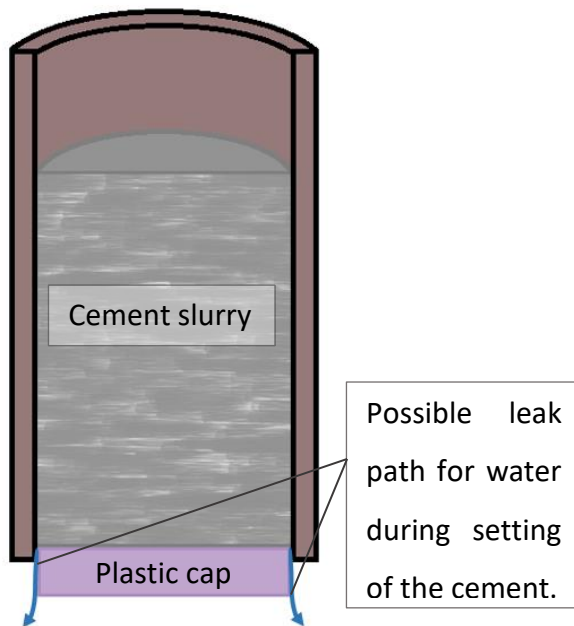
Figure 4.24: Illustration of possible leak of water during setting of cement.

When the cement slurry was well mixed and homogeneous it was poured into a measuring cup, approximately 60 ml, to make sure all specimens had the same amount of cement. The 60 ml of cement slurry was then poured into the casing onto the plastic cap and left to cure for two days. Unfortunately, the plastic cap did not provide very effective seal and did allow some of the water to escape past the cap during the setting of the cement, this is illustrated in Figure 4.24. When the cement was set the plastic cap was removed before testing.

4.3.1.2 Temperature cycling of CC-I

To study the effect of temperature on cement and cement – casing bonding, the specimens have been exposed to temperature in oven. After every temperature cycle the specimens were tested for leakage, this is discussed in more detail below. Figure 4.25 shows the temperature cycling profile; where time zero is when they were mixed. The specimens have been exposed to four cycles of 108°C and one cycle of 200°C; where one cycle begins at room temperature and ends when it reaches back to the same temperature after the exposure to the temperature changes. When the specimens were taken out of the oven the outside of the casings were cooled with running water (approx. 9°C), making sure to only wetting the outside of the casing so the cement would not get wet before testing. This was done to create a worsen scenario with rapid cooling, and to make sure the specimens were cool enough to avoid evaporation of water when testing. Then the specimens were left at room temperature for a few minutes and after a short period the temperature would eventually rise towards the room temperature, this is shown in Figure 4.25 where the temperature goes to 9°C after the high temperatures and then quickly up to 21°C.
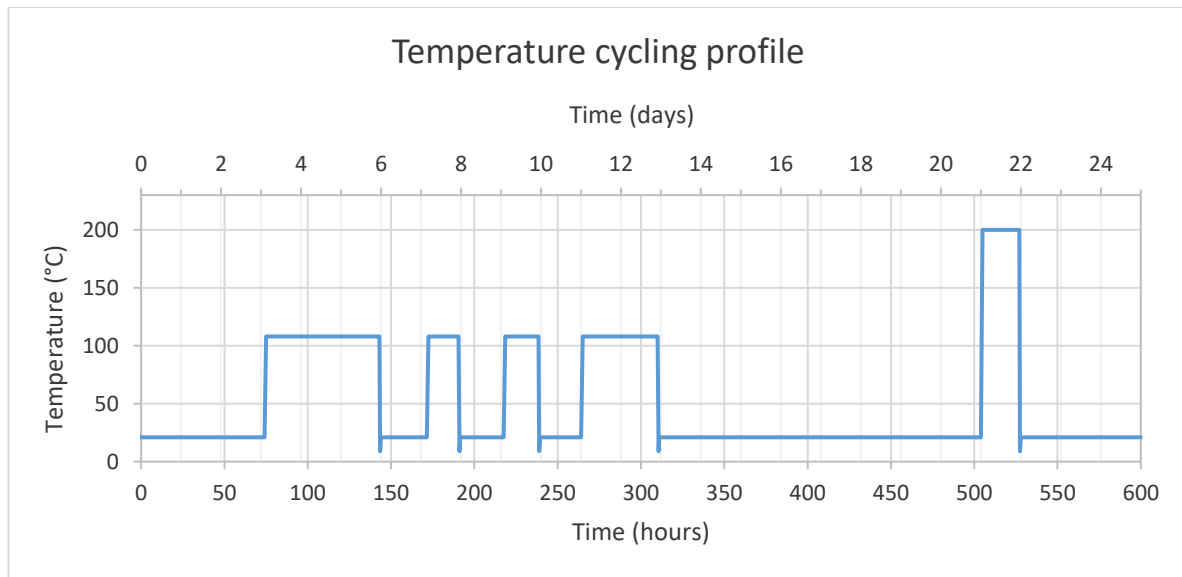
Figure 4.25: Temperature cycling loading profile of CC-I.

4.3.1.3 Leakage of CC-I

To study the sealing capability of the cement a leakage test was designed and executed. Water was poured onto the cement and a cup was placed under the specimen to catch any leakage. Figure 4.26 shows the setup for the leakage test. First, the specimens were tested for leakage before exposing them to high temperature. Two days after mixing, water was poured onto the cement and left at normal conditions for 24 hours. After 24 hours with water on top the leakage was measured (in weight) and the results are illustrated in Figure 4.27. It shows that the control (CC-I-1) did not allow water to migrate through it, and neither did the specimen containing CF (CC-I-2). Comparing CC-I-3 and CC-I-4, a couple of things
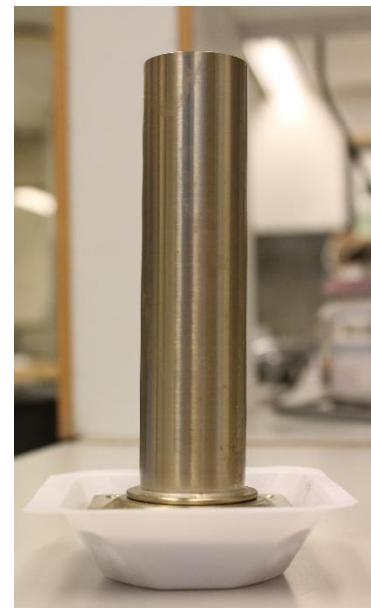
Figure 4.26: Setup for leakage test for CC-I and CC-II.

can be observed: (1) when only Nano silica was added to the cement slurry it allowed leakage, and (2) with increased amount of Nano silica the leakage was increased. However, when both Nano silica and CF was added to the cement (CC-I-8) it did not allow leakage. When comparing the specimens with micro minerals additives, CC-I-5, -6 and -7, it showed that all allowed leakage, but out of these micro quartz had the least leakage. Furthermore, when these minerals were together added to the cement (CC-I-9) it showed no leakage.
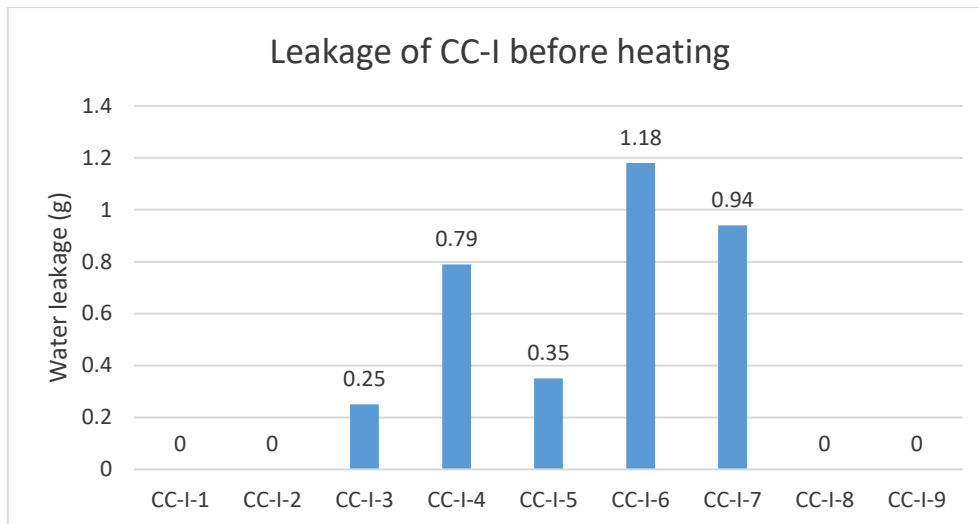
Figure 4.27: Leakage of CC-II after 24 hours with water on top, before exposure to high temperature.

After the first leakage test the specimens were put in an oven at 108°C for three days, as shown on the temperature profile in Figure 4.25, then they were taken out of the oven and cooled down. Thereafter, a leakage test was executed in a same manner as described above, where water was poured onto the cement and left with water on top for 24 hours. This test was performed three more times with various times in the oven; shown on the temperature profile. The amount of water leakage is illustrated in Figure 4.28, where the first temperature cycle is referred as "1st cycle, 108°C" and so forth. As shown in Figure 4.28, some of the specimens had increased leakage which worsened with every cycle. However, some specimens did not follow this trend, which was not expected. This could be because when they were taken out of the oven, water was poured on top of the cement and, although it allowed water to travel through it, it also absorbed a part of it. This could have continued the hydration process, allowing the cement to further develop its strength and its bonding with the casing, i.e. allowing it to regain its strength and bonding after being exposed to the high temperature. Also, the results illustrated in Figure 4.28, show similar results as before exposure to high temperature in terms of which specimen had the least and the most leakage. Where CC-I-1, -2, -8 and -9 had no leakage before exposing them to high temperature, and showed very small amount of leakage after temperature cycling; excluding CC-I-9 after the 4th cycle, it had significantly more leakage than after the previous cycles.
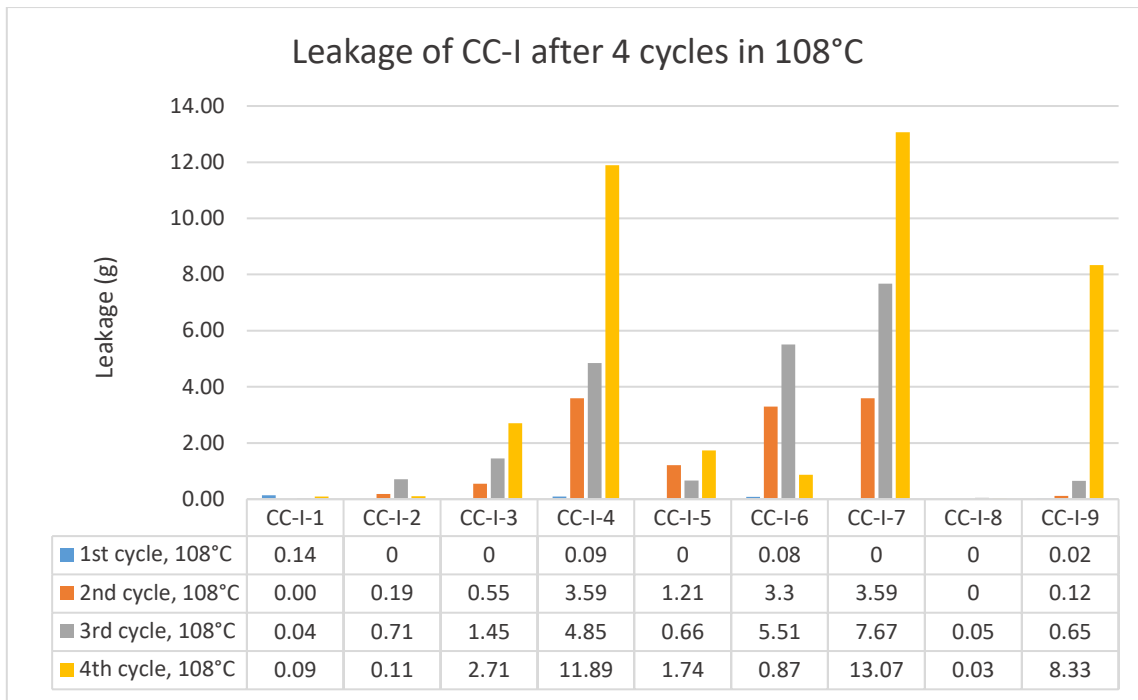
Figure 4.28: Leakage of CC-I after 24 hours with water on top after each temperature cycle, a total of four cycles.

After a few days it was decided to see if the specimens that had near zero leakage could withstand even higher temperature. Eight days after they were taken out of the oven, after the 4th cycle, they were put in an oven at 200°C. After 24 hours in the oven the specimens were taken out and cooled as before. It was observed that some specimens had slightly loose cement inside the casing, where they moved a bit when pressed with small force with a finger. Leakage was tested by pouring water onto the plugs as before. The next day none of the specimens had any water on top, meaning that they did not hold the water that was poured onto them over night. Consequently, the leakage was unsatisfactory as it did not represent the true leakage over a 24 hour period; it is expected that more leakage had been measured if more water had been available.

To see if the specimens had regained their bonding by curing for six days at normal conditions, another leakage test was executed. The results are illustrated in Figure 4.29. Four specimens had no water on top the next day (CC-I-3, -4, -6 and -7) and were therefore expected to have more leakage than measured, these are marked with a red plus sign on the chart. The other specimens had regained the cement – casing bond and improved the leakage, but the only specimen that performed better than the control was CC-I-2. This decreased measured leakage after standing at normal conditions for six days is mostly due to the casing coming

43

back to its original length and the cement has expanded, and the hydration process continued after water was allowed back into the system.
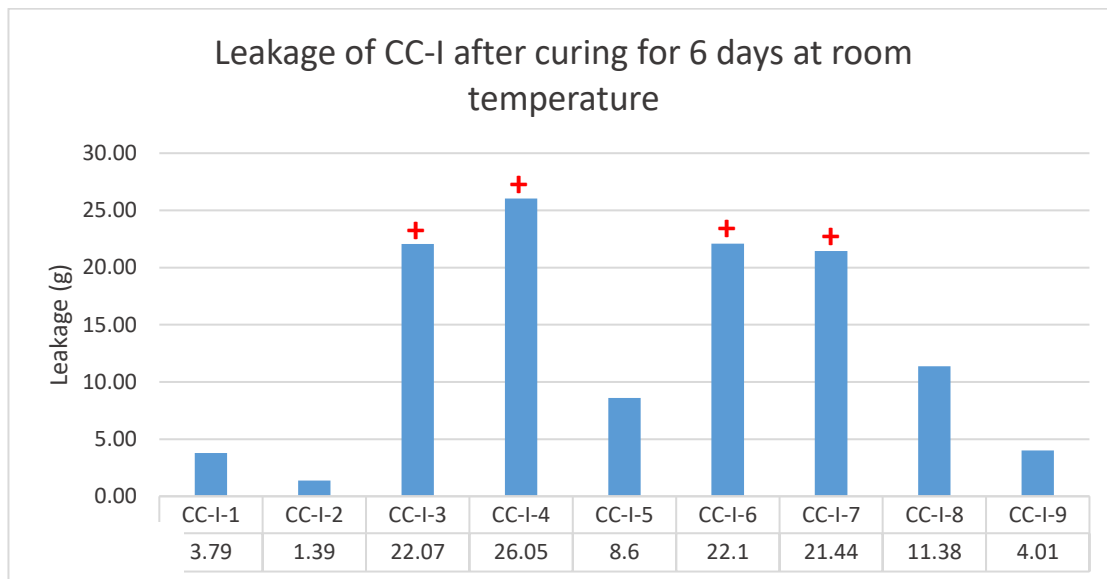
Figure 4.29: Leakage of CC-I after 24 hours with water on top, after curing at normal conditions for six days, after a 200°C temperature cycle.

From this leakage experiment it can be concluded that none of the additives had significantly improved the performance compared with the control. Some even significantly worsened the sealing capability, but combination of additives showed improvement to some extent or were at a similar level as the control.

4.3.1.4 Bond strength of CC-I

After the leakage tests a bond strength test was performed, where the specimens were placed upside down on a table and a steel rod, with the same diameter as the inner diameter of the casing, was placed onto the cement. A force was applied on the steel rod until the cement plug would move, this force needed to move the cement was then used to calculate the bond strength using eq. (3.10). The setup of the bond strength test is shown in Figure 4.30 and the results are illustrated in Figure 4.31. Unfortunately, a failure occurred during testing of CC-I-2 and a correct force was not measured, it is therefore not included on the chart.

As shown on Figure 4.31, CC-I-5 had significantly higher bond strength than any other specimen, almost 150 kPa, or 215% of the control value (115% increase). CC-I-5 also performed well on the leakage test indicating that micro quartz has a really positive affect on both preventing leakage and increasing bond strength with casing when exposing to temperature cycles. Furthermore, all other specimens had either lower bond strength than the control or had an insignificant increase in bond strength, where CC-I-4, and CC-I-6 had very similar bond strength compared with the control, about 70 kPa. When comparing CC-I-3 and CC-I-4 (0.25% and 0.5% bwoc Nano silica, respectively), it seems to be a correlation between the amount of Nano silica in cement and its bond strength with casing. Where 0.25% bwoc decreased the strength

Figure 4.30: Setup of a shear bond strength test.

significantly, but by increasing it to 0.5% its bond strength increased towards the bond strength of the control. Furthermore, micro $CaCO_3$ and micro feldspar (CC-I-6 and CC-I-7, respectively) seem to have very little effect on the bond strength of the conventional cement. When CF and Nano silica were both mixed with the cement (CC-I-8), it showed significant decrease in bond strength compared with the control.

Figure 4.31: The shear bond strength of CC-I after five temperature cycles.

4.3.2 Type 2 Casing – Cement bonding (CC-II)

The second batch of casing – cement was designed, called CC-II. The idea behind the slurry design was based on the leakage test results obtained from the CC-I (section 4.3.1). In the newly design, the mixture of the slurry additives from CC-I and new other additives were formulated. The bond strength had not yet been tested when CC-II were made.

4.3.2.1 Preparation of CC-II

14 cement slurries were mixed with various additives and their composition (in % bwoc) is listed in Table 4.5. The same type of casing as for CC-I was used, i.e. table leg casing. The specimens were mixed in a same way as CC-I, but in addition the silicone and O-ring rubber were first mixed with the dry cement and then with water, while the latex was first mixed with the water before mixing it with the dry cement. When preparing the acid treated silicone the mass loss due to the acid treatment was underestimated and consequently, CC-II-8 had smaller amount of rubber compared to CC-II-7, -9 and -10, this is marked with * in Table 4.5.

Table 4.5: Composition of Casing – Cement-II
*Smaller than planned due to underestimation of mass loss during acid treatment

Specimen name	Water (% bwoc)	Cement (% bwoc)	Additive/-s	Amount additives (% bwoc)
CC-II-1	60	100	-	-
CC-II-2	60	100	Carbon fibre	0.10
			Nano silica	0.10
CC-II-3	60	100	Carbon fibre	0.10
			Nano silica	0.20
CC-II-4	60	100	Carbon fibre	0.10
			Micro quartz	2.00
CC-II-5	60	100	Nano silica	0.15
			Micro quartz	2.00
CC-II-6	60	100	Carbon fibre	0.05
			Nano silica	0.08
			Micro quartz	2.00
CC-II-7	60	100	Silicone rubber UT	1.30
CC-II-8	60	100	Silicone rubber AT	0.57*
CC-II-9	60	100	O-ring rubber UT	1.30
CC-II-10	60	100	O-ring rubber AT	1.30
CC-II-11	60	100	Nano graphene	0.10

CC-II-12	60	100	Latex	4.00
CC-II-13	60	100	Latex	4.00
			Nano silica	0.10
CC-II-14	60	100	Latex	4.00
			Nano graphene	0.10

4.3.2.2 Temperature cycling of CC-II

Instead of 108°C as for CC-I it was decided to increase the temperature to 200°C. The specimens were exposed to four such cycles, where they were left in the oven for one to three days at a time. When taken out of the oven the specimens were cooled down, as for CC-I, to approx. 9°C with running water, without getting water inside the casings. The temperature cycling profile is shown in Figure 4.32.
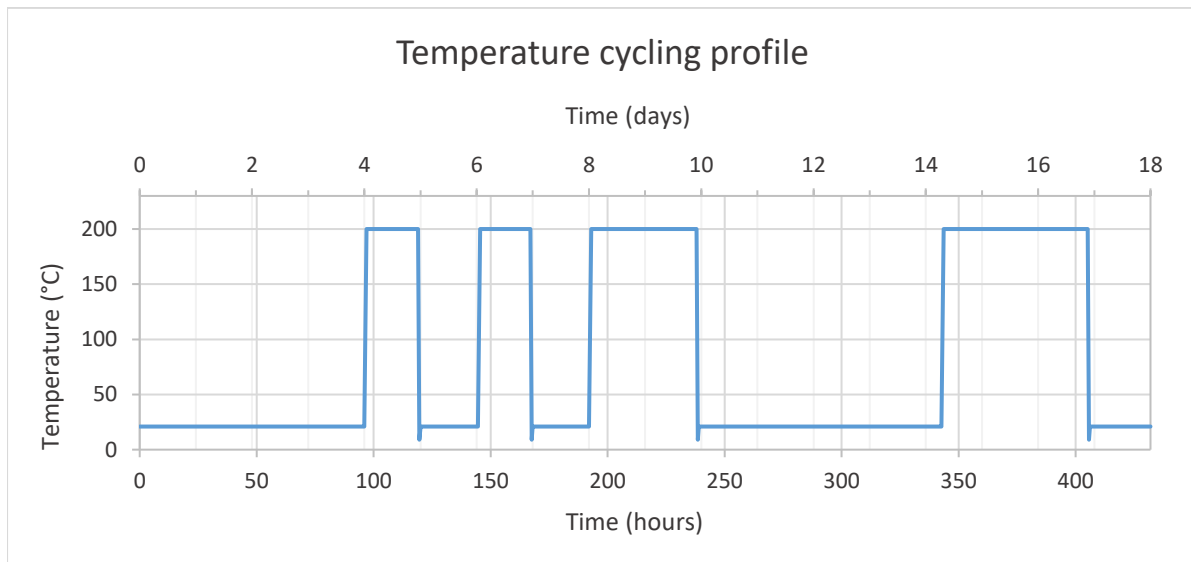
Figure 4.32: Temperature cycling loading profile of CC-II.

4.3.2.3 Leakage of CC-II

The specimens were first tested for leakage before exposure to high temperature. This was done three days after the mixing of the cement slurries. Water was left on top of the cement, and after 24 hours no specimen had any leakage.

After the first leakage test the specimens were put in an oven at 200°C, and after one day they were taken out and cooled before testing. It was observed that many specimens had a loose cement inside the casing. This is most likely due to the expansion of the casing and the

shrinkage of the cement when exposed to high temperature; the shrinkage of cement is discussed in section 4.4.5 . The leakage was tested as before, where water was poured onto the cement and left on it for 24 hours. Initially the cement absorbed a fair bit of the water so water was added on top of the cement as needed, and the leakage was measured each time. Then they were left overnight and the leakage was measured after 24 hours. Unfortunately, many specimens had no water left on top and where therefore assumed to have more leakage then measured. These were concluded to have unsatisfactory resistance against the high temperature and/or shrank too much and completely lost their bonding with casing. The specimens that held water after the first cycle were CC-II-1, -3, -4, -5, -7 and -8. The leakage of these after 24 hours with water on top after three temperature cycles are illustrated in Figure 4.33. The specimens that allowed water to migrate through them too quickly, i.e. they did not hold any of the top water overnight, are marked with a red plus sign, indicating that these were expected to have more leakage. As shown on Figure 4.33, after the 1st cycle the control was one of the specimens that did not allow water to migrate too fast through it, but did still allow a rather large amount of leakage. Also, there were three specimens that performed better than the control after the 1st cycle, these were CC-II-5, -7, and -8, mixture of Nano silica and quartz, silicone UT, and silicone AT, respectively. After the 2nd cycle, CC-II-1, -4 and -5 were too damaged to hold any water overnight. Furthermore, only two specimens that were able to resist three temperature cycles of 200°C were CC-II-7 and CC-II-8. This shows that CF, quartz and silicone can increase the endurance of conventional cement in high temperature, in terms of leakage.

Leakage of CC-II after 3 cycles in 200°C

	CC-II-1	CC-II-3	CC-II-4	CC-II-5	CC-II-7	CC-II-8
■ 1st cycle	18.29	27.42	22.43	12.89	15.5	2.3
■ 2nd cycle	59.49	30.44	31.95	39.73	16.6	10.86
■ 3rd cycle	61.51	36.36	29.8	35.73	25.77	24.25
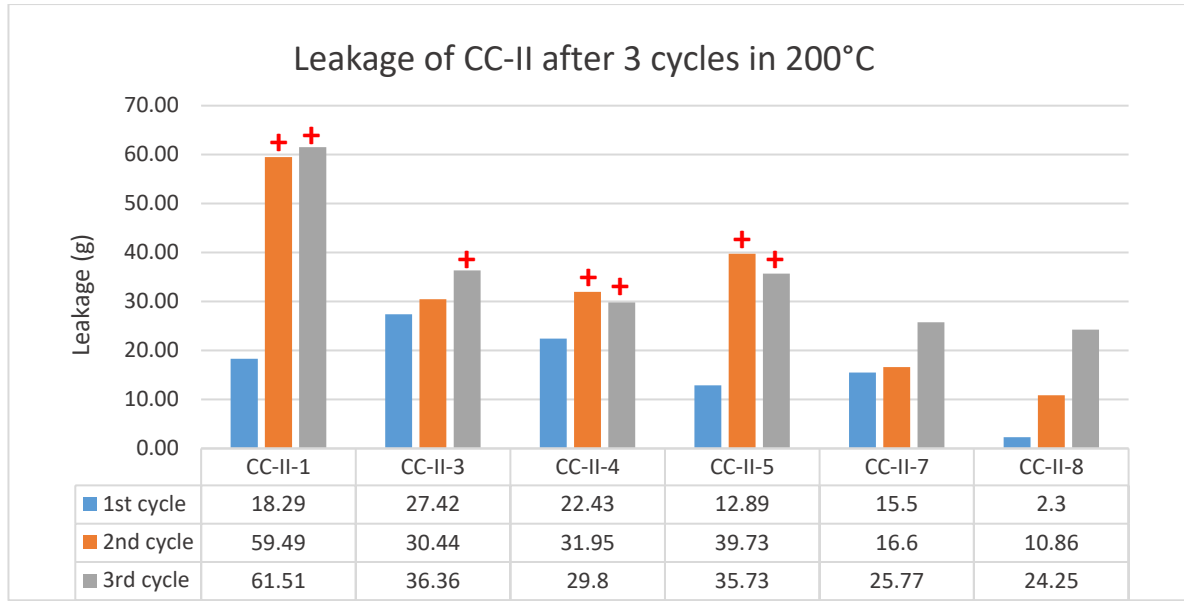
Figure 4.33: Leakage of CC-II after 24 hours with water on top after each temperature cycle, a total of three cycles.

It must be noted that the cement that was loose inside the casing after heating had regained its bond after water was allowed back into the system, and were no longer loose. After standing in room temperature for four days, the specimens were tested for leakage to see if they had healed themselves. Water was poured onto the cement and water leakage was measured after 30 min, 160 min and 6 hrs with water on top, this is illustrated in Figure 4.34. It shows that after six hours many specimens had little or no leakage, and had therefore regained their bonding with casing, especially CC-II-7 ,-8, -9 and -10.

Leakage of CC-II after curing for 4 days at room temperature

	CC-II-1	CC-II-2	CC-II-3	CC-II-4	CC-II-5	CC-II-6	CC-II-7	CC-II-8	CC-II-9	CC-II-10	CC-II-11	CC-II-12	CC-II-13	CC-II-14
■ 30 min	9.40	13.15	1.03	2.39	0.48	0.77	0.15	0.00	0.00	0.00	0.53	0.56	1.81	0.00
■ 160 min	29.83	32.70	6.76	16.34	1.59	5.37	0.32	0.00	0.00	0.00	1.75	2.17	5.81	1.17
■ 360 min	50.11	51.71	18.17	34.43	3.37	13.43	0.40	0.15	0.68	0.49	3.11	4.63	8.32	2.18

Figure 4.34: Leakage of CC-II measured at different times with water on top of the cement; after four days of curing after the 3rd cycle.

To see if any specimen could resist the high temperature after the cement had regained its bonding with casing, they were put back into the oven at 200°C, the 4th cycle. However, after the 4th cycle no specimen held any water overnight and were therefore concluded to be too damaged.

4.3.2.4 Bond strength of CC-II

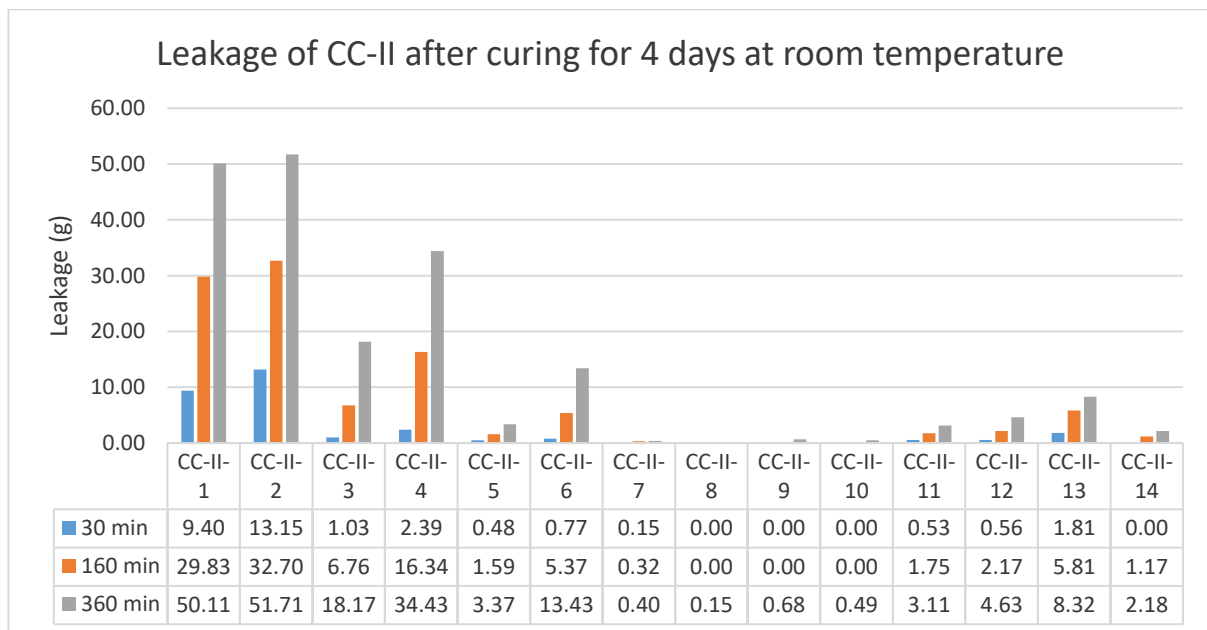A bond strength test was executed on CC-II after the leakage tests, in a same way as for CC-I, and the results are illustrated in Figure 4.35. Firstly, it shows that CC-II-9 and CC-II-10 were off the scale with a bond strength greater than 700 kPa. This is because the force needed to push out the cement was greater than the maximum force measureable by the instrument and consequently the test had to be stopped before the cement moved. However, even though the true bond strength was not measureable, this suggest that O-ring rubber improves the self-healing ability of the cement by a large factor when left at normal conditions with water in the system. Secondly, when comparing CC-II-12, -13 and -14, which all contained latex, one can see that both CC-II-12 and CC-II-14 had a significantly higher bond strength compared with the control, while CC-II-13 had zero bond strength. From this it can be assumed that latex has a good bond strength effect on the cement when alone or when mixed with Nano graphene, while latex mixed with Nano silica has a damaging effect. Furthermore, CC-II-2 also showed a higher bond strength than the control, meaning that mixture of CF and Nano silica can improve the bond strength of conventional cement by a small factor. Moreover, many specimens had a zero bond strength, these were too loose to be measured as they could easily be move inside the casing by gravity alone.
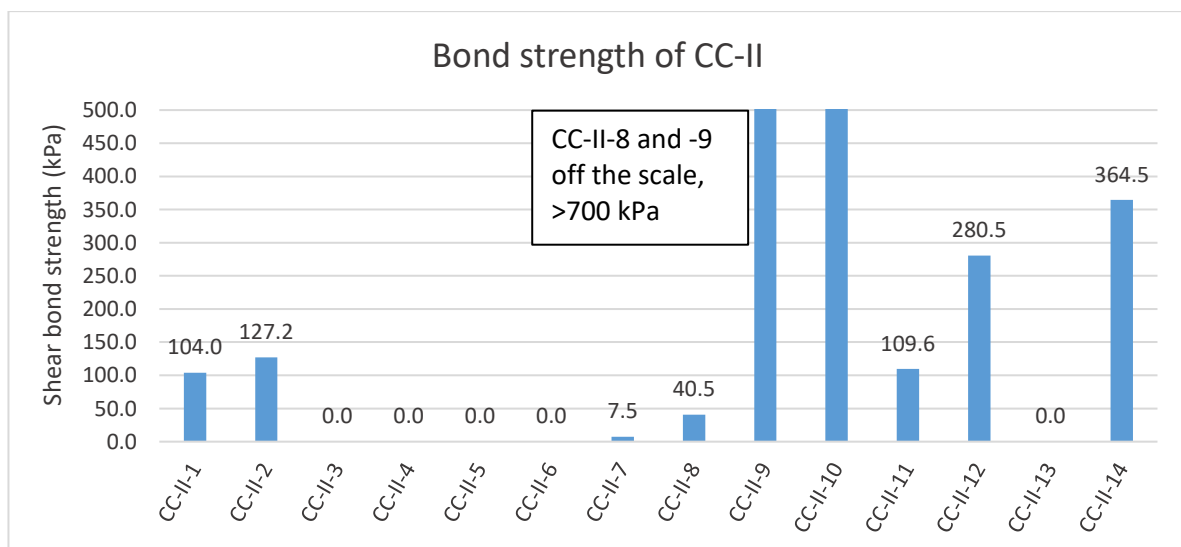

Figure 4.35: The bond strength of CC-II after four temperature cycles.

4.3.3 Type 3 Casing – Cement bonding (CC-III)

The third batch of casing – cement was designed, called CC-III. The idea behind the slurry design was based on the leakage test results obtained from the CC-I and CC-II (section 4.3.1 and 4.3.2). To test different portions and mixtures of the additives. Also, to further study if the acid treated silicone performed little better than the untreated silicone in CC-II because it had less amount of silicone or because of the fact it was acid treated.

4.3.3.1 Preparation of CC-III

Nine specimens were mixed and their composition is illustrated in Table 4.6. More silicone was prepared with acid treatment and a steel pipe casing, described in section 4.1.2 (see Figure 4.2 (b)), was prepared to represent more realistic casing. The specimens were mixed in the same way as before and poured into the casing onto a cap on its bottom; the cap was to keep the cement slurry in place while setting. Two days after mixing the cap was removed from the bottom before testing.

Table 4.6: Composition of casing – cement-III.

Specimen name	Water (% bwoc)	Cement (% bwoc)	Additive/-s	Amount additives (% bwoc)
CC-III-1	60	100	-	-
CC-III-2	60	100	Silicone rubber UT	0.80
CC-III-3	60	100	Silicone rubber AT	0.80
CC-III-4	60	100	Silicone rubber AT	1.10
CC-III-5	60	100	Silicone debris AT	0.80
CC-III-6	60	100	O-ring rubber AT	0.80
CC-III-7	60	100	Silicone rubber AT	0.40
			O-ring rubber AT	0.40
CC-III-8	60	100	Silicone rubber AT	0.80
			Carbon fibre	0.10
			Nano silica	0.15
			Micro quartz	0.70
			Micro $CaCO_3$	0.70
			Micro feldspar	0.70
CC-III-9	60	100	Silicone rubber AT	1.10
			Carbon fibre	0.10
			Nano silica	0.15
			Micro quartz	1.00
			Micro $CaCO_3$	0.50
			Micro feldspar	0.50

4.3.3.2 Temperature cycling of CC-III

The specimens were exposed to four temperature cycles at 200°C. When taken out of the oven the specimens were cooled down, as for earlier tests, to approx. 9°C. The temperature cycling profile is shown in Figure 4.36.
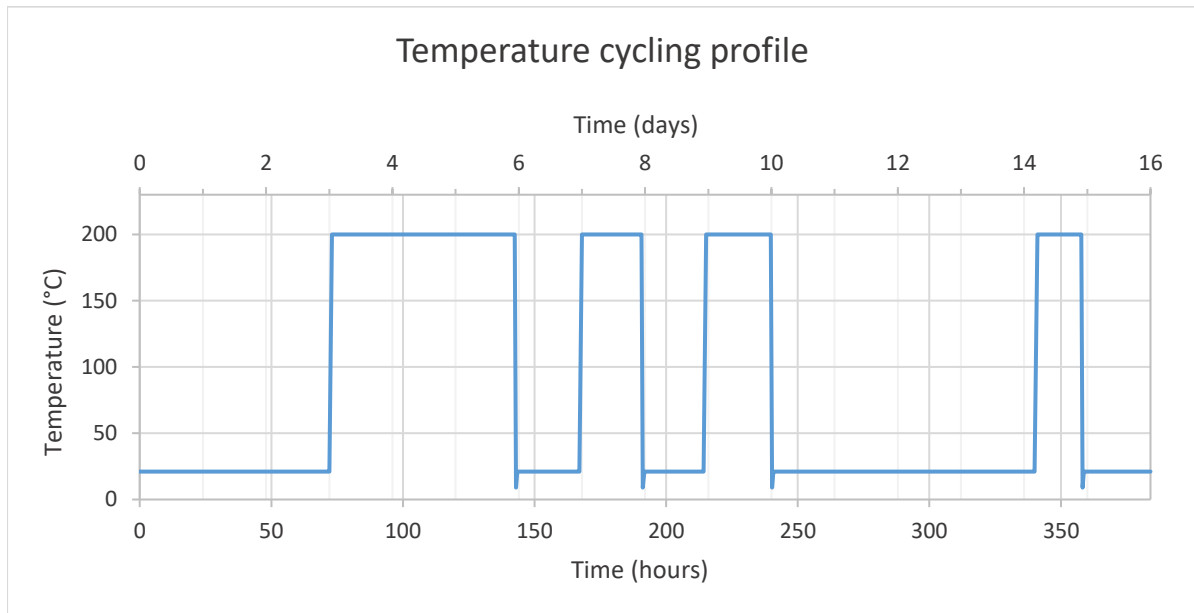

Figure 4.36: Temperature cycling loading profile of CC-III

4.3.3.3 Leakage of CC-III

First, the specimens were tested for leakage two days after mixing by leaving water on top of the cement over a 24 hours period. The setup for the leakage test is shown in Figure 4.37. No water leakage was observed for any of the specimens. Thereafter, they were put into an oven at 200°C and then tested for leakage. The leakage after 24 hours with water on top of the cement is shown in Figure 4.38 for the first three cycles. It shows that after the 1st cycle, many specimens did not have much leakage after 24 hours. The specimens with less leakage than the control after the 1st cycle were CC-III-2, -3, and -9. After the 2nd cycle most of the specimens had dramatically more leakage compared with the 1st cycle, especially CC-III-6 which had the most leakage after the 2nd cycle. Two specimens, CC-III-4 and CC-III-9, did not worsen so much after the 2nd cycle, but rather had similar amount of leakage as

Figure 4.37: Setup for leakage test of CC-III.

52

after the 1st cycle. Additionally, these had the least amount of leakage after the 2nd cycle. After the 3rd cycle only two specimens held water overnight, and those how did not are marked with a red plus sign on Figure 4.38, indicating that these were expected to have more leakage than measured. The two specimens that held water overnight were CC-III-2 and CC-III-4, both containing silicone rubber, UT and AT respectively.
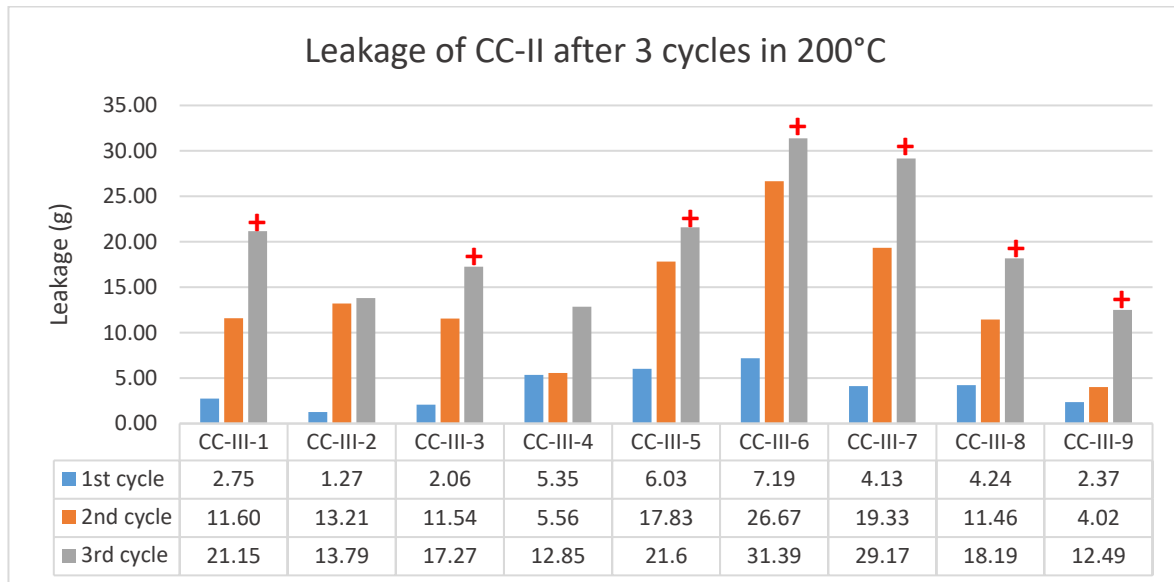
Leakage of CC-II after 3 cycles in 200°C

	CC-III-1	CC-III-2	CC-III-3	CC-III-4	CC-III-5	CC-III-6	CC-III-7	CC-III-8	CC-III-9
■ 1st cycle	2.75	1.27	2.06	5.35	6.03	7.19	4.13	4.24	2.37
■ 2nd cycle	11.60	13.21	11.54	5.56	17.83	26.67	19.33	11.46	4.02
■ 3rd cycle	21.15	13.79	17.27	12.85	21.6	31.39	29.17	18.19	12.49

Figure 4.38: Leakage of CC-III after 24 hours with water on top after a total of three temperature cycles.

The leakage was also measured at different time periods with water on top. Figure 4.39 illustrates the leakage development with time after the 3rd cycle measured after 15, 60, 140 and 170 min. It shows how that in the beginning the leakage was rapid for the specimens with the most leakage, then had a decreasing slope after longer period of time. However, for the specimens with little leakage in the beginning had relatively steady slope of leakage over the whole period of 170 min.
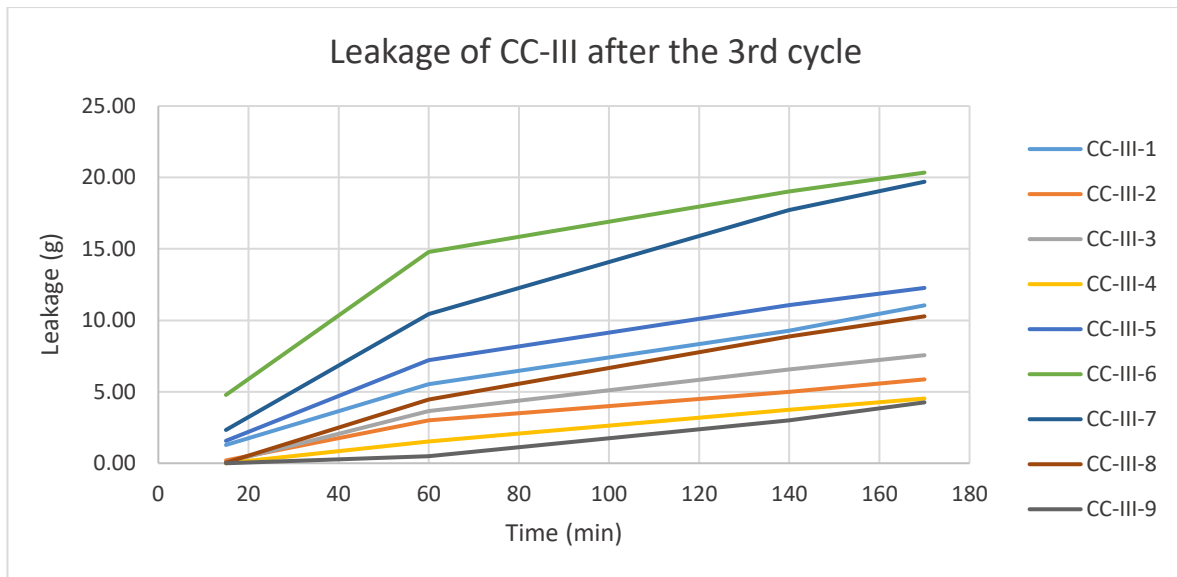
Figure 4.39: Leakage of CC-III after the 3rd cycle of the first 170 minutes with water on top of the cement.

To see if the cement plugs had regained their bond after the 3rd cycle a leakage test was performed tree days after they were taken out of the oven. The leakage after 24 hours with water on top is illustrated in Figure 4.40. This showed that all specimens had improved the sealing capability and were performing similarly or even better than after the 2nd cycle. The biggest surprise here was how small amount of leakage CC-III-6 had, as it had the most leakage after all previous temperature cycles, but was now with the least amount of leakage. This can indicate that the O-ring rubber has good self-healing ability. Other specimens with significantly less leakage than the control were CC-III-2, -3, and -4, all containing silicone as the only additive.
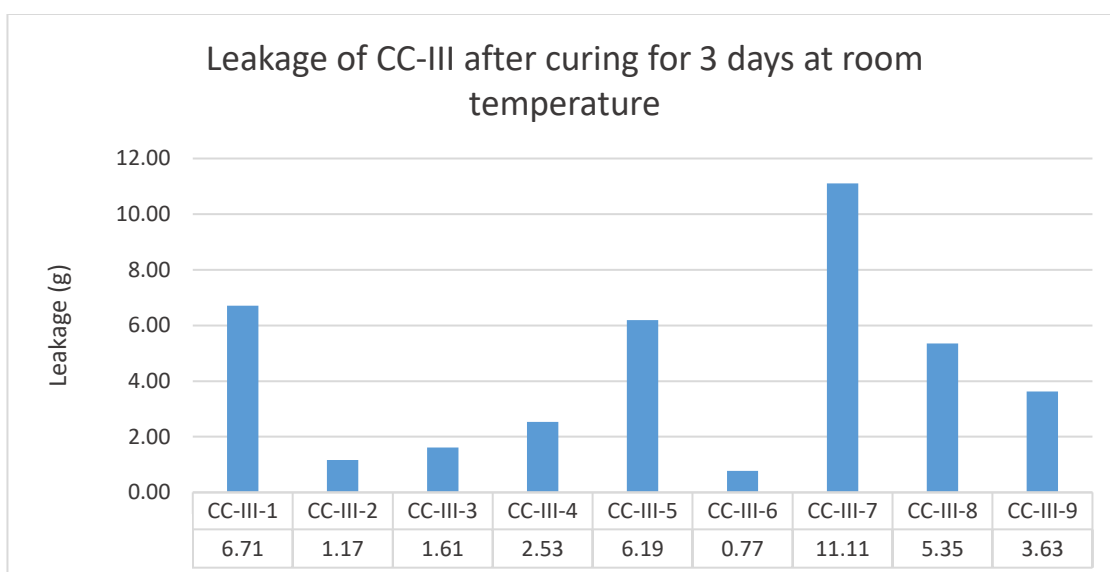

Figure 4.40: Leakage of CC-III after 24 hours with water on top of the cement, after curing for 3 days after the 3rd cycle.

54

After this the specimens were put back into an oven at 200°C, and the leakage was tested as before. The leakage was measured at different time periods and water added when needed, then water was left on top overnight. Only one specimen held water overnight, namely CC-III-4, but it had 10.8 g leakage after 24 hours. The leakage development over the first 270 minutes is illustrated in Figure 4.41. It shows that the control had the most leakage after 270 minutes and that CC-III-6 had again lost its ability to resist flow of water through it or past it.
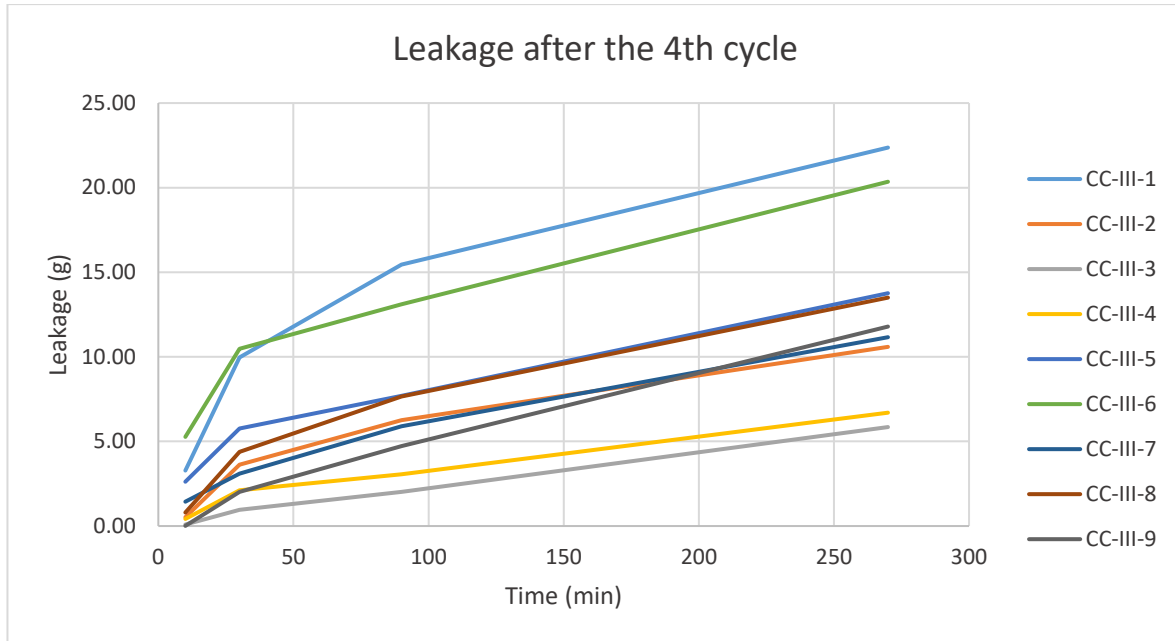

Figure 4.41: Leakage of CC-III the first 270 minutes with water on top after the 4th cycle.

4.3.3.4 Bond strength of CC-III

After the leakage test the bond strength was measured and calculated. The results are illustrated in Figure 4.42. It shows that the control had very little bond strength, and all other specimens had much greater bond strength, except CC-III-6 (containing O-ring rubber AT) which had zero bond strength. The specimens with the greatest bond strength were CC-III-4 and CC-III-7, with about 68 kPa. This indicates that acid treated silicone both alone and in combination with acid treated O-ring rubber can improve the bond strength of cement significantly, when exposed to temperature cycling. Furthermore, CC-III-2, -3, -8 and -9 had a bond strength between 40 kPa and 50 kPa, which is significantly higher than of the control. When comparing these four specimens with one another, all containing silicone but the two latter containing other additives in addition, it appears to improve the bond strength insignificantly by adding these additives along with the silicone to the cement slurry.
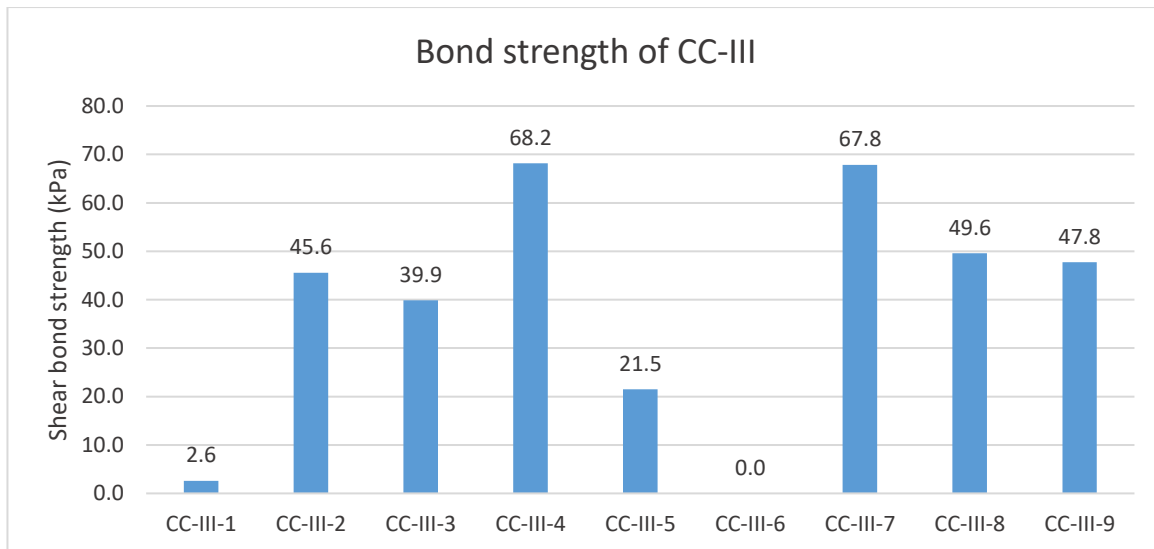
Figure 4.42: The bond strength of CC-III after four temperature cycle.

4.4 Cement Core Plug (CCP)

To characterize the physical and elastic properties of the cement slurry composition designed in section 4.3.3 (Table 4.6), a total of nine cylindrical cement core plugs (CCP) have been prepared. The specimens were prepared in a same way as the CC-III. Each specimen with the same components will have the same numbering, for instance CCP-2 will have the same composition as CC-III-2. The mixed cement slurry was poured in a plastic cup, 67x33 mm (length x diameter) dimension, and left for six days. They were removed from the plastic cup and it was observed that a large amount of the rubber had migrated to the top of the plug. This created an uneven surface and was therefore sanded to even out the surface. This was done to all the specimens to create a smooth top and bottom, and to make all specimens approx. the same size. Figure 4.43 shows the top of CCP-4 before and after sanding. After sanding, the specimens were immersed in water at room temperature and were left in water bath for three days to study the absorption and sonic development over time in water. Thereafter, they were put into an oven at 200°C to study its effect on their properties. Figure 4.44 illustrates the temperature profile of the specimens, also showing the time in water bath with a thick blue line, just before they were put into an oven.
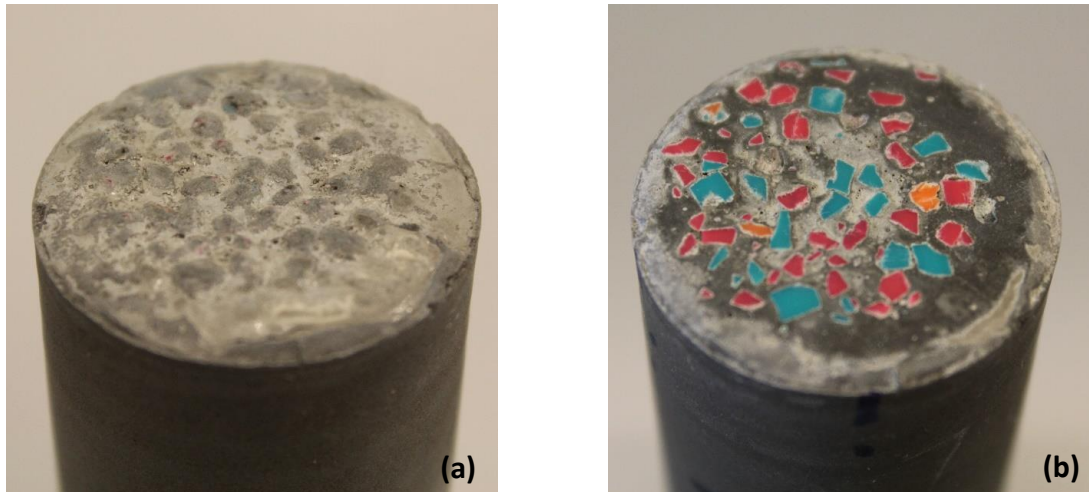
Figure 4.43: (a) CCP-4 after removal from the mould; (b) CCP-4 after sanding the top surface.
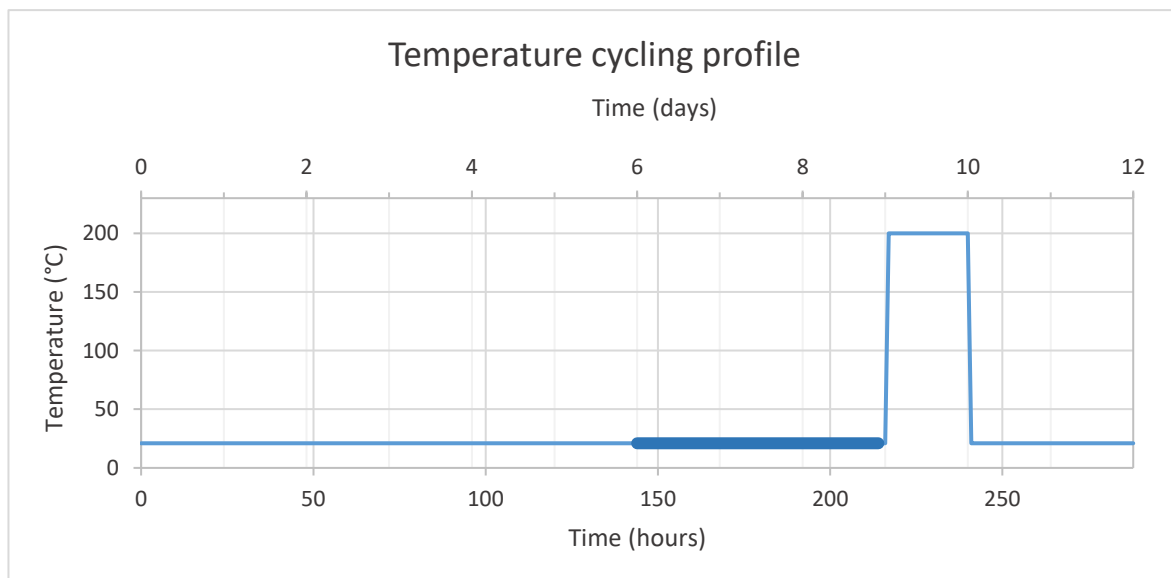

Figure 4.44: Temperature cycling loading profile of CCP, also showing the time in water bath with a thick blue line.

4.4.1 Mass change of CCP

After three days in water the fluid absorption had stabilised, and Figure 4.45 illustrates the mass change in percent, calculated using eq. (3.1). It shows that after just one day in water most specimens had increased in mass by about 9%. However, two specimens, CCP-5 and CCP-7, had much less water absorption than the rest with about 6.5% increase in mass after 3 days in water. These contained silicone debris alone and mixture of acid treated silicone and O-ring rubber, respectively. The specimen with the third least absorption was CCP-9, with

8.72% increase in mass after 3 days in water. The rest of the specimens had a similar absorption, a change in mass between 9.5% and 10.5% after 3 days.
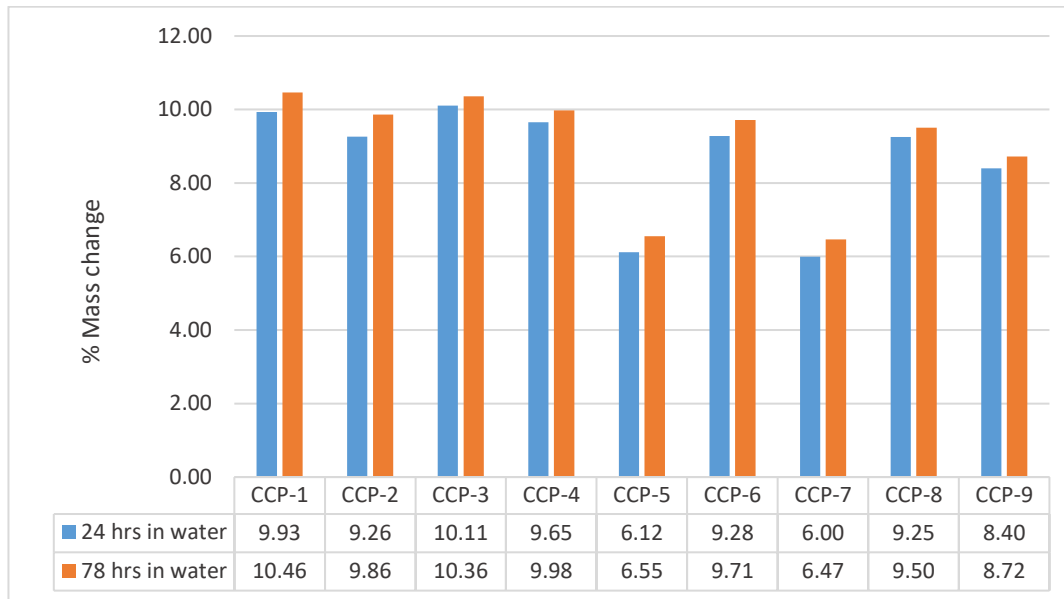

	CCP-1	CCP-2	CCP-3	CCP-4	CCP-5	CCP-6	CCP-7	CCP-8	CCP-9
24 hrs in water	9.93	9.26	10.11	9.65	6.12	9.28	6.00	9.25	8.40
78 hrs in water	10.46	9.86	10.36	9.98	6.55	9.71	6.47	9.50	8.72

Figure 4.45: Percent mass change of the cement core plugs after 24 and 78 hours in water.

After three days in water the specimens where put into an oven at 200°C to see how much mass would be lost by heating and allowing pore water to evaporate. The change in mass after 24 hours in 200°C is illustrated in Figure 4.46, it shows the mass reduction from the original mass in percent. All specimens had similar mass loss, which was more than 22% of their original mass. The specimen with the least mass loss was CCP-3 and the one with the most mass loss was CCP-5, with -22.20% and -24.40% mass change, respectively. This value signifies the amount of pore water and other moisture in the cement paste that evaporates in the oven, drying the specimen. From this one can conclude that cement is highly subjected to high heat and low pressure where it will lose a large amount of its pore water, and none of the additives used had any significant improvement in terms of maintaining its mass.
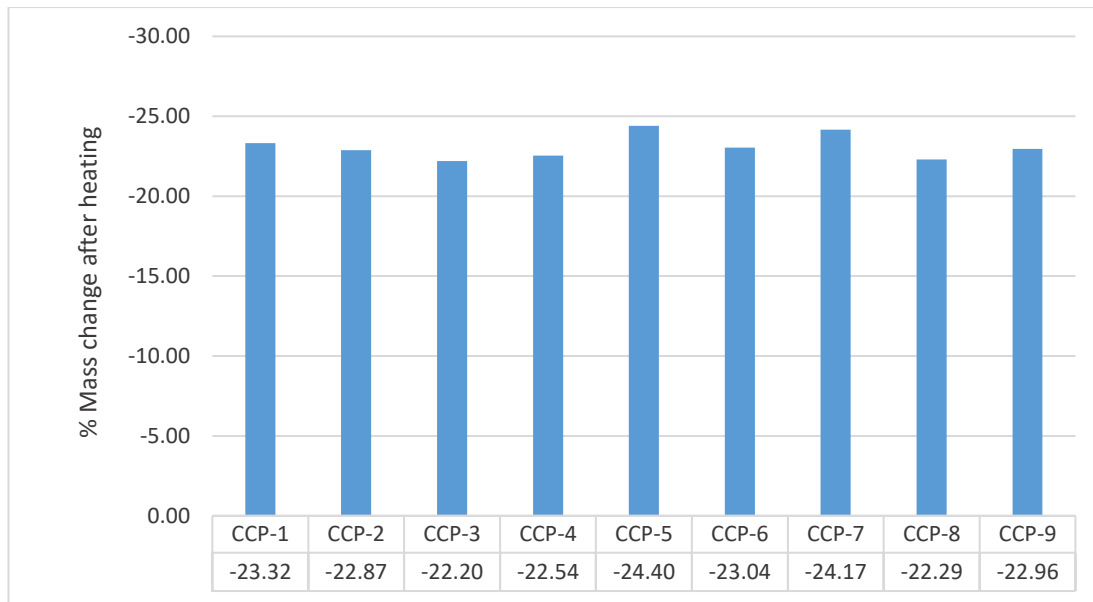
Figure 4.46: Percent mass change of the cement core plugs after 24 hours in 200°C.

4.4.2 Resistivity of CCP

There is a correlation between how high of a resistivity cement has and how well it can resist a flow through its pores, i.e. the higher the resistivity the higher the permeability will be. The resistivity of the specimens was measured after three days in water and calculated using eq. (3.9). The results are illustrated in Figure 4.47, which shows that the two specimens with the highest resistivity were CCP-2 and CCP-7, 9.27 kΩm and 9.17 kΩm, respectively. This means that untreated silicone, and a mixture of acid treated silicone and O-ring rubber mixed with the cement can make the cement more impermeable. However, the increased resistivity of CCP-2 and CCP-7 compared with the control was insignificant. Furthermore, all other specimens had a lower resistivity than the control, and the lowest resistivity was measured in CCP-6.
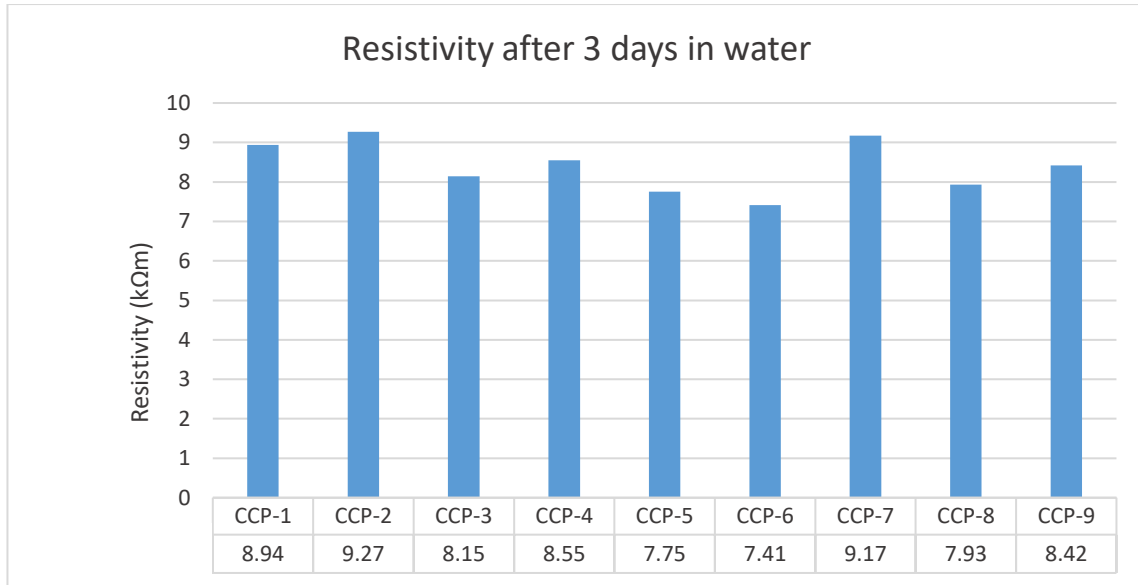
Figure 4.47: Resistivity of the cement core plugs after 3 days in water.

4.4.3 P-wave velocity of CCP

The P-wave velocity of the plugs from the sonic measurements is illustrated in Figure 4.48. These were used to calculate the dynamic elastic modulus in section 4.4.4 .
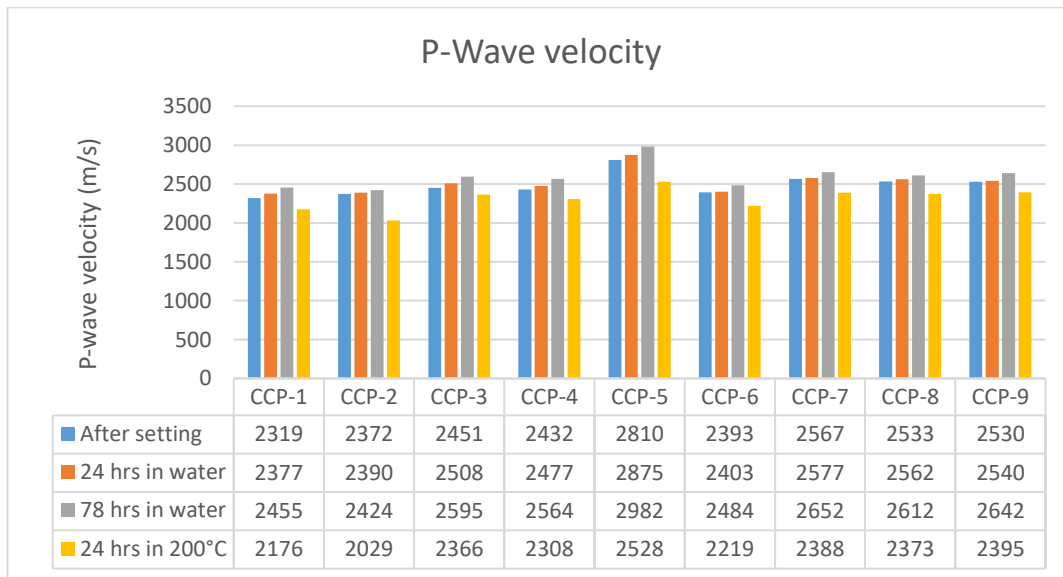

Figure 4.48: Primary wave velocity of CCP.

4.4.4 Dynamic elastic modulus of CCP

The dynamic elastic modulus (E*) from the sonic measurements is an indirect method to measure the elasticity of cement, the higher E* the less is cement deformed by pressure, making it more brittle. The E* was calculated using eq. (3.5), where the P-wave velocity was

60

obtained from the sonic measurements. The sonic was first measured six days after mixing, then for three days in water, and lastly after one day in 200°C. Figure 4.49 illustrates the calculated E* for the specimens (a) after setting (6 days after mixing), (b) after one day in water, (c) after three days in water, and (d) after one day in the oven. As shown in Figure 4.49, at first all specimens showed the same development of the E* over time, where it increased with a relatively steady slope from before the specimens were immersed in water to when they had been in water for three days. This increase is mostly because the hydration process is still ongoing, increasing the C-S-H gel volume, making it denser, and the fact that the cement is absorbing water. Then after heating in 200°C for one day all specimens had a dramatically decreased value of E*. Another observation is that CCP-5 had significantly higher E* than all other specimens. This could be because of the small particle size of silicone debris, which could have similar effect on the cement slurry as micro silica or even Nano silica, increasing both the rate of hydration and the compressive strength, but possibly making it more brittle. Another speculation is that the amount of sulphur and oxygen, which is in relatively high amount on the silicone debris' surface, could have this effect. The specimen with the second highest E* was CCP-7 (mixture of silicone and O-ring rubber AT). When comparing the specimens to the control one can see that the control had lower E* than all the specimens for all measurements, with one exception, CCP-2 had the lowest value of E* after three days in water and after heating.
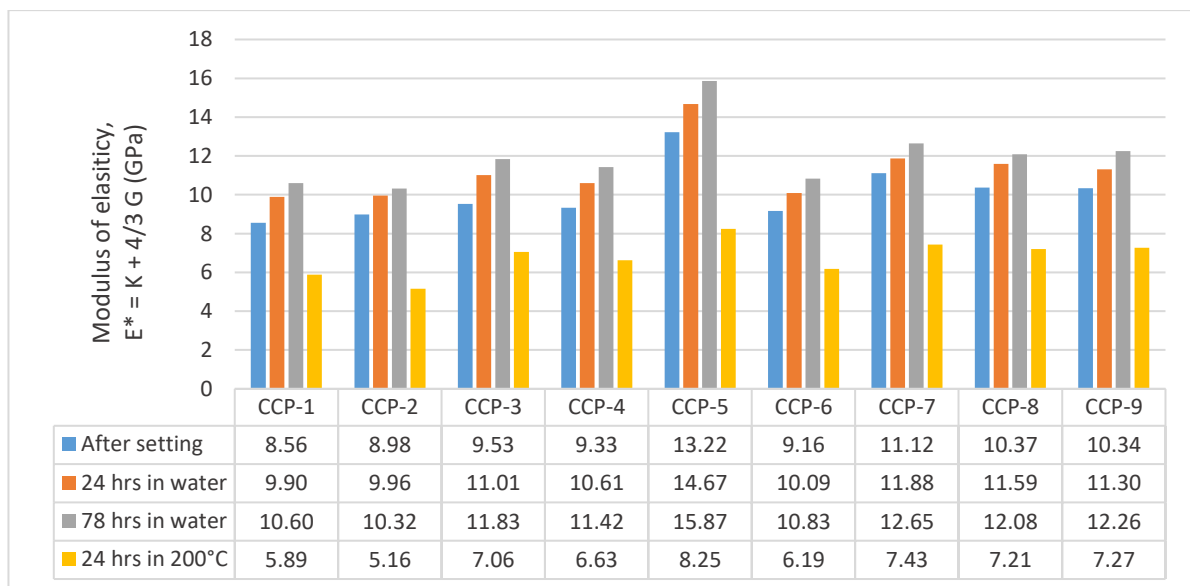
	CCP-1	CCP-2	CCP-3	CCP-4	CCP-5	CCP-6	CCP-7	CCP-8	CCP-9
After setting	8.56	8.98	9.53	9.33	13.22	9.16	11.12	10.37	10.34
24 hrs in water	9.90	9.96	11.01	10.61	14.67	10.09	11.88	11.59	11.30
78 hrs in water	10.60	10.32	11.83	11.42	15.87	10.83	12.65	12.08	12.26
24 hrs in 200°C	5.89	5.16	7.06	6.63	8.25	6.19	7.43	7.21	7.27

Figure 4.49: Dynamic elastic modulus (E) of the cement core plugs after setting, 24 hours in water, 78 hours in water, and 24 hours in 200°C.*

4.4.5 Shrinkage analysis of CCP

Shrinkage of the plugs was analysed based on volume changes. Both the length and the diameter of the specimens were measured at four places on every specimen. The average value was used to calculate the volume. It was ensured that the place of which the length and diameter was measured was always at the same place by marking it. The volume change was then calculated using eq. (3.2), and the volume change, in percent, over the period the specimens were in water bath is illustrated in Figure 4.50. It shows that some specimens shrank while in water, but for some specimens it appears to be no correlation between time in water and shrinkage or swelling. This shrinkage and swelling of the specimens are so small that it can merely be uncertainties in the measurements. However, the shrinkage of CCP-3 was relatively large, a shrinkage of almost 0.4%.
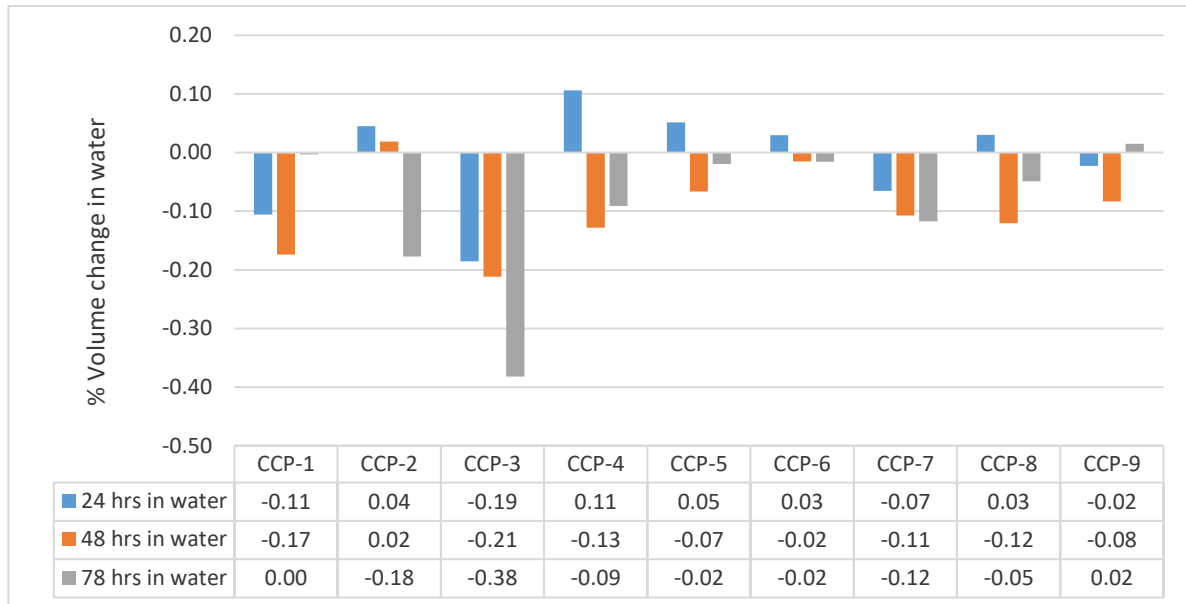

	CCP-1	CCP-2	CCP-3	CCP-4	CCP-5	CCP-6	CCP-7	CCP-8	CCP-9
24 hrs in water	-0.11	0.04	-0.19	0.11	0.05	0.03	-0.07	0.03	-0.02
48 hrs in water	-0.17	0.02	-0.21	-0.13	-0.07	-0.02	-0.11	-0.12	-0.08
78 hrs in water	0.00	-0.18	-0.38	-0.09	-0.02	-0.02	-0.12	-0.05	0.02

Figure 4.50: The % volume change of the CCP from the original after 24, 48 and 78 hours in water

The shrinkage of the specimens after 24 hours in 200°C is illustrated in Figure 4.51. It shows how the cement shrinks dramatically when heated in an oven at 200°C, where all specimens shrank more than 1.7% compared to their original volume. The specimens which showed the least shrinkage were CCP-2 and CCP-9, with 1.71% and 1.76% volume loss, respectively. In addition, these two plugs also showed less shrinkage as compared with the control plug.
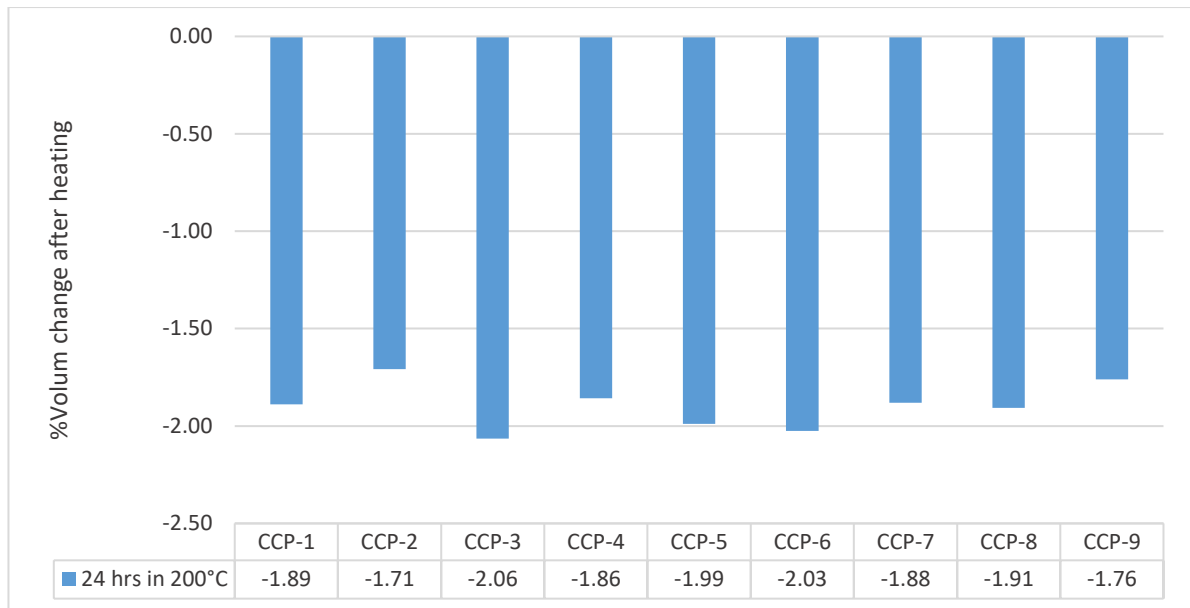
Figure 4.51: The % volume change of CCP from the original after 24 hours in 200°C.

4.4.6 Destructive compressional test

4.4.6.1 UCS of CCP

The UCS of the core plugs, calculated using eq. (3.6), is illustrated in Figure 4.52. For an easier comparison with the control (CCP-1), a red line was drawn over the graph showing the value of the control. Additionally, a percentage of the control was calculated by dividing the UCS value of the each plug with the control's value. This percentage is shown on the data table in Figure 4.52 (% of CCP-1), where any increase or decrease in UCS compared to the control shows higher or lower percentage than 100, respectively (this comparison with the control is also shown on the figures in the whole section 4.4.6). As shown on Figure 4.52, CCP-5 had a significantly higher UCS than any other specimen, and 63% higher UCS than the control. Other specimens with significantly higher UCS compared with the control were CCP-9, -3, and -7, which had 29%, 26%, and 21% higher UCS than the control, respectively.
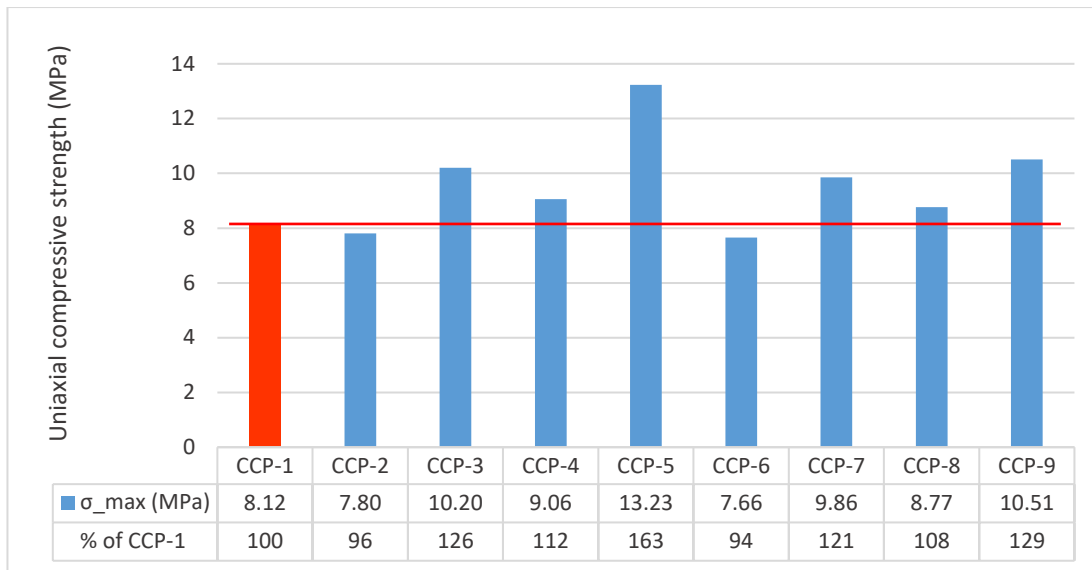
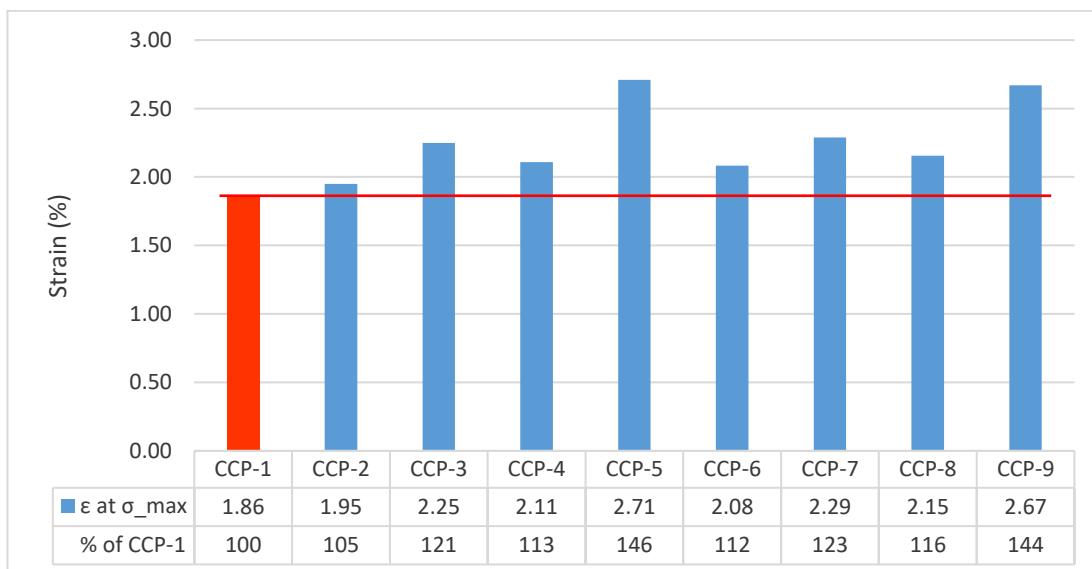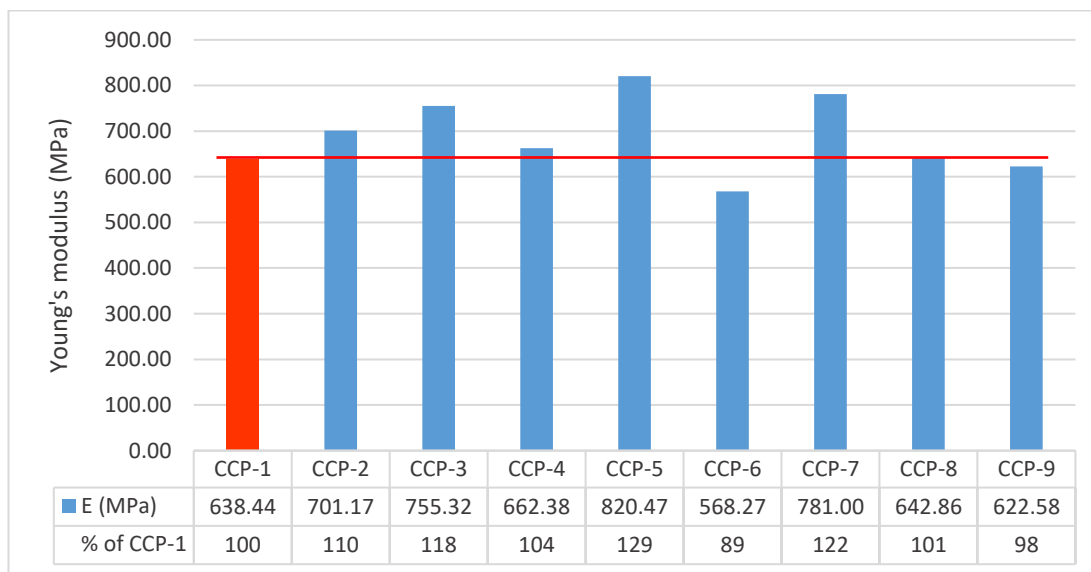| σ_max (MPa)	CCP-1	CCP-2	CCP-3	CCP-4	CCP-5	CCP-6	CCP-7	CCP-8	CCP-9
σ_max (MPa)	8.12	7.80	10.20	9.06	13.23	7.66	9.86	8.77	10.51
% of CCP-1	100	96	126	112	163	94	121	108	129

Figure 4.52: The UCS of the cement core plugs, showing the UCS percentage of the control, where the control is 100%.

4.4.6.2 Deformation of CCP

The deformation, or the strain, of the specimens at the time of failure is shown in Figure 4.53. This describes how much the cement is deformed before it fails. There is a relation between how much a specimen deforms and how ductile it is, where a long deformation is associated with high ductility. As shown on Figure 4.53, all specimens had more deformation at failure than the control, where CCP-5 and CCP-9 deformed the most with about 2.7% deformation.

ε at σ_max	CCP-1	CCP-2	CCP-3	CCP-4	CCP-5	CCP-6	CCP-7	CCP-8	CCP-9
ε at σ_max	1.86	1.95	2.25	2.11	2.71	2.08	2.29	2.15	2.67
% of CCP-1	100	105	121	113	146	112	123	116	144

Figure 4.53: The strain of the cement core plugs, showing the strain percentage of the control, where the control is 100%.

4.4.6.3 Elastic modulus of CCP

Another factor that describes the ductility of a material is the Young's modulus (E). A higher E value is associated with stiffer and brittle material and lower E value with a ductile material. The E value of the specimens is illustrated in Figure 4.54. Its shows that the lowest value of E was obtained in CCP-6, with 11% lower E than the control. All other specimens had higher value of E compared with the control or had almost the same value. Moreover, CCP-5 had the highest E value, 29% higher than of the control.

	CCP-1	CCP-2	CCP-3	CCP-4	CCP-5	CCP-6	CCP-7	CCP-8	CCP-9
■ E (MPa)	638.44	701.17	755.32	662.38	820.47	568.27	781.00	642.86	622.58
% of CCP-1	100	110	118	104	129	89	122	101	98

Figure 4.54: The Young's modulus (E) of the cement core plugs, showing the E percentage of the control, where the control is 100%.

4.4.6.4 Resilience

For better describing a desired property of cement, one can combine the UCS and the modulus of elasticity (or the strain), called the resilience (R). Which describes the amount of energy absorbed by the plug until reaching the maximum stress, UCS. A high UCS is always desirable, but in combination with a low value of E will make the material able to withstand high pressure and at the same time deform without damaging its structural strength. The R was calculated using eq. (3.8). The results are illustrated in Figure 4.55. The results show that CCP-5 absorbs much more energy than the rest. Comparing with the additive free plug (the control), CCP-5 had double resilience value. Even though CCP-5 had higher modulus of elasticity, the specimen recorded a higher energy storage (R). This is due to its great UCS compared with the rest, and the long deformation before failure. Another specimen that had significantly increased R was CCP-9, which had 72% increased R compared with the control.

This high value of R is due to its relatively high UCS and low E. Furthermore, Figure 4.55 shows that almost all cement systems improved the resilience of a conventional cement with some amount, apart from CCP-6 and CCP-2.
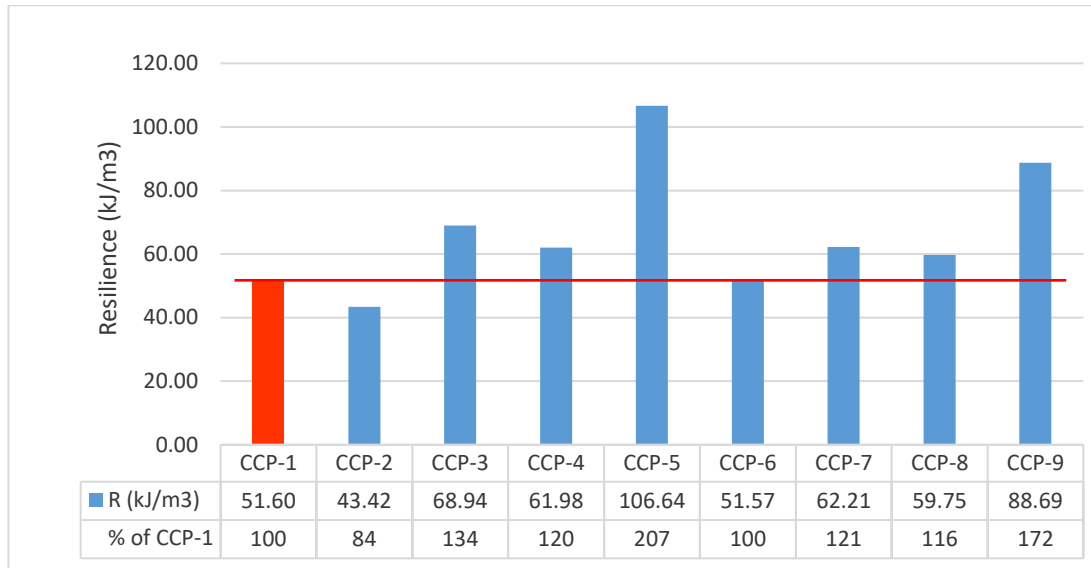

	CCP-1	CCP-2	CCP-3	CCP-4	CCP-5	CCP-6	CCP-7	CCP-8	CCP-9
■ R (kJ/m3)	51.60	43.42	68.94	61.98	106.64	51.57	62.21	59.75	88.69
% of CCP-1	100	84	134	120	207	100	121	116	172

Figure 4.55: The resilience (R) of the cement core plugs, showing the R percentage of the control, where the control is 100%.

From this destructive test one can see that silicone debris (CCP-5) has really positive effect on the strength of cement. Also, a mixture of silicone, micro minerals, carbon fibre and Nano silica (CCP-9) improves the cement's strength significantly.

4.5 UCS-V_p Modelling

Among others, Horsrud [45] derived a correlation equation that relates the uniaxial compressive strength with the sonic velocity (P-wave). The model has been derived based on several rock specimens taken from the North Sea shale formation. The models reads:

$$C_0 = 0.77V_p^{2.93} \qquad (4.1)$$

Where,

C_0 is the uniaxial compressive strength (UCS) (Mpa);

V_p is the P-wave velocity (km/s).

In this thesis, the UCS measured with destructive test (section 4.4.6) data were used to model with the P-wave velocity of the core plugs measured in section 4.4.3 . The modelling result with R² = 0.8477 is given as:

$$C_0 = 0.9634 V_p^{2.7055} \qquad\qquad (4.2)$$

Figure 4.56 shows the comparison between this thesis model (eq. (4.2)) and literature Horsrud's model (eq. (4.1)). As shown, both models look quite similar with different coefficient and exponents.

Since Horsrud model is used for predicting UCS in the drilling formation, this thesis author believes that the model developed in this thesis may have a potential to be used in sedimentary rock. Unfortunately, due to short research period, the author was not able to find literature data and test the model.
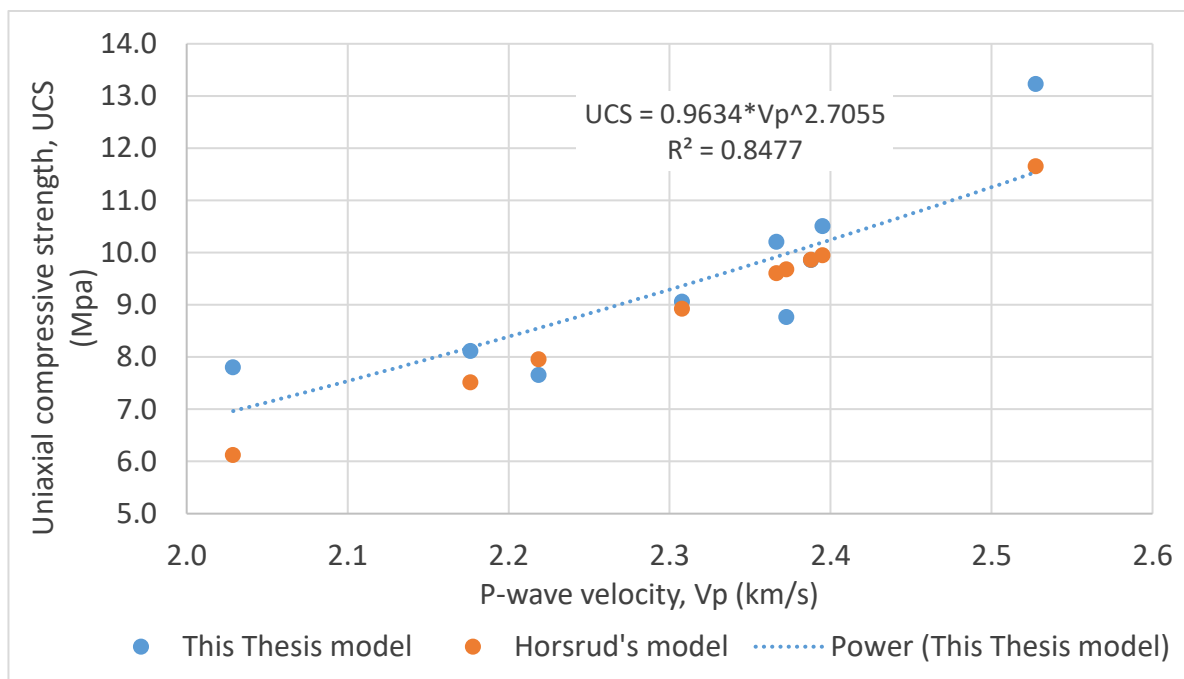
Figure 4.56: UCS vs V_p modelling and comparison with Horsrud's literature model.

4.6 Casing – Cement – Casing

To study the differences between having a cement plug inside a casing and outside of a casing, and how it reacts to high temperature, a brief test was designed where cement was placed in between two steel pipes. This test was only carried out for cement with no additives; conventional cement with 0.6 WCR. Figure 4.57 shows the set cement between one pipe with a large diameter and one with a small diameter. Three days after mixing the specimen was put into an oven for 24 hours at 200°C. Both before the specimen was put into an oven and as soon as it was taken out, the diameters of the pipes were measured to study their expansion rate. Their diameters were measured at both ends of the pipes, and the average

was used to calculate their linear expansion coefficient. After heating the inner pipe was pulled with small force to see if the cement plug had lost its bonding with either of the pipes. It was observed that the cement moved with the inner pipe along the outer pipe, i.e. it had lost its bonding with the outer pipe but not the inner pipe. Moreover, on the bottom of the specimen one fairly wide crack and one narrower crack, opposite form each other, this is shown in Figure 4.58 (a). After the measurements the specimen
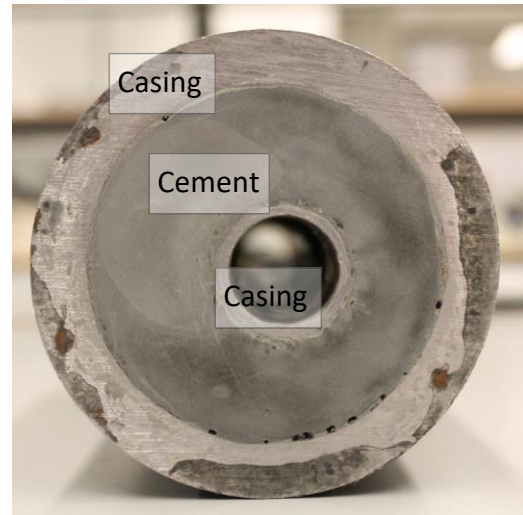
Figure 4.57: A cement plug between two casings; one with large diameter and one with small diameter.

was immersed in water at room temperature to study if the cement would regain its bonding. After 24 hours in water the pipe's diameters were measured and it was observed that the cement had re-bonded with the outer pipe, the narrower crack was invisible to the naked eye and the wider crack had decreased (see Figure 4.58 (b)).

The specimen was then put back into the oven at 200°C for the second time to study if the cracks would further develop and to get two measurements of the thermal expansion. After 24 hours it was taken out of the oven and it was observed that the cement had lost its bonding with the outer pipe and the large crack seemed to have enlarged and many small cracks were visible, this is shown in Figure 4.58 (c). Figure 4.58 (d) shows how the cement was able to move from its original place. Also, as soon as the specimen was taken out of the oven the diameters were measured. The expansion coefficient from the cross-sectional area, α_A, of the pipes were calculated using eq. (3.12), and the linear expansion from the circumference, α_C, was calculated using eq. (3.11). Table 4.7 illustrates these values after both temperature cycles, and their averages. The diameter for calculating the expansion from the circumference was the one in contact with the cement, i.e. for the outer pipe the inner diameter was used, and for the inner pipe the outer diameter was used. These diameters were used because the expansion of these effect the cement the most. Where the outer pipe will move away the cement, losing the bond, and the inner pipe will expand towards it, creating tension. For the outer pipe the difference between the two coefficients are quite large, this is because it has a relatively thick wall and the inner diameter expands with higher rate than the outer

diameter. This gives a significantly larger value of α_C compared with α_A. For the inner casing a large differences in the coefficients was observed when comparing the measurements after the 1st and the 2nd temperature cycle. A possible explanation for this is that the cement continued the hydration process while it was in the water bath after the 1st cycle, and further developed its strength giving it more resistance against the expansion of the pipe. Another reason for this can be an error in the measurements, a digital calliper was used with an accuracy of ±0.005 mm. However, this is moderate error and a more probable inaccuracy is due to human errors, where only a small inaccuracy in the measured diameter can lead to a relatively large variation in the expansion coefficient. Nonetheless, the average value of the coefficients were similar indicating that the outer diameter and the cross-sectional area expanded with almost the same rate.

Table 4.7: The linear expansion coefficient of the outer and inner pipes, after two temperature cycles, calculated from both the cross-area (α_A) and the circumference (α_C)

	Outer pipe			Inner pipe		
	1st cycle	2nd cycle	Average	1st cycle	2nd cycle	Average
α_A $(10^{-6}\ K^{-1})$	1.66	2.02	1.84	7.89	3.64	5.77
α_C $(10^{-6}\ K^{-1})$	9.09	9.91	9.50	8.9	6.67	7.79

As shown in Figure 4.58, these expansions of the pipes both fractured the cement plug and resulted in lost bonding with the pipe. Where the inner pipe generated a tension from the inside of the cement, weakening its structure and creating possible leak paths for fluid to migrate through it. Also, the outer pipe expanded more than the cement allowing the cement to move freely inside it, and creating additional leak paths along the interface.
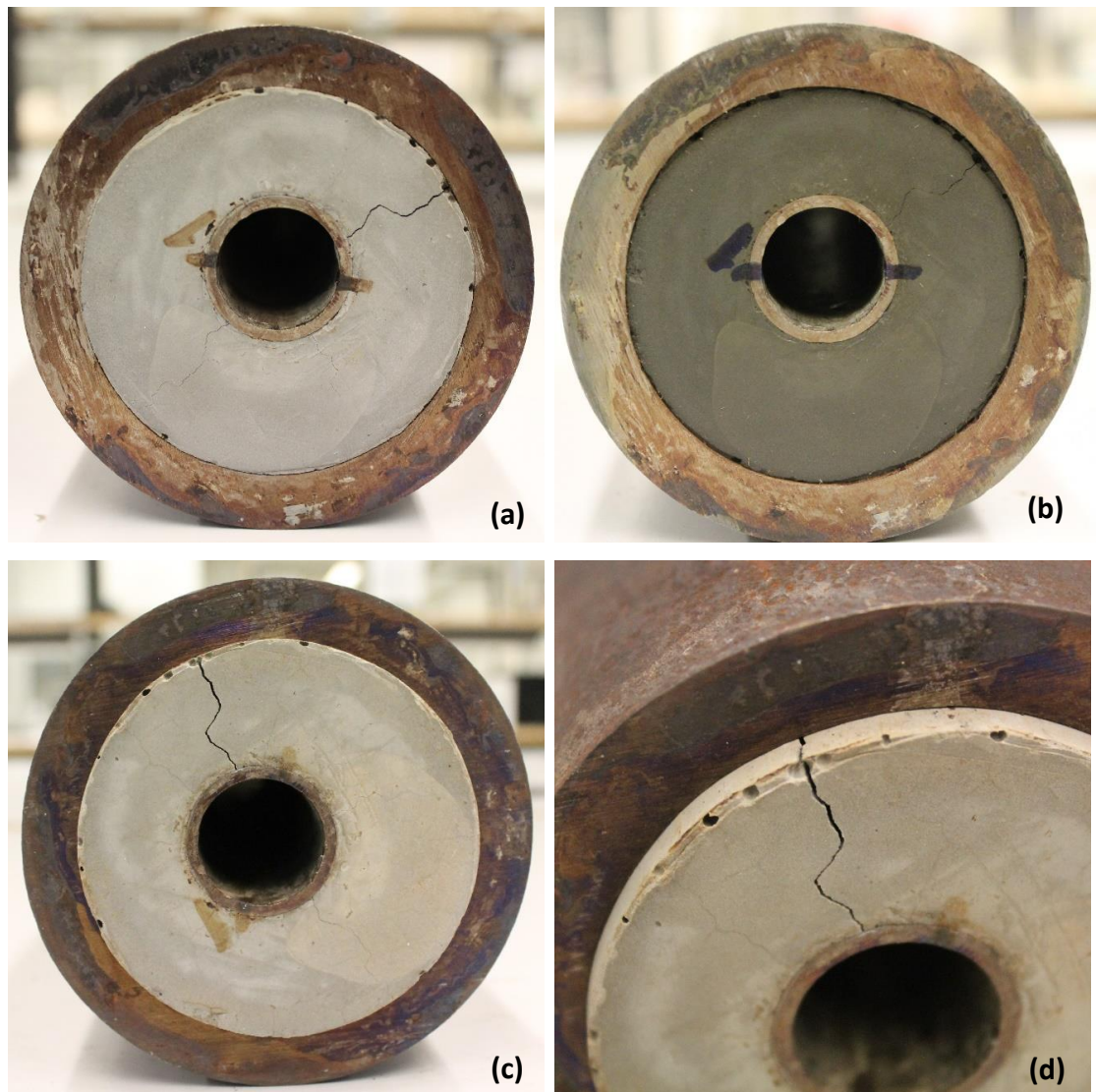
Figure 4.58: The bottom of the casing – cement – casing specimen after: (a) 1st temperature cycle, (b) water bath for 24 hours, and (c) 2nd temperature cycle. (d) Showing the loose cement plug and a closer look of the crack.

4.7 Formation – Cement – Casing (FCC) bond

A test was designed to simulate a cemented casing in a well, where the cement is pumped between the casing and the formation, creating a seal between the formation and the casing, among others. The choice of cement system was mostly based on the destructive compressional test, but partly on the shear bond strength test. The formation – cement – casing specimens are referred as FCC and is used in the following sections.

4.7.1 Preparation of FCC

A porous concrete block, 6 cm thick, was used to exemplify a formation and for the casing a steel pipe casing was used. The type of casing is the same as for the one used for CC-III (see

section 4.3.3). Initially, an attempt was made to scale down the 9 $^5/_8$" casing in a 12 ¼" open hole to a laboratory scale. Therefore a 32 mm hole was required for the 25 mm casing already available. Unfortunately, the smallest drill bit available was 38 mm, which was then used to drill holes through the concrete blocks. If the 25 mm casing is still used to exemplify the 9 $^5/_8$" casing, a 38 mm hole will exemplify a roughly 14 $^5/_8$" hole. This is reasonable because even though a 12 ¼" hole is drilled a likely scenario can be a washout or collapse, increasing the size of the open hole.
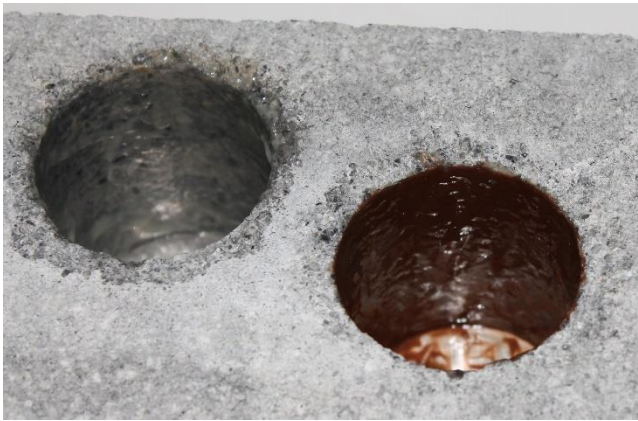
Figure 4.59: The small scale borehole with applied mud cake: WBM on the left and OBM on the right.

To study the effect of water based mud (WBM) and oil based mud (OBM) on the cement bonding with the formation two simple mud systems were prepared. The WBM was mixed with 6/100 ratio of bentonite/water, and the OBM had 80/20 oil/water ratio. The mud was applied on the borehole wall to create a thin mud cake, this is shown in Figure 4.59, where the mud cake from the WBM is on the left and OBM on the right. A plank was clued on one side of the block, closing that end of the hole to hold the cement inside while setting. The casing was placed in the centre of the borehole before pouring the mixed cement between the casing and the borehole wall. The composition of the cement slurries is illustrated in Table 4.8. All cement slurries were poured in two holes, one with WBM and one with OBM. The control (FCC-1) however was additionally poured in a dry hole without any mud cake.

Table 4.8: Composition of Formation – Cement – Casing.

Specimen name	Water (% bwoc)	Cement (% bwoc)	Additive/-s	Amount additives (% bwoc)
FCC-1	60	100	-	-
FCC-2	60	100	Silicone rubber AT	0.80
FCC-3	60	100	Silicone debris AT	0.80
FCC-4	60	100	Silicone rubber AT	0.40
			O-ring rubber AT	0.40
FCC-5	60	100	Silicone rubber AT	1.10
			Carbon fibre	0.10
			Nano silica	0.15
			Micro quartz	1.00
			Micro CaCO$_3$	0.50
			Micro feldspar	0.50

Five days after the cement was mixed and poured in the borehole the plank under the concrete block was removed. Figure 4.60 (a) shows the set cement of the control in a dry well, water based well and oil based well, from left to right. When the bottom of the specimens were examined it was noted that the mud seemed to have damaged the cement. This was because when the mud cake was applied on the borehole wall a portion of the mud fell on the bottom leaving a very thin layer on the bottom. Figure 4.60 (b) shows the bottom of the controls in a dry well, water based well and oil based well, from left to right. It shows that the dry well had relatively smooth surface, the well with WBM had rather rough surface where it looked like the cement had partially corroded, and the well with OBM had large air pockets.

Figure 4.60: The set cement in a dry well, well with WBM and well with OBM, from left to right. (a) The top of the specimens, and (b) the bottom of the same specimens.

4.7.2 Temperature cycling of FCC

Five days after mixing the cement and pouring it into the wells the specimens were put into an oven at 200°C for 24 hours. This was to study if the cement could withstand the extreme heat in addition to the expansion of the casing. The temperature cycling profile is illustrated in Figure 4.62. After 24 hours in the oven all specimens had some cracks both on top of the cement and on the bottom ranging

Figure 4.61: After one temperature cycle the cement had fractured due to heating and expansion of the casing.

from the casing towards the formation, this is shown in Figure 4.61. All specimens had about 4-6 cracks on the top and 2-3 on the bottom. There was not much difference between each specimen concerning the size and number of cracks. The specimens were at normal conditions for three days before the shear bond strength test was executed.
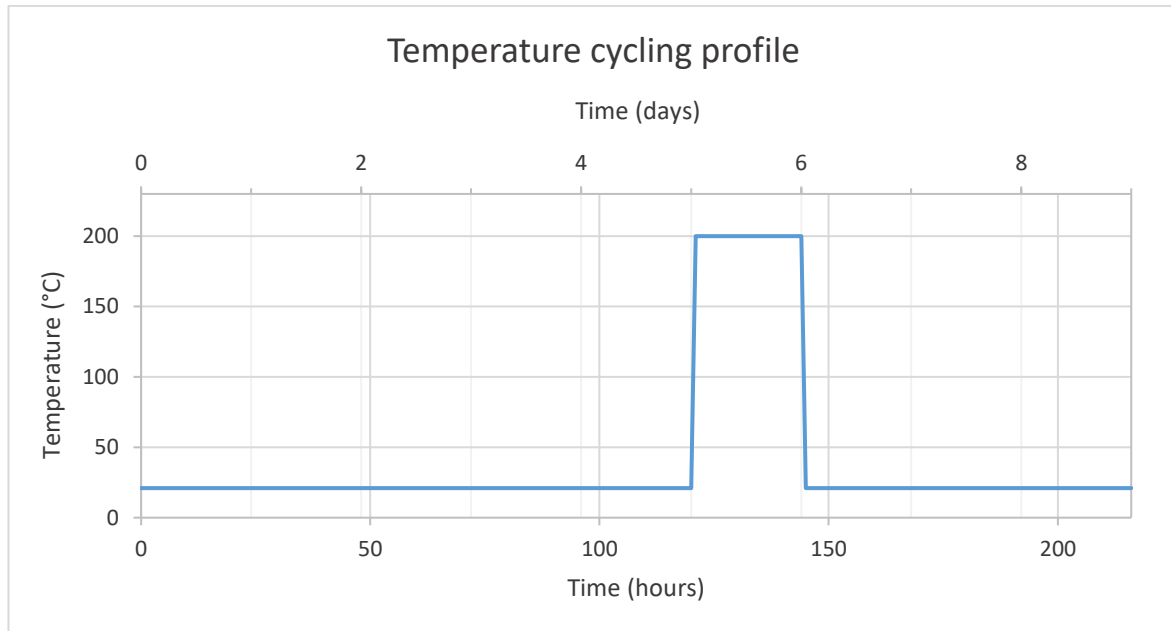
Figure 4.62: Temperature cycling loading profile of FCC

4.7.3 Shear bond strength of FCC

The shear bond strength was tested by applying a force on top of the casing until the cement would lose its bonding with either the casing or the formation. Figure 4.63 shows the setup for the test. Figure 4.64 shows an illustration of the specimen's cross-section during testing, showing the forces acting on the interfaces of a specimen. Before the specimen loses its bond at either of the interfaces the forces must remain equal according to Newton's third law, i.e. for all component of the system to remain still, all forces must be equal. It is assumed that the forces inside the cement are of the same extent at the interfaces, i.e. the force acting on the formation – cement interface is equal the force acting on the cement – casing interface. Furthermore, when the force reaches a certain magnitude the bond will break at one of the interfaces, this will indicate the weak point of the system and the force needed to break the bond at the weak point.

Figure 4.63: Setup for the shear bond strength test of the FCC specimens.
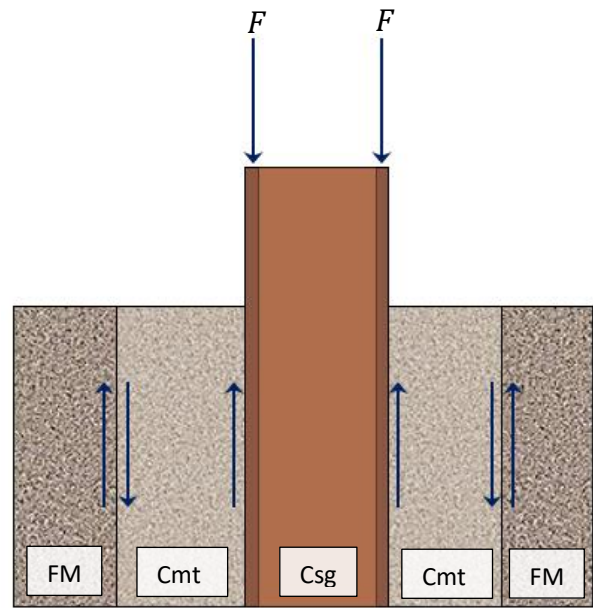
Figure 4.64: Illustration of the cross-section of a specimen showing the forces influencing the bond at the interfaces during testing.

Three days after the specimens were taken out of the oven the bond strength test was executed. Where force was applied on top of the casing until either the casing alone or the cement and casing together would move. The weak point from the test of each specimen is listed in Table 4.9, where FM stands for the formation – cement interface, and Csg. stands for cement – casing interface. As shown in Table 4.9 the weak point was for the majority of the specimens at the formation – cement interface. Also, all specimens in a well with an oil based mud cake had a weak point at the formation. This indicates that the OBM has a damaging effect on the bond strength of cement. Furthermore, the control (FCC-1) had better bond strength with the formation in water based formation than with the casing; this was also true for a dry borehole, but that was expected.

Table 4.9: The shear bond weak point of FCC, where FM stands for the formation – cement interface, and Csg. for the cement – casing interface.

	Mud		
	WBM	OBM	Dry
FCC-1	Csg.	FM	Csg.
FCC-2	Csg.	FM	-
FCC-3	FM	FM	-
FCC-4	FM	FM	-
FCC-5	FM	FM	-

The maximum force needed to move a specimen was used to calculate the shear bond strength using eq. (3.10). Where the surface area used was at the interface of weak point, i.e. when the weak point was at the formation – cement interface the surface area of the cement in contact with the formation was used, and when the weak point was at the cement – casing

interface the surface area of the cement in contact with the casing was used. Unfortunately, due to technical issue, the force needed to move the casing of FCC-2 in a WBM was not measured.

The bond strength at the weak point is illustrated in Figure 4.65. Note that this is only for the weak point and therefore is the comparison between these not a comparison between the different bond strengths with formation only nor with casing only, but rather the weaker case of these two. However, for the case of OBM all specimens had a weak point at the formation – cement interface. This shows that the strongest formation – cement bond strength with OBM was found to be FCC-4, with 61 kPa, but only 11% higher than of the control, which is insignificant. All other specimens had lower bond strength with formation in well with OBM. For the wells with WBM both FCC-3 and FCC-5 had significantly higher bond strength at the weak point compared with the control, a 31.8% and 37.5% increase, respectively. However, even though FCC-3 and FCC-5 had the highest bond strength in WBM, they were also highly affected by changing the mud from water based to oil based. This decreased the bond strength of FCC-3 and FCC-5 by 73.3% and 66.7%, respectively. Another observation that must be noted is that the control had a significant difference in bond strength for the dry well and the well with WBM. These were expected to have the same values because both had the weak point at the cement – casing interface and should not be affected by the mud. A possible explanation for this is that during setting of the cement the water in the system was able to migrate into the formation of the dry formation. This could decrease the WCR and change the properties of the cement, where it could be more brittle and/or more subjected to the expansion of casing. This would be easier in a dry formation opposed to a formation with a mud cake because the mud cake would act as a barrier for the water, preventing it to escape.

Figure 4.66 shows cement plugs after they were removed from formations with (a) water based mud cake and (b) oil based mud cake. It shows how a part of the mud cake had bonded with the cement not allowing the cement to bond with the formation itself.
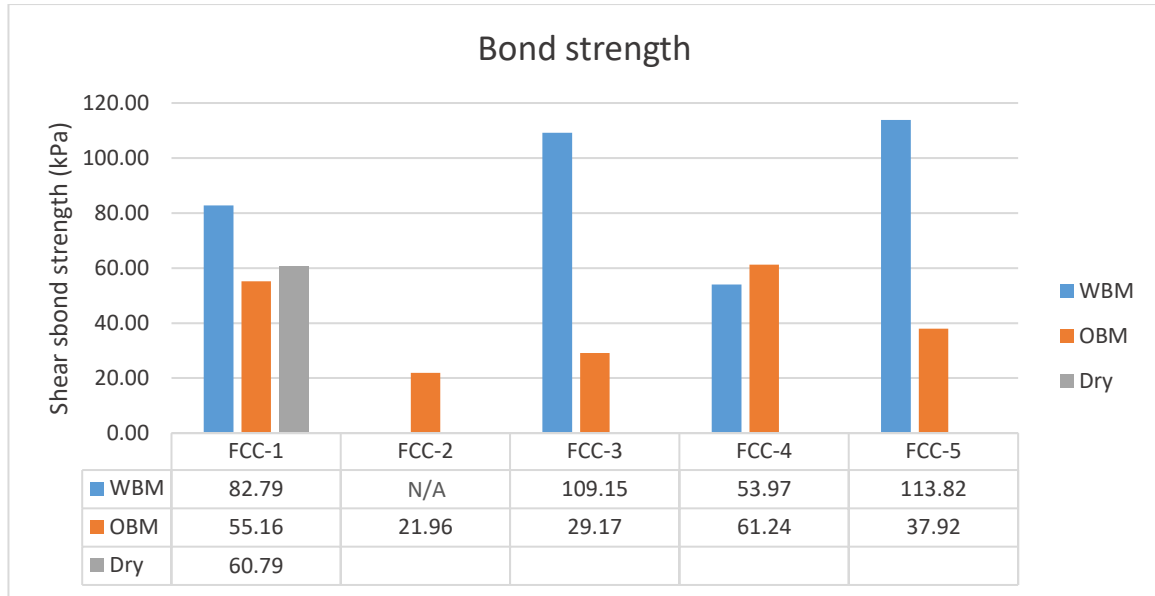
Figure 4.65: The shear bond strength at weak point of FCC.
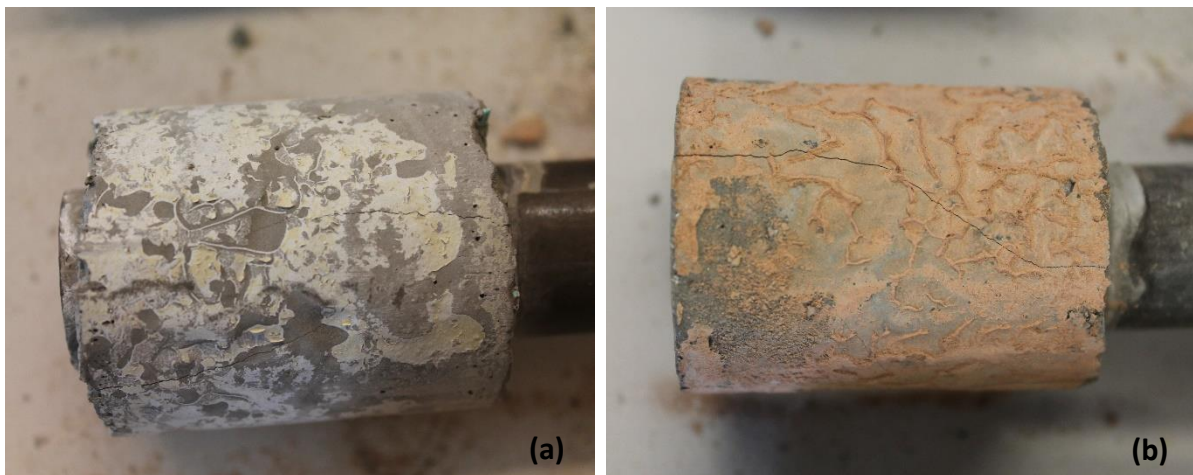
Figure 4.66: Cement plugs after they were removed from a formation with (a) WBM; and (b) OBM.

5   Summary and Discussion

In the experiments a G class cement was used with water-to-cement ratio 0.6 using fresh water. Various additives were mixed with the cement and their effect on the properties of the cement was studied when exposed to high temperature. In this chapter the various tests and experiments performed in this study will be discussed and compared with each other.

5.1 Thermal expansion

Two types of casings were used in the Casing – Cement experiments, nickel based steel table leg and steel pipe. The table leg casing had a linear expansion coefficient of 13.90×10^{-6} K^{-1} calculated from the increased circumference of the casing. This means that a pipe with for instance a circumference of 88.40 mm at 21°C will increase to 88.62 mm at 200°C, this will increase the annulus area from 621.93 mm^2 to 625.02 mm^2, which is 0.50% area increase. This 3.1 mm^2 does not sound very much but this can be enough to break the bonding at the casing – cement interface, especially when in combination with the shrinkage of cement. The steel pipe casing had a linear expansion coefficient of 9.55×10^{-6} K^{-1}, also calculated from the increased circumference. This means that a pipe with a circumference of 67.06 mm at 21°C will increase to 67.18 mm at 200°C, this will increase the annulus area from 357.87 mm^2 to 359.09 mm^2, which is 0.34% area increase. The differences in the expansion coefficient between these two casing types does not seem to be significant, but a little less expansion can decrease its effect on the bonding between the cement and the casing significantly. The values used in the examples above are the averages from the casings used in the experiments.

5.2 Casing – Cement

To study how cement will react to high temperature changes when inside a casing, a casing was filled with cement and left to set. When the cement and the casing are exposed to high temperatures the casing will expand and the cement will dry out and shrink. This can seriously damage both the structure of the cement and its bonding with the casing. This is the worst case in scenario and in reality the cement would most likely not dry out inside the well because of the high pressure keeping the fluid in the pores of the cement, despite the high temperature. Also, when the cement is pumped down into the casing the casing has most likely already expanded and would not expand much after the cement is in place. Hence, this

experiment was to study how well cement can retain its bond with the casing despite the expansion of casing when exposed to the harsh environment, and how well it can regain its bonding afterwards. This was done with two different tests: (1) leakage tests after each temperature cycle, where water was left on top of the cement for 24 hours and then the leakage was measured; and (2) after this a bond strength test was executed were the cement was pushed out of the casing.

5.2.1 Leakage

In the first Casing – Cement design (CC-I), cement was filled inside a table leg casing and the specimens were exposed to 108°C in an oven. After four 108°C cycle loadings and leakage tests, the results showed that the additive free control system was found to be able to withstand the given temperature decently. This was also true for cement with additives such as carbon fibre (CF) alone, and in a combination with Nano silica. Furthermore, when micro quartz, $CaCO_3$ and feldspar were all used together as additives a small amount of leakage was measured for the first three cycles, but after the forth cycle it seemed to have lost its ability to keep water from migrating through it or past it. After four temperature cycles of 108°C, which did not have much of an impact on the conventional cement, it was decided to increase the temperature to 200°C. However, after the first cycle in 200°C no specimen could hold any water. The specimens were left at normal conditions for six days and it showed that almost all had regained their bonding with casing. Three specimens had significantly improved the leakage after six days namely, the cement without additives, with carbon fibre (CF), and with mixture of the micro minerals.

For the second batch (CC-II), a table leg casing was also used and they were exposed to 200°C temperature cycles. The leakage test showed that many specimens did not withstand this high temperature and had very high leakage rate after just the first cycle. These were specimens who contained O-ring rubber, latex, or Nano graphene. On the other hand, the additives that improved the conventional cement were: (a) acid treated (AT) silicone rubber, (b) untreated (UT) silicone rubber, (c) micro quartz in combination with CF and Nano silica, and (d) CF in combination with Nano silica. After the third temperature cycle the specimens were left at room temperature for four days before testing for leakage again. This showed that many specimens that performed poorly after the temperature cycles had regained bonding and had very little leakage. This was especially noticeable for the cement mixed with

latex, Nano graphene and O-ring rubber. Also, the cement with both silicone rubber and a combination of quartz and Nano silica had regained its bonding and had very little leakage. When the leakage rate of the specimens containing silicone and O-ring rubber is compared it seems that the acid treatment provided slightly better performance for both rubber types in terms of preventing migration of water through or past the cement.

For the third batch (CC-III) a different casing was used, a steel pipe casing. The steel pipe casing had a smaller expansion coefficient, reducing the effect of the expansion. The specimens were exposed to 200°C temperature loading cycles, and after three cycles it showed that the following additives had improved the ability to prevent migration of water compared with cement with no additives: (a) silicone as the only additive, both AT and UT, and (b) acid treated silicone in combination with CF, Nano silica, quartz, $CaCO_3$ and feldspar. After the third cycle the specimens were left at room temperature for three days. This showed that all specimens had regained its bonding but the one who had the most improvement by curing for three days was the one mixed with acid treated O-ring rubber, where it had the most leakage right after the temperature cycles but had the least amount of leakage after curing for 3 days. After the fourth cycle the only specimen that held any water over night was the one mixed with 1.1% bwoc acid treated silicone.

5.2.2 Bond strength

A shear bond strength test was performed on the casing – cement specimens where a force was applied on top of the cement until it would lose its bonding with the casing. This force needed to move the casing was then used to calculate the shear bond strength. This test was performed after the specimens had been exposed to temperature cycling.

From the first two casing – cement batches (CC-I and CC-II), which had the same type of casing, the one that stands out is that the cement mixed with only O-ring rubber, AT and UT, had significantly higher bond strength than any other, going off the scale with over than 700 kPa bond strength. Other additives that showed increased bond strength compared with the additive free cement of any significant were: (a) micro quartz, (b) latex alone, (c) latex and Nano graphene, and (d) CF with Nano silica (0.1% bwoc each). These had the following increase in bond strength: (a) 115%, (b) 170%, (c) 251%, and (d) 22%. This showed that even though latex and O-ring rubber had a large amount of leakage after the temperature cycles

they had regained their sealing ability and their bond strength when water was introduced back into the system. Despite they had completely lost their bond with the casing after the cycles, as they were loose inside the casing.

The bond strength of the third batch (CC-III) was overall lower compared with the previous batches. This is because another type of casing was used with smaller diameter and made of different material. Only one specimen had lower bond strength than the cement with no additives, namely, the one containing O-ring rubber. This shows that the O-ring rubber did not regain its bonding as for the previous cases, and had zero bond strength. The cement with no additives had very low bond strength, only 2.6 kPa. The additives that improved the bond strength the most were: (a) 1.1% bwoc acid treated silicone, and (b) a mixture of acid treated silicone and O-ring rubber, 0.4% bwoc each. These had a bond strength of (a) 68.2 kPa and (b) 67.8 kPa.

5.3 Cement Core Plug

Cylindrical cement core plugs were created with the same composition as CC-III to study their physical properties. Both a none-destructive and a destructive experiments were executed.

5.3.1 None-destructive test

The water absorption was studied by leaving the core plugs in water bath for three days. The more water the cement absorbs the more likely it will allow other fluids to migrate through it. All specimens absorbed some amount of water and increased in weight. It showed that the least water absorption was measured for the cement with silicone debris alone, and the cement with a mixture of AT silicone and AT O-ring rubber as additives. These had a significantly less water absorption compared with the other specimens, only about 6.5% increase in weight after three days in water. Whereas, the other specimens had an increase in weight from 8.5% to 10.5% after three days in water. Furthermore, during the three days in water the cement with 0.8% bwoc AT silicone decreased in volume by almost 0.4%.

The resistivity of cement is related to how easily fluid can migrate through its pores. After three days in water bath the resistivity was measured. It showed that all specimens had either a lower resistivity than the conventional cement or an insignificantly higher resistivity. So,

according to the measured resistivity the additives used did not improve the conventional cement in terms of resisting a flow through its pores.

After three days in water bath the specimens were put into an oven at 200°C. After a day in the oven the specimens had all lost on average 23% of their original weight and 1.9% of their original volume. This lost can be quite severe, especially when in combination with the expansion of steel. For instance, if cement is inside a steel casing and is exposed to high increase in temperature, the casing will expand and the cement will shrink. Ultimately, this could break the bonding between the cement and the casing. Another example is where the cement is outside the steel pipe, and instead of moving away from each other, as in the previous example, they will move towards each other generating a tension in the cement that could lead to fracturing the cement.

The dynamic modulus of elasticity (E*) was calculated from the sonic measurements. This is an indirect method to measure the elasticity of cement, where a high E* means that a cement will deform by a small percentage when pressure is applied, making it more brittle. It was observed that while in water all the specimens had and increased E* each day, this is because the hydration process was still ongoing and the cement was still developing its strength. However, after a day in 200°C the E* dramatically decreased for all specimens. All specimens had a similar E* except the one with silicone debris as an additive, it had significantly higher E*. After three days in water it had almost 50% higher E* than the cement with no additives.

5.3.2 Destructive test

A destructive uniaxial compressional test was performed where an axial force was applied to the cement core plugs until failure. The uniaxial compressive strength (UCS) can then be calculated from the force needed to break the plug. This was done after the plugs had been in 200°C for a day and then left at normal conditions for a few days; without immersing them back in water.

From this test it showed that silicone debris had very good effect on the strength of the cement. It had very high UCS compared with the others specimen, it had 63% higher UCS than the additive free cement. It also had a very high deformation before failure and a high Young's modulus (E). Consequently, it had very high resilience (R), or a 46% increased R compared with the cement without additives.

Another specimen that showed a high R was a specimen with mixture of many additives, it contained 1.1% bwoc acid treated silicone, 0.1% CF, 0.15% Nano silica, 1% quartz, 0.5% $CaCO_3$, and 0.5% feldspar. This mixture of additives improved the resilience of the conventional cement by 72%. It had this high value of resilience due to its ductile property, where it had a low E and a high deformation before failure.

Other additives that improved the resilience were acid treated silicone as the only additive and in a combination with acid treated O-ring rubber. Where 0.8% bwoc AT silicone had a 34% increase, 1.1% bwoc AT silicone had a 20% increase, and AT silicone and AT O-ring rubber together (0.4% bwoc each) gave an increase of 21% to the resilience.

5.4 Formation – Cement – Casing

A small-scale wellbore was created to study how some additives effect the bond strength of cement with casing on one hand and formation with mud on the other hand. 38 mm well was drilled into a concrete block, casing was place in its centre and then cement slurry was poured between the formation and the casing, creating a seal. For each cement slurry composition two wells were prepared, namely one with water based mud cake and one with oil based mud cake. After curing for five days the specimens were put into an oven at 200°C for 24 hours. After heating it was observed that the cement of all specimens had formed cracks, were cracks ranged from the casing to the formation.

The specimens were left at normal conditions for a few days after they were taken out of the oven, before testing the bond strength. The bond strength of the specimens was tested by applying a force on top of the casing until the bond would fail at either the formation – cement interface or the cement – casing interface. The place where the bond failed indicates the weak point of the system. For the wells with oil based mud cake the weak point was always at the formation – cement interface. In these wells the greatest bond strength was measured in cement mixture with 0.4% bwoc AT silicone and 0.4% bwoc AT O-ring rubber. The second greatest bond strength in oil based well was the conventional cement. In the wells with water based mud cake, the specimens with the greatest bond strength at weak point were cement with (a) 0.8% bwoc AT silicone as additive, and (b) a mixture of additives: silicone, CF, Nano silica, quartz, $CaCO_3$ and feldspar.

6 Conclusion

The main focus of this experimental work was to improve the properties of conventional cement when exposed to high temperature by mixing it with various additives. Based on the results the following conclusions were attained:

With respect to the conventional cement, the addition of the following additives showed the best results:

- 1.1% acid treated silicone, 0.1% carbon fibre, 0.15% Nano silica, 1% Micro quartz, 0.5% micro CaCO3 and 0.5% micro feldspar
  - Increased the bond strength with steel pipe casing by 1,738% after four temperature cycles.
  - 6.7% less shrinkage after heating.
  - Increased the UCS by 29%.
  - Increased the maximum strain by 44%.
  - Decreased the Young's modulus by 2%.
  - Increased the resilience by 72%.
  - Increased the bond strength at weak point in WBM formation by 37%.
  - Decreased leakage by 42% on average.
- 0.8% bwoc acid treated silicone rubber
  - Increased the bond strength with steel pipe casing by 1,435% after four temperature cycles.
  - Increased UCS by 26%.
  - Increased the maximum strain by 21%.
  - Increased the resilience by 34%.
  - Decreased leakage by 30% on average.
- 1.1% bwoc acid treated silicone rubber
  - Increased the bond strength with steel pipe casing by 2,523% after four temperature cycles.
  - 1.6% less shrinkage after heating.
  - Increased UCS by 12%.
  - Increased the maximum strain by 13%.

- □ Increased the resilience by 20%.

- □ Decreased leakage by 15% on average.

- 0.8% bwoc acid treated silicone debris

  - □ Increased the bond strength with steel pipe casing by 727% after four temperature cycles.

  - □ Increased the UCS by 63%

  - □ Increased the maximum strain by 46%

  - □ Increased the resilience by 107%

  - □ Increased the bond strength at weak point in WBM formation by 32%

  - □ However, it increased the leakage by 55% on average.

- 0.4% bwoc acid treated silicone and 0.4% acid treated O-ring rubber

  - □ Incresed the bond strength with steel pipe casing by 2,508% after four temperature cycles.

  - □ Increased the UCS by 21%.

  - □ Increased the maximum strain by 23%.

  - □ Increased the resilience by 21%.

  - □ Increased bond strength with formation with OBM by 11%.

  - □ However, it increased leakage by 61% on average.

- 0.1% carbon fibre and 0.1% Nano silica,

  - □ Increased the bond strength with table leg casing by 22.3% after exposure to four temperature cycles.

  - □ Had similar leakage.

Treating silicone rubber with acid resulted in increased uniaxial strength, increased maximum elongation and increased resilience. However, it decreased the bond strength by 13%.

Treating O-ring rubber with acid resulted in less leakage but it still had very much leakage after temperature cycling. However, O-ring rubber seem to be very good at regaining its bond strength when water is allowed back into the system and left at room temperature for a few days.

Please note that this conclusion is based on experimental results. However, for statistical purpose and to check the repeatability of the results, it is important to do several experiments.

7 Recommendation for further work

From the experience gained from this experimental work I suggest the following investigation to further study the findings:

- Perform an experiment to study different quantities of silicone debris, and in a mixture with other additives, for instance with carbon fibre, quartz and possibly acid treated silicone. In this study 0.8% bwoc silicone debris improved the mechanical properties of cement significantly, but was not tested with other additives or different quantities.

- Study the acid resistance of the optimum cement compositions found in these experiments.

- Compare the performance of acid treated silicone and silicone debris as additives with for instance silica flour and fly ash. These have been used as additives to cement or partially replaced the cement to improve the temperature resistance. A comparison with these could indicate if silicone rubber is better or worse additive or a mixture of all could be the optimal solution.

- Increase the exposure time of O-ring rubber to acid. One minute was the exposure time in the experiments and it did not affect the surface very much. A longer exposure time could create more micro cracks on its surface, allowing better bonding with the cement's particles.

- Expose the cement to high temperature in a pressure chamber where the cement would not lose all its moisture. In the experiments the cement was completely dried when exposed to high temperature, and a more realistic scenario would be a higher pressure and the cement would not completely dry out.

- During the leakage test not enough water was left on top of the cement overnight and a precise leakage was often not measured over a 24 hours period. Therefore a more water should be available for correct leakage measurements.

- Perform a different leakage test of cement inside a casing scenario where air pressure is applied on one side and gradually increased, and on the other side the pressure is measured to study if pressure leakage is observed through/past the cement plug.

- Study the effect of the setting conditions, e.g. perform an experiment where the cement is allowed to set in high temperature and high pressure.

References

[1]   Birgit Vignes, "Contribution to well integrity and increased focus on well barriers from a life cycle aspect," PhD, Faculty of Science and Technology, University of Stavanger, Stavanger, 2011.

[2]   Richard J. Davies, Sam Almond, Robert S. Ward, Robert B. Jackson, Charlotte Adams, Fred Worrall*, et al.*, "Oil and gas wells and their integrity: Implications for shale and unconventional resource exploitation," *Marine and Petroleum Geology,* vol. 56, pp. 239-254, 2014.

[3]   Stefan Bachu and Theresa L. Watson, "Possible indicators for CO2 leakage along wells," researchgate.net Jan. 2006.

[4]   SPE International. (2015). *Geothermal drilling and completion*. Available 13/06/2017: http://petrowiki.org/Geothermal_drilling_and_completion

[5]   Erik B. Nelson and Dominique Guillot, *Well Cementing*, 2nd ed. Sugar Land, Texas: Schlumberger, 2006.

[6]   NORSOK Standard D-010, "Well integrity in drilling and well operations," 2013.

[7]   Kjell Corneliussen, Folke Sorli, Hilde Brandanger Haga, Carlos Antonio Menezes, Eli Tenold, Bruno Grimbert*, et al.*, "Well Integrity Management System (WIMS) - a systematic way of describing the actual and historic integrity status of operational wells," 2007.

[8]   Arash Shadravan, Mohammadreza Ghasemi, and Mehrdad Alfi, "Zonal Isolation in Geothermal Wells," in *Fortieth Workshop on Geothermal Reservoir Engineering*, 2015, pp. 26-28.

[9]   SPE International. (2015). *Geothermal reservoir engineering*. Available 13/06/2017: http://petrowiki.org/Geothermal_reservoir_engineering

[10]   SPE International. (2017). *Well integrity thermal*. Available 13/06/2017: http://petrowiki.org/Well_integrity_thermal

[11]   SPE international. (2014). *Cement composition and classification*. Available 13/06/2017: http://petrowiki.org/Cement_composition_and_classification#cite_ref-r3_2-2

[12]   Dr. Jeff Thomas and Dr. Hamlin Jennings. (2014). *The Science of Concrete*. Available 13/06/2017: http://iti.northwestern.edu/cement/monograph/Monograph5_1.html

[13]   Ashok Kumar Santra, Peter Boul, and Xueyu Pang, "Influence of Nanomaterials in Oilwell Cement Hydration and Mechanical Properties," 2012.

[14]   Rahul C. Patil and Abhimanyu Deshpande, "Use of Nanomaterials in Cementing Applications," 2012.

[15]   Ehsan Ghafari, Hugo Costa, Eduardo Júlio, António Portugal, and Luisa Durães, "The effect of nanosilica addition on flowability, strength and transport properties of ultra high performance concrete," *Materials & Design,* vol. 59, pp. 1-9, 2014.

[16]   Raymond M. Reilly, "Carbon Nanotubes: Potential Benefits and Risks of Nanotechnology in Nuclear Medicine," *The Journal of Nuclear Medicine,* vol. 48, July 2007.

[17]   Mohammad Rahimirad and Javad Dehghani Baghbadorani, "Properties of Oil Well Cement Reinforced by Carbon Nanotubes," 2012.

[18]   Kazi P. Fattah, Noha M. Hassan, and Adil Tamimi, "Effect of adding polar impurities on carbon nanotubes and concrete bonding strength," presented at the 10th International Conference on Composite Science and Technology, 2015.

[19]   Serdar Aydın and Bülent Baradan, "Effect of pumice and fly ash incorporation on high temperature resistance of cement based mortars," *Cement and Concrete Research,* vol. 37, pp. 988-995, 2007.

[20]   Li Li, Matthew Kellum, and Angela Doan, "In-situ Tensile Strength Testing: Awareness of Variations with Testing Environment," 2016.

[21]   Waqas Mushtaq, "Experimental Study of Cement-Formation Bonding," MSc, Petroleum Engineering, Norwegian University of Science and Technology, 2013.

[22]   Xiaofeng Zhao, Zhichuan Guan, Minglei Xu, Yucai Shi, Hualin Liao, and Jia Sun, "The Influence of Casing-Sand Adhesion on Cementing Bond Strength," *PLOS ONE,* vol. 10, 2015.

[23]   Sara Sgobba, Giuseppe Carlo Marano, Massimo Borsa, and Marcello Molfetta, "Use of Rubber Particles from Recycled Tires as Concrete Aggregatefor Engineering Applications," presented at the Second International Conference on Sustainable Construction Materials and Technologies, Ancona, Italy, 2010.

[24]   M. A. Yazdi, J. Yang, L. Yihui, and H. Su, "A Review on Application of Waste Tire in Concrete," *International Journal of Civil, Environmental, Structural, Construction and Architectural Engineering,* vol. 09, pp. 1635-1640, 2015.

[25]   X. Colom, F. Carrillo, and J. Cañavate, "Composites reinforced with reused tyres: Surface oxidant treatment to improve the interfacial compatibility," *Composites Part A: Applied Science and Manufacturing,* vol. 38, pp. 44-50, Jan. 2007.

[26]   Fang Xu, Chao Peng, Jing Zhu, and Jianping Chen, "Design and evaluation of polyester fiber and SBR latex compound-modified perlite mortar with rubber powder," *Construction and Building Materials,* vol. 127, pp. 751-761, 11/30/ 2016.

[27]   Shenzhen Chenggong. *Class G Oil Well Cement*. Available 13/06/2017: http://www.chngn.com/product_show.asp?id=1595&class_id=298

[28]   Les Ciments Artificiels Tunisiens S.A. *Class G HSR: Oil well cement*. Available 13/06/2017: http://www.cat.colacem.com/Products.aspx?Folder=Products&ID=86&mId=102

[29]   Jesus de La Fuente. *Graphene - What is it?* Available 13/06/2017: https://www.graphenea.com/pages/graphene#.WQL7rdKGPIV

[30]   Otakar Frank. (2015). *Graphene*. Available 13/06/2017: http://www.nanocarbon.cz/research.html

[31]   David Barthelmy. *Quartz Mineral Data*. Available 13/03/2017: http://webmineral.com/data/Quartz.shtml#.WP29mdJ97IU

[32]   Hershel Friedman. *The Mineral Quartz*. Available 13/06/2017: http://www.minerals.net/mineral/quartz.aspx

[33]   A. C. Akhavan. (2013). *The Silica Group*. Available 13/06/2017: http://www.quartzpage.de/gen_mod.html

[34]   W. A. Deer, R. A. Howie, and J. Zussman, *Framework silicates: Feldspars*, 2nd ed. London: The Geological Society, 2001.

[35]   Siim Sepp. *Anorthosite and labradorescence*. Available 13/06/2017: http://www.sandatlas.org/anorthosite-and-labradorescence/

[36]   David Barthelmy. *Labradorite Mineral Data*. Available 13/06/2017: http://webmineral.com/data/Labradorite.shtml#.WP9iHdJ9600

[37]   Muskid, "Ternary phase diagram of the feldspars (at 900 °C) modified from N.N. Greenwood, A. Earnshaw - Chemistry of Elements (1998) - p. 357.," ed, 2016.

[38]   Industrial Minerals Association - North America. *What is Calcium Carbonate?* Available 13/06/2017: http://www.ima-na.org/page/what_is_calcium_carb

[39]   Hershel Friedman. *The Mineral Aragonite*. Available 13/06/2017: http://www.minerals.net/mineral/aragonite.aspx

[40]   Hershel Friedman. *The Mineral Calcite*. Available 13/06/2017: http://www.minerals.net/mineral/calcite.aspx

[41]   David Barthelmy. *Calcite mineral data*. Available 13/06/2017: http://webmineral.com/data/Calcite.shtml#.WP8a79J97IX

[42]   The National Institute for Occupational Safety and Health, "Occupational safety and health guideline for calcium carbonate," 1995.

[43]   David Barthelmy. *Aragonite mineral data*. Available 13/06/2017: http://webmineral.com/data/Aragonite.shtml#.WP7-itJ97IU

[44]   ZOLTEK. (2017). *Carbon Fiber*. Available 13/06/2017: http://zoltek.com/carbonfiber/

[45]   Per Horsrud, "Estimating Mechanical Properties of Shale From Empirical Correlations," vol. 16, p. 6, June 2001.

Appendix

Appendix A: SEM images

O-ring rubber before acid treatment:
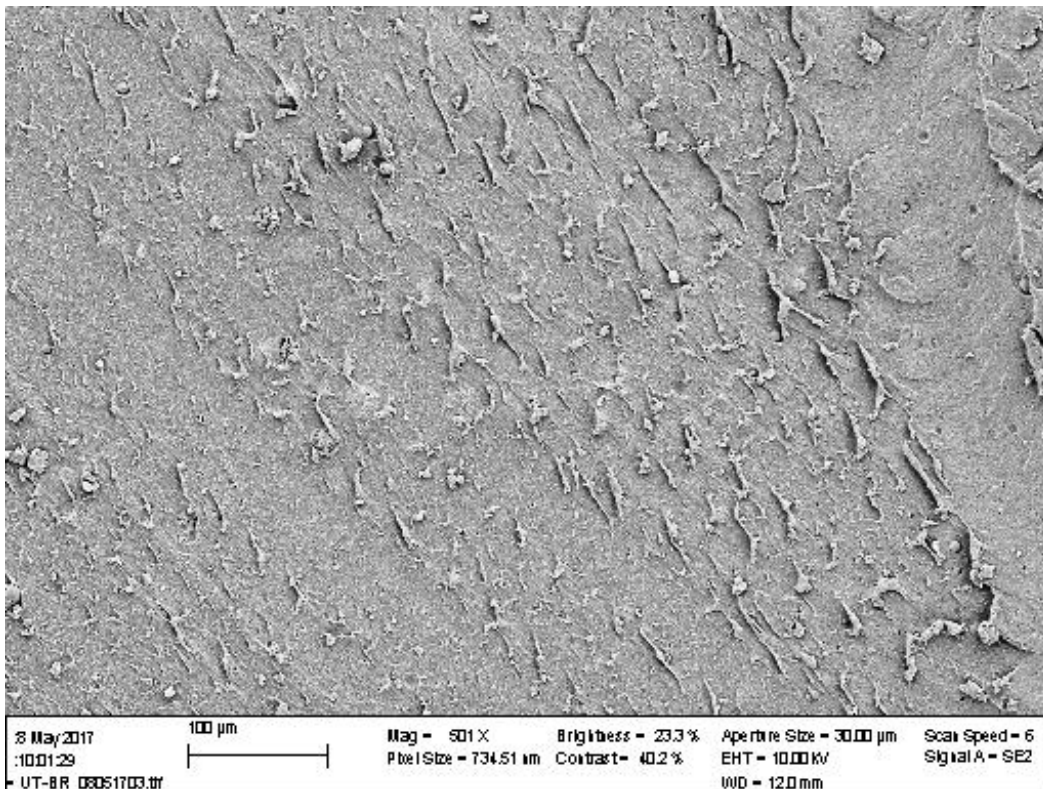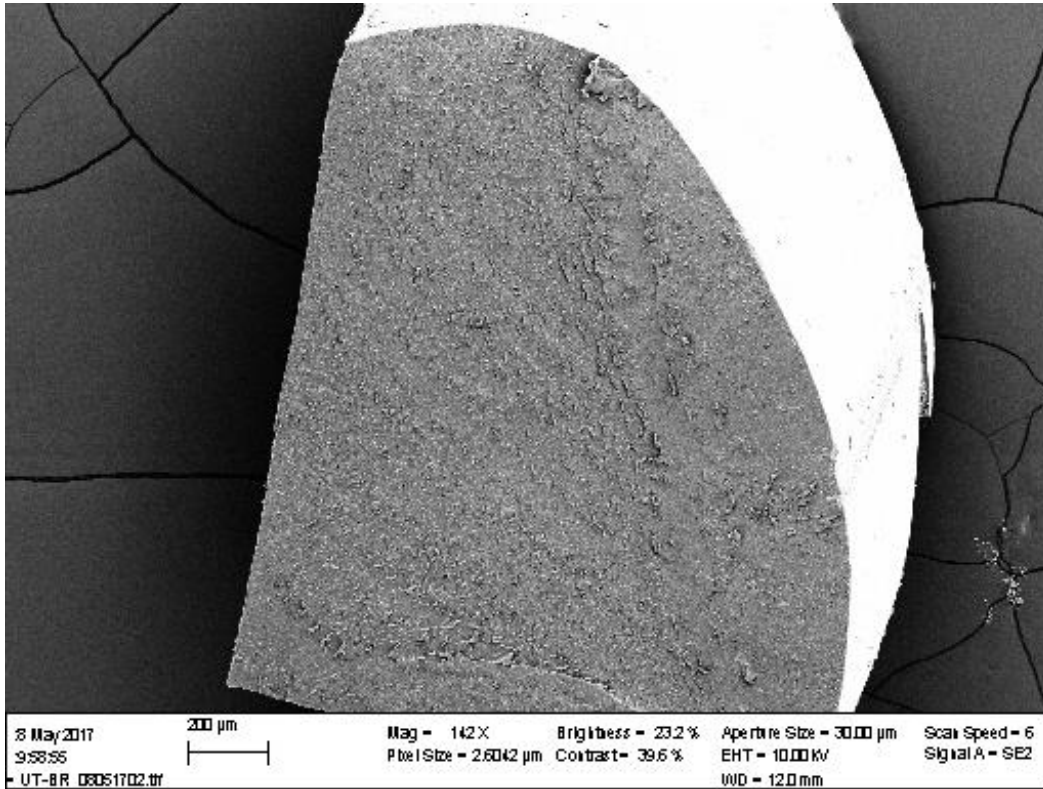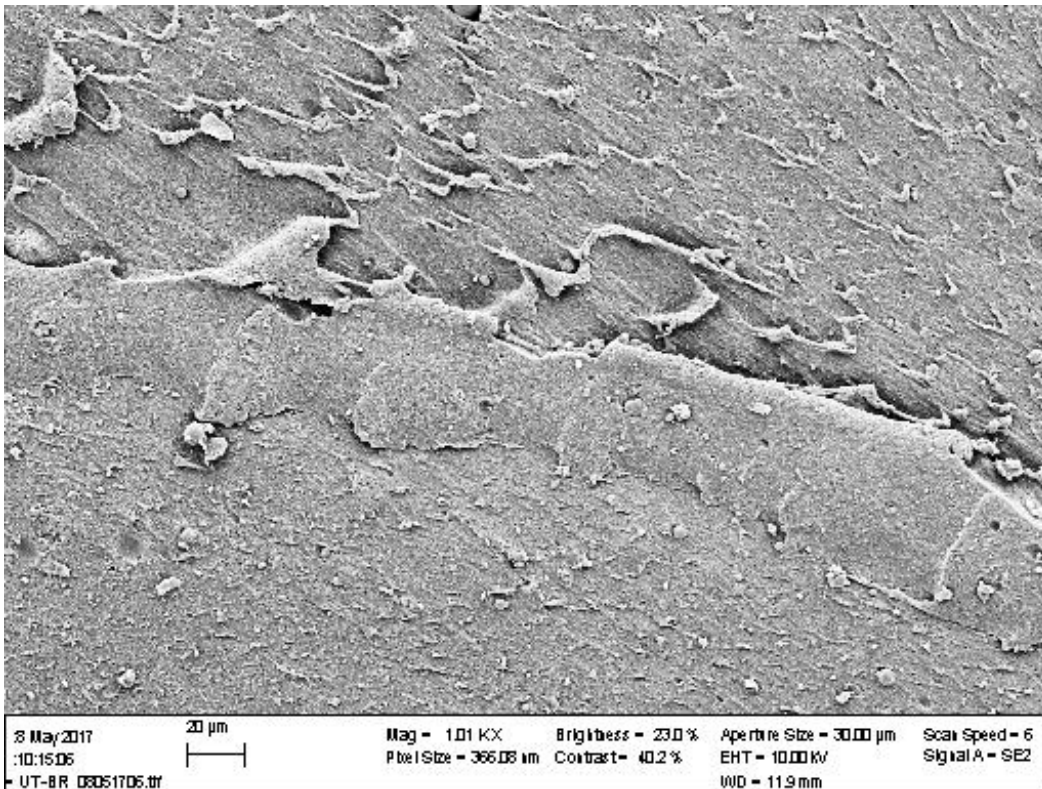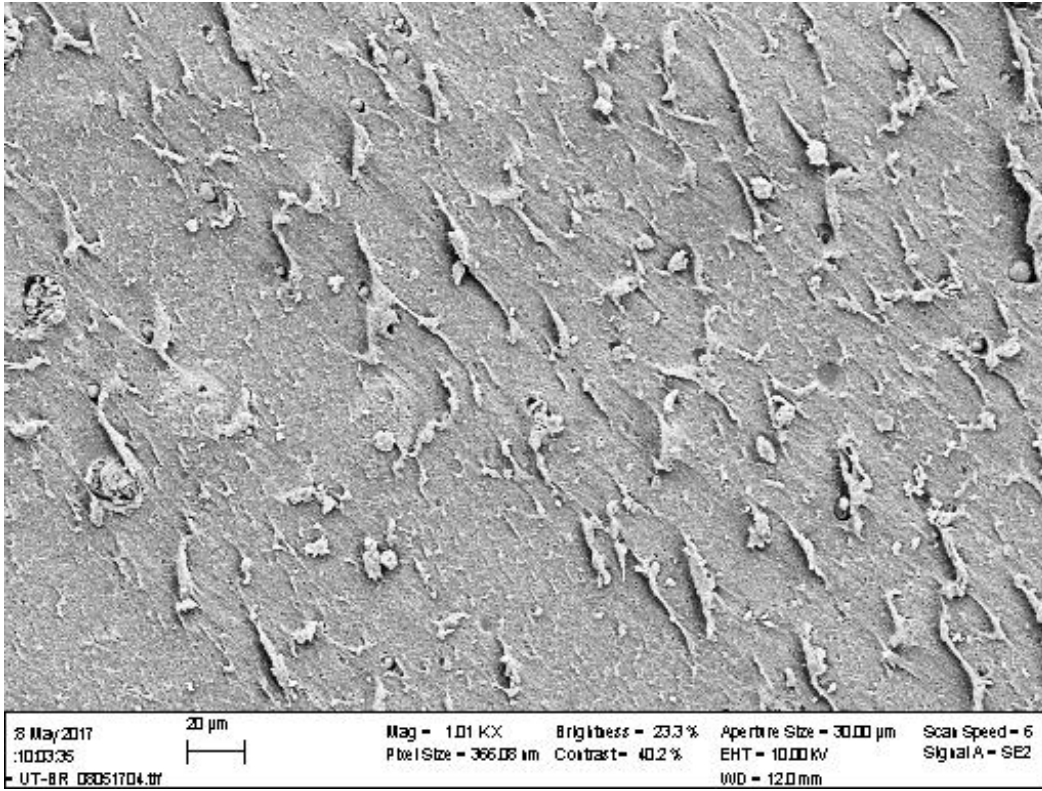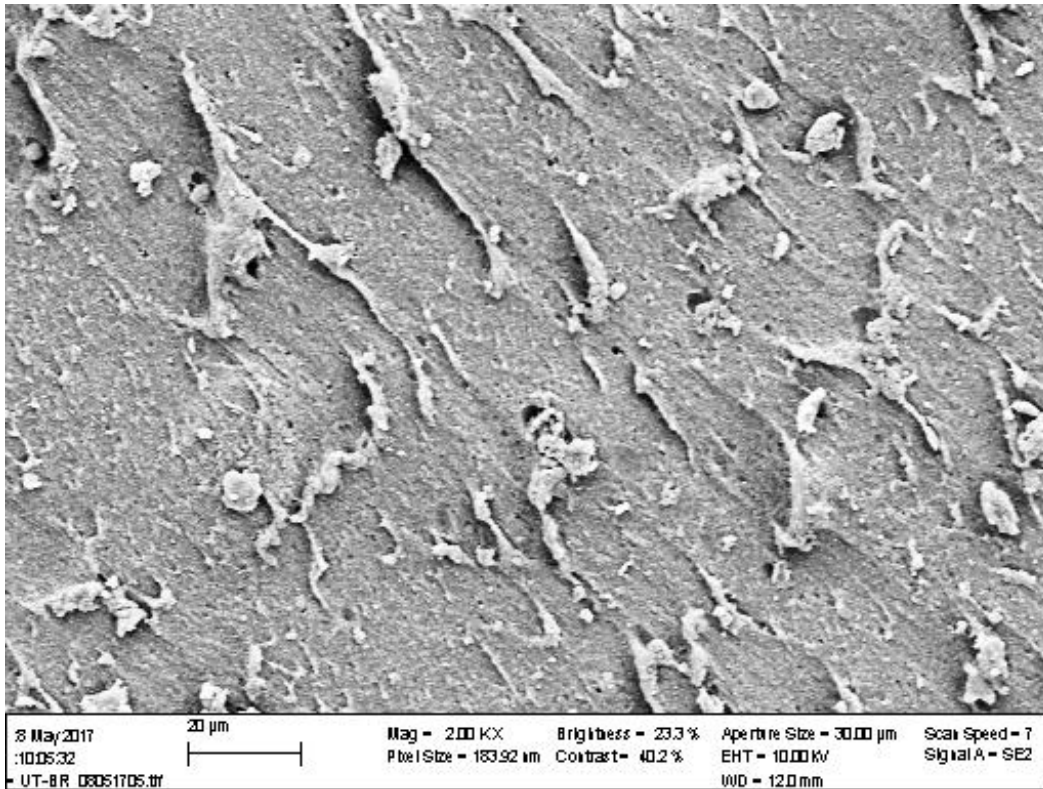
O-ring rubber after acid treatment:
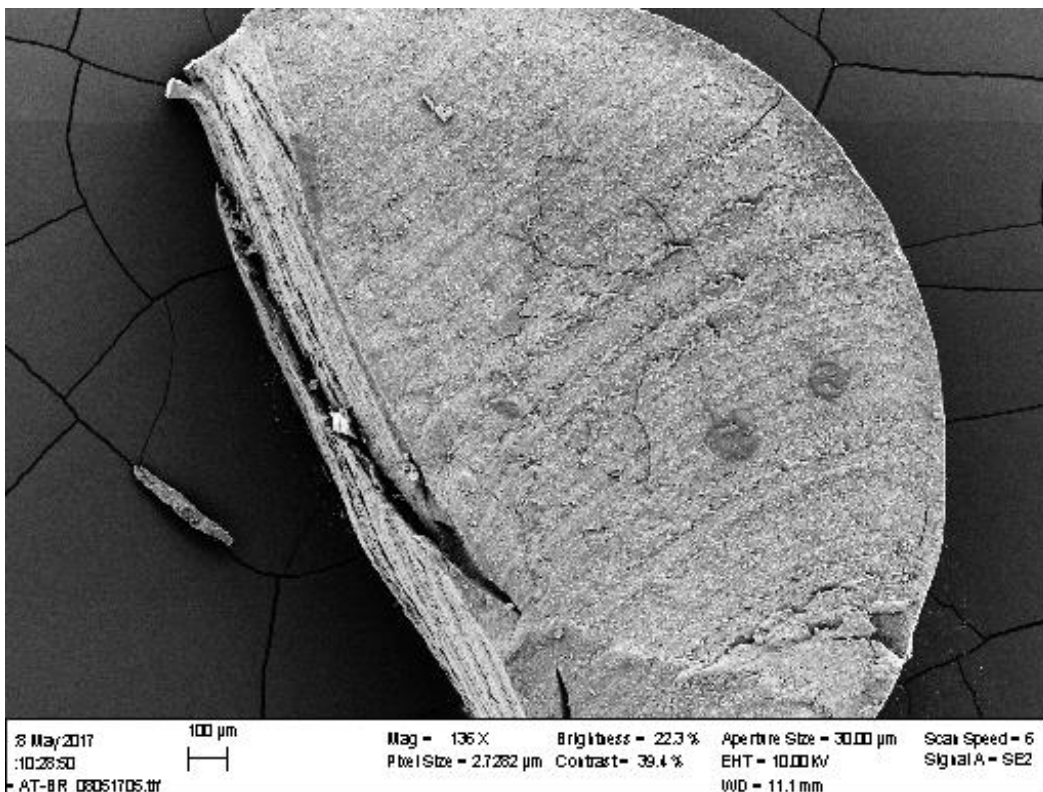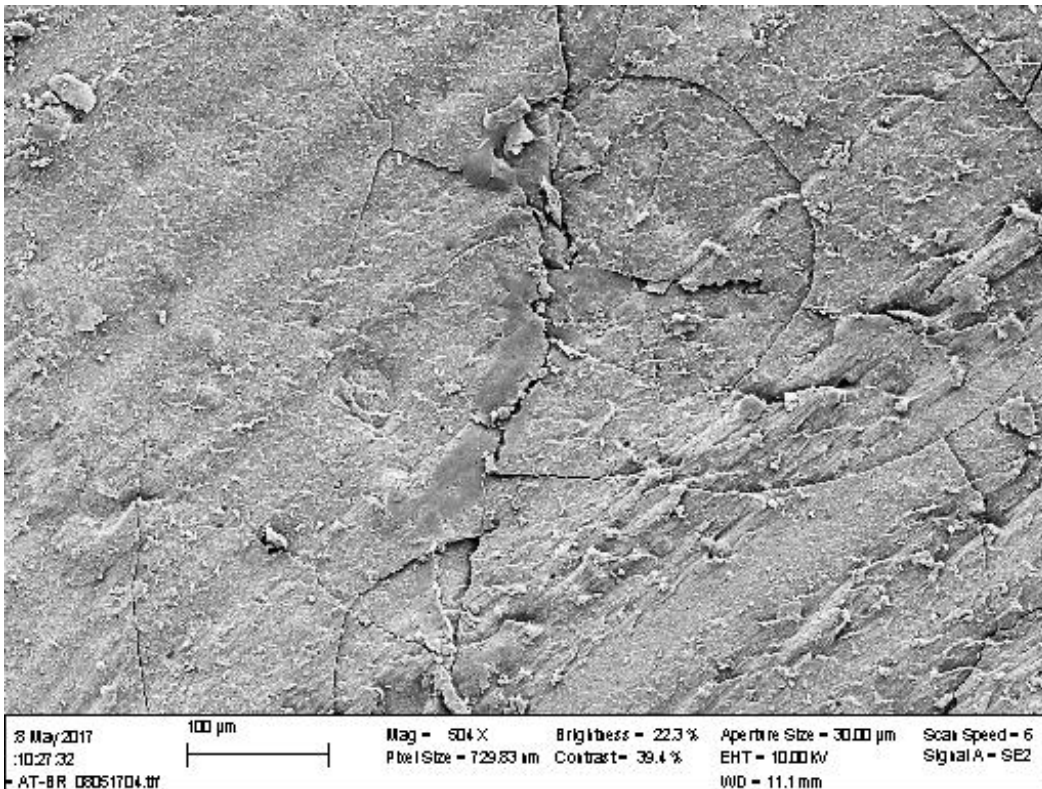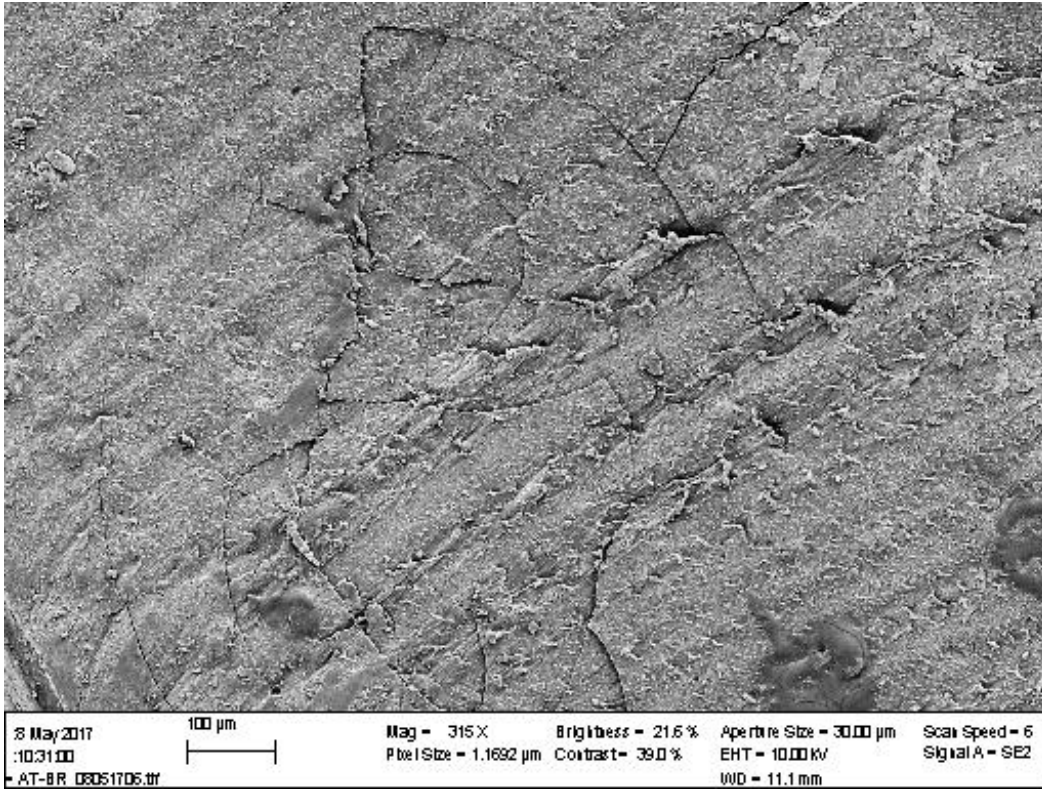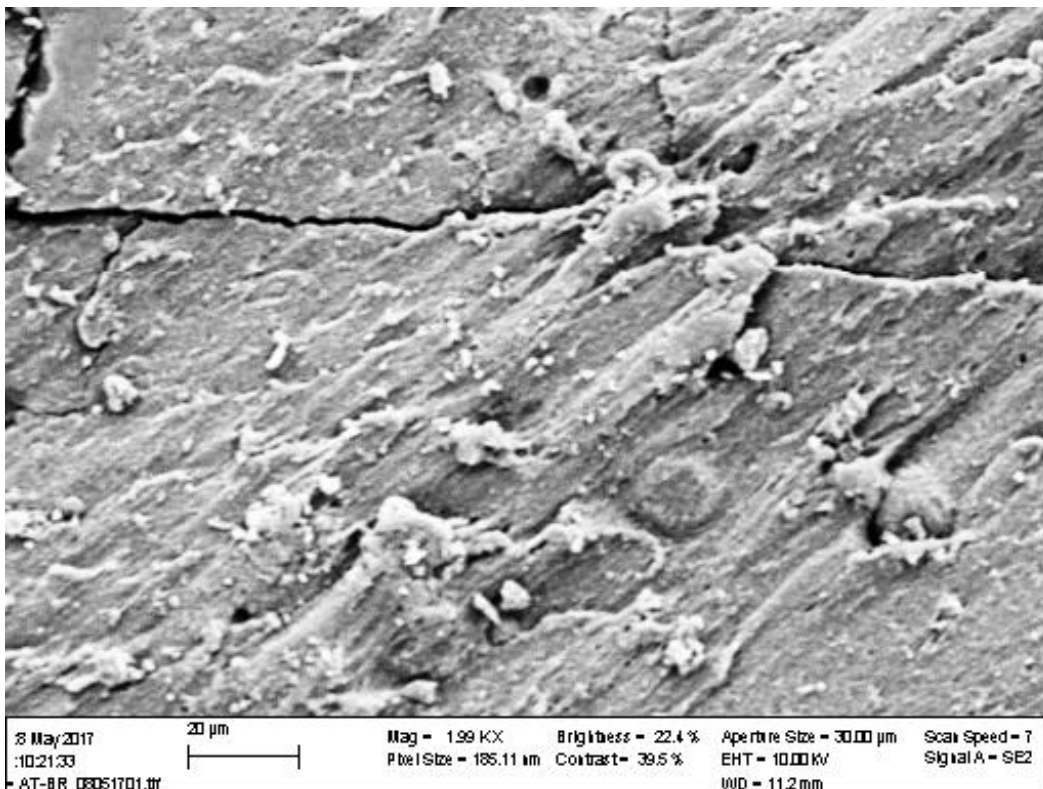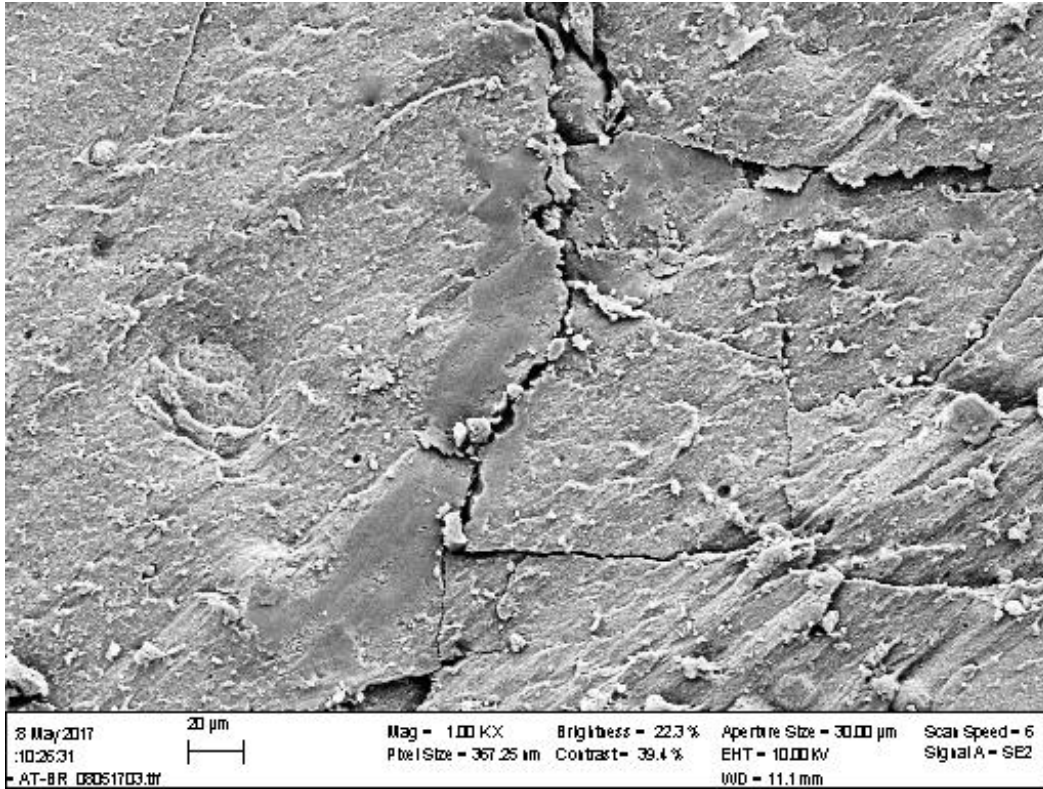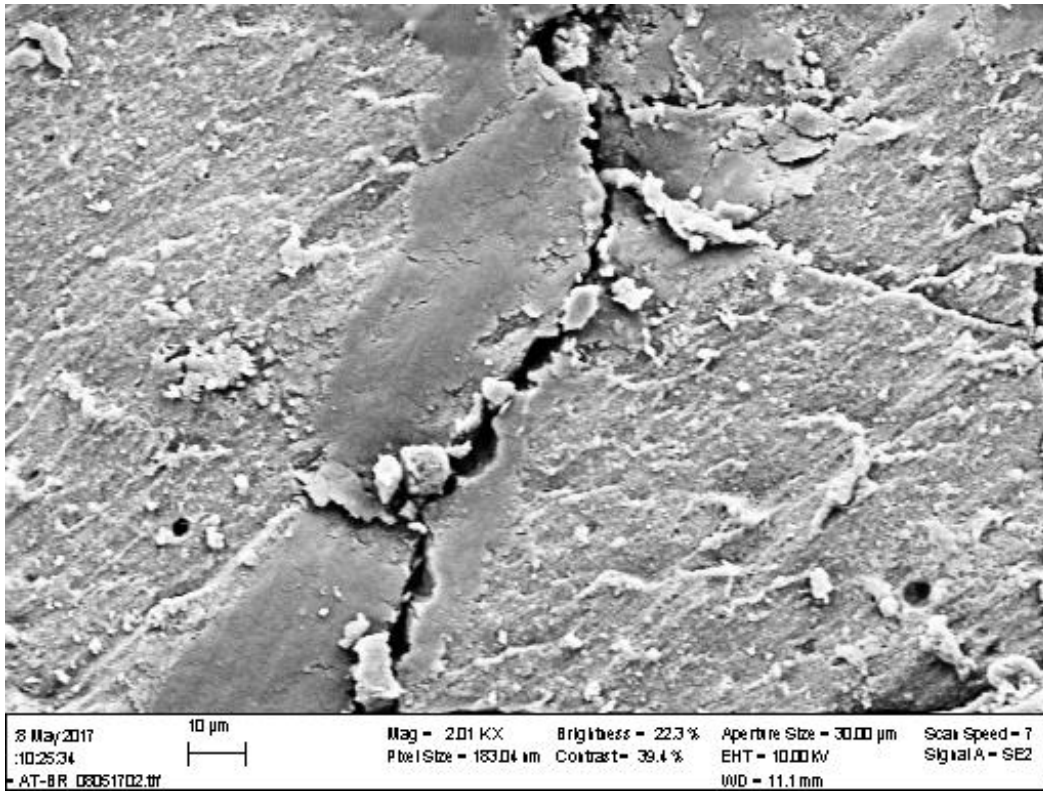
Silicone rubber before acid treatment:
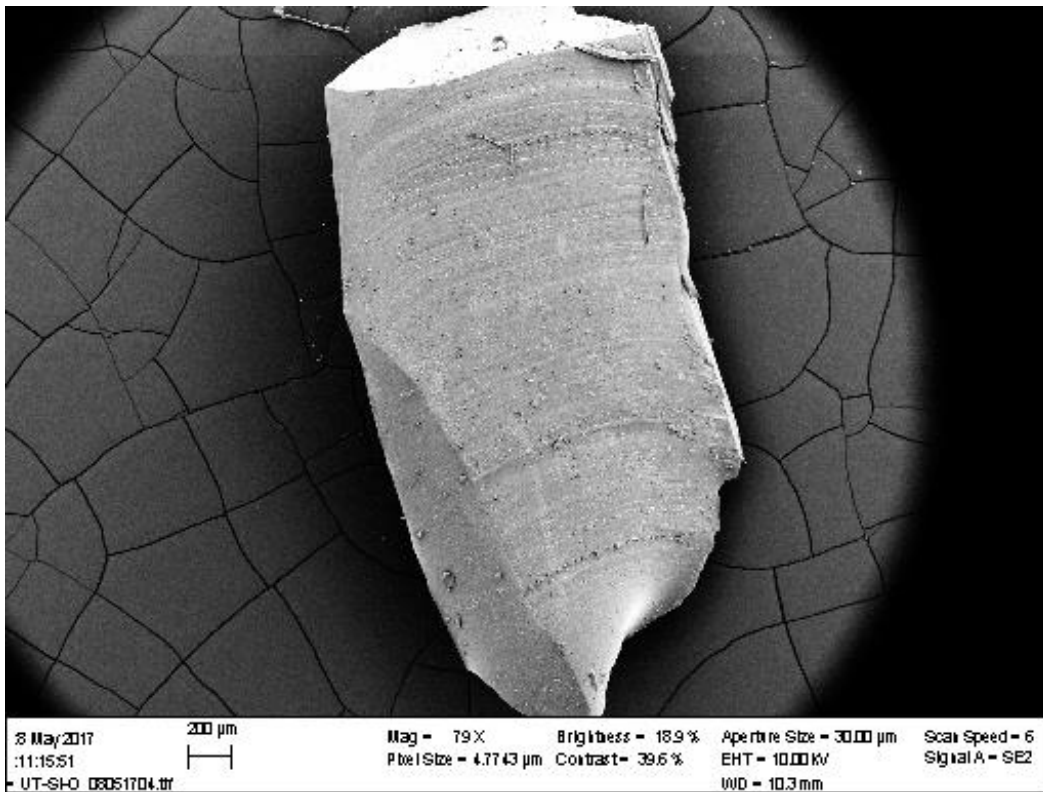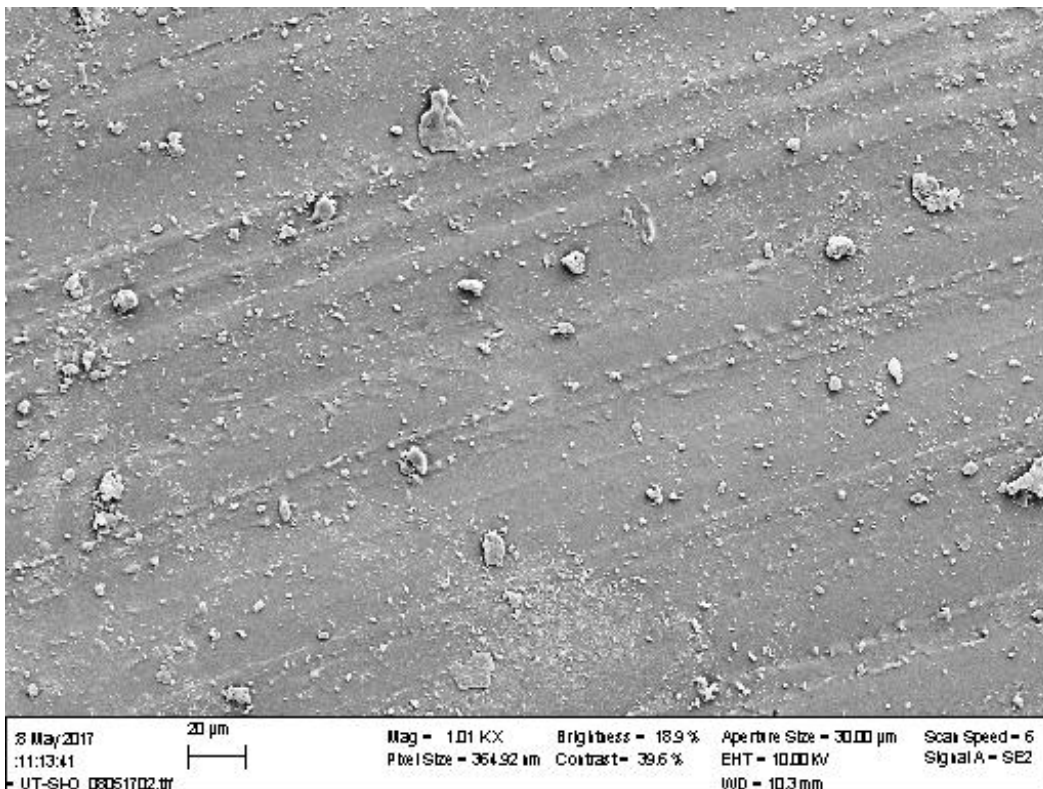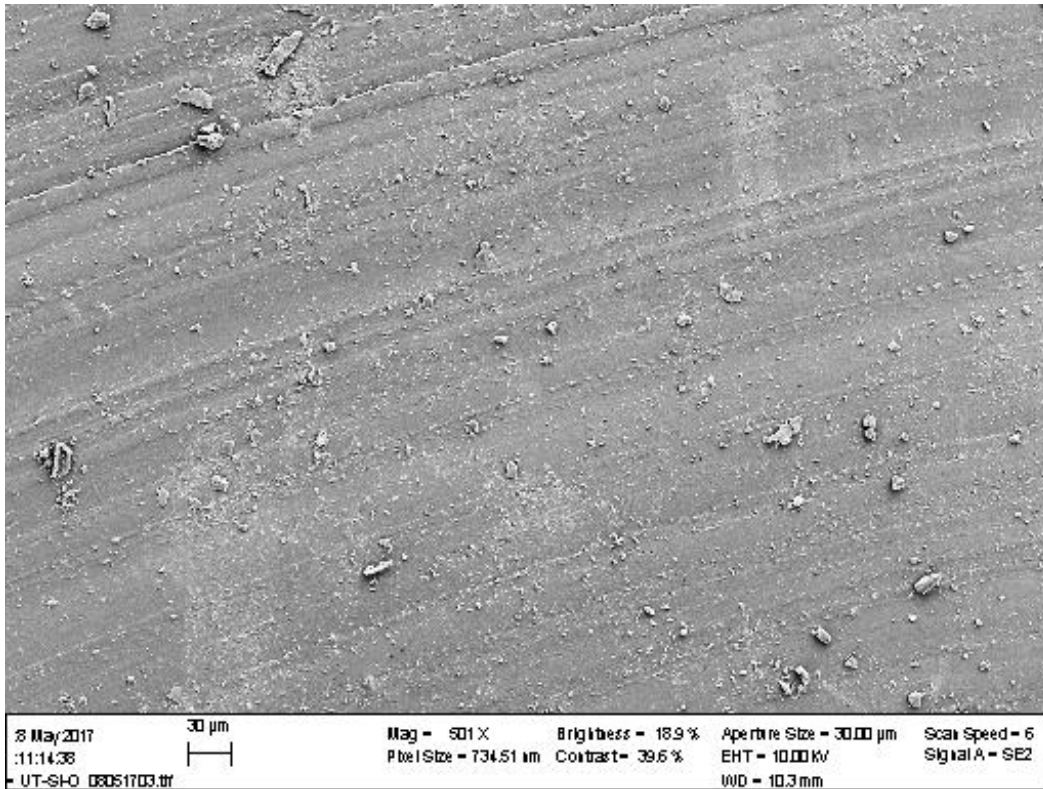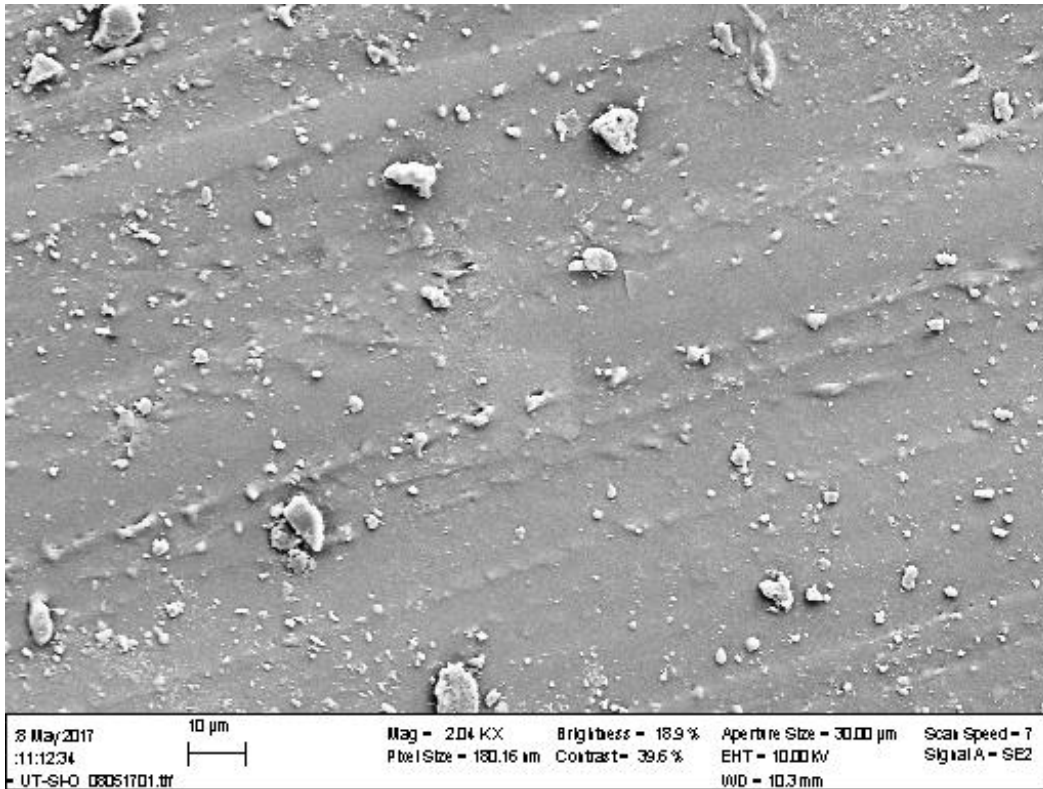
Silicone rubber after acid treatment:
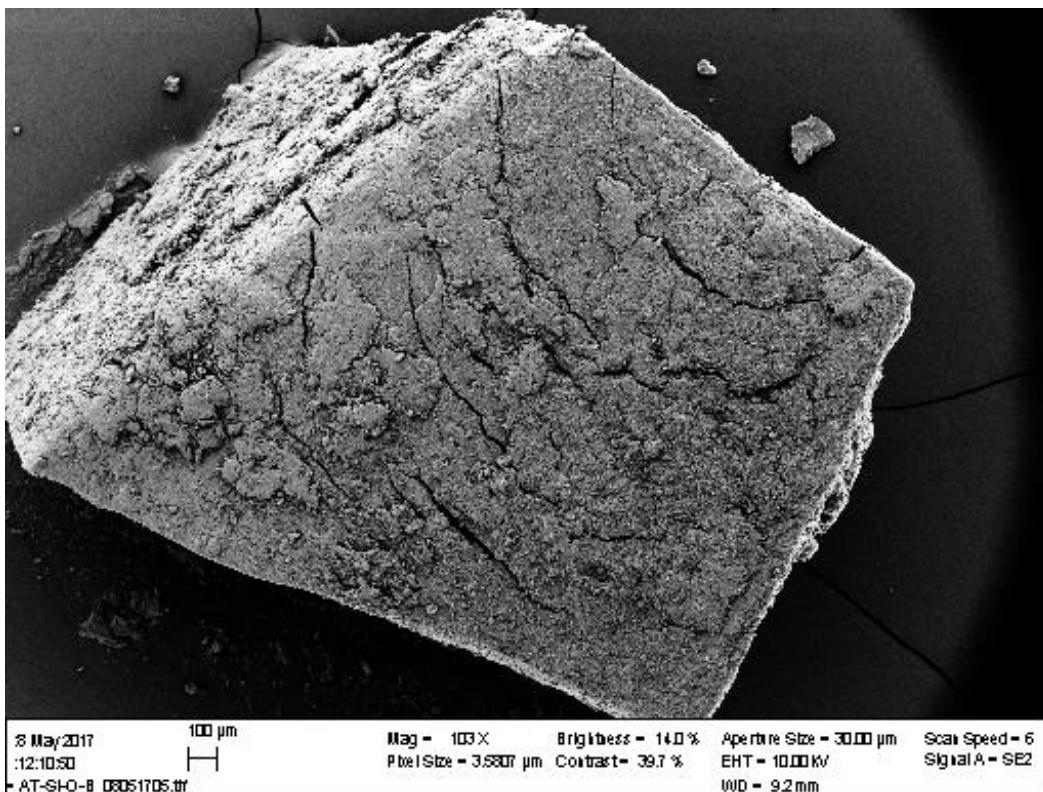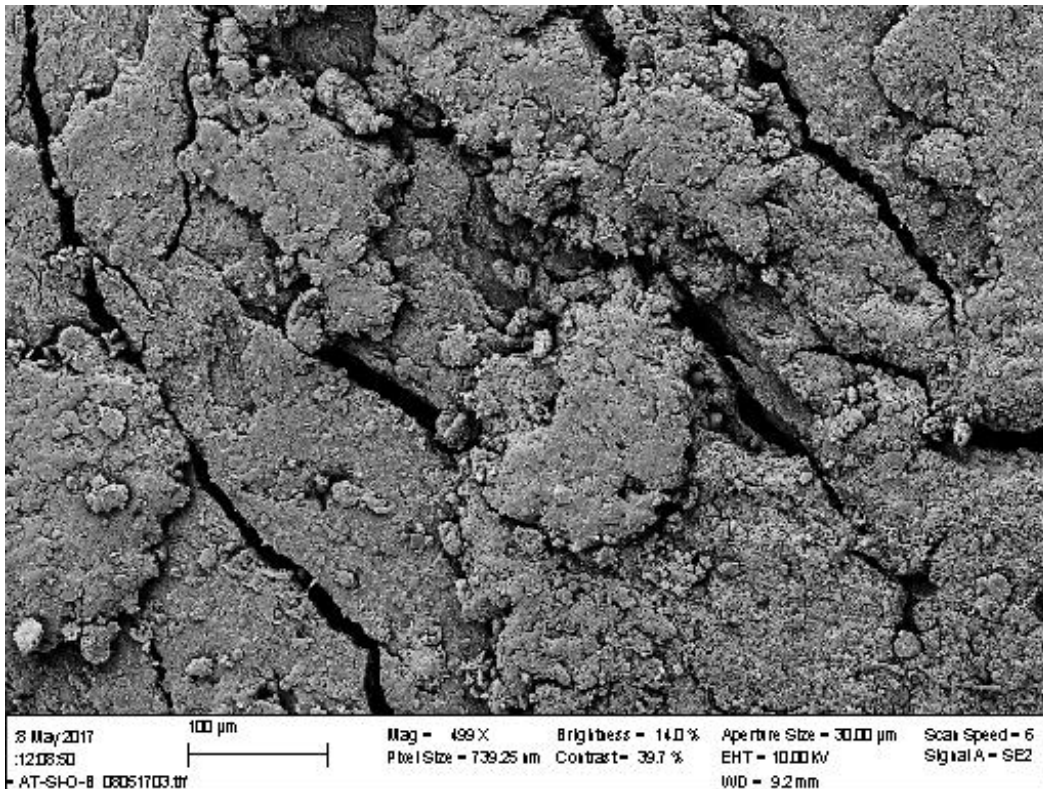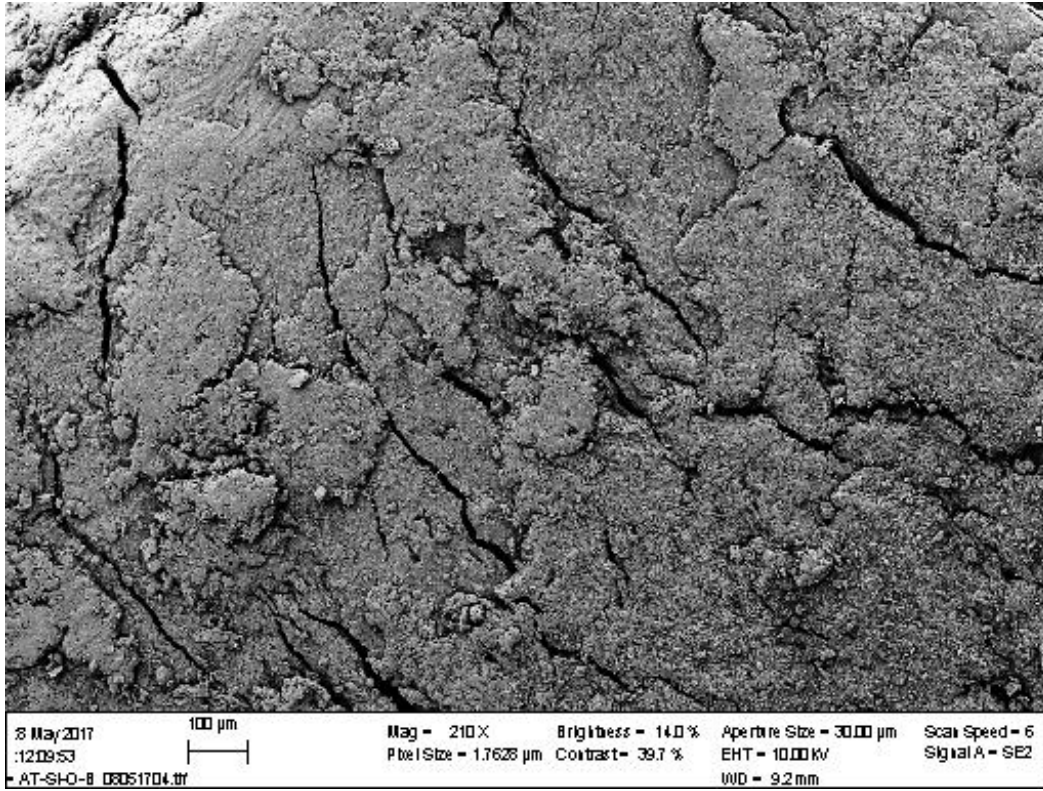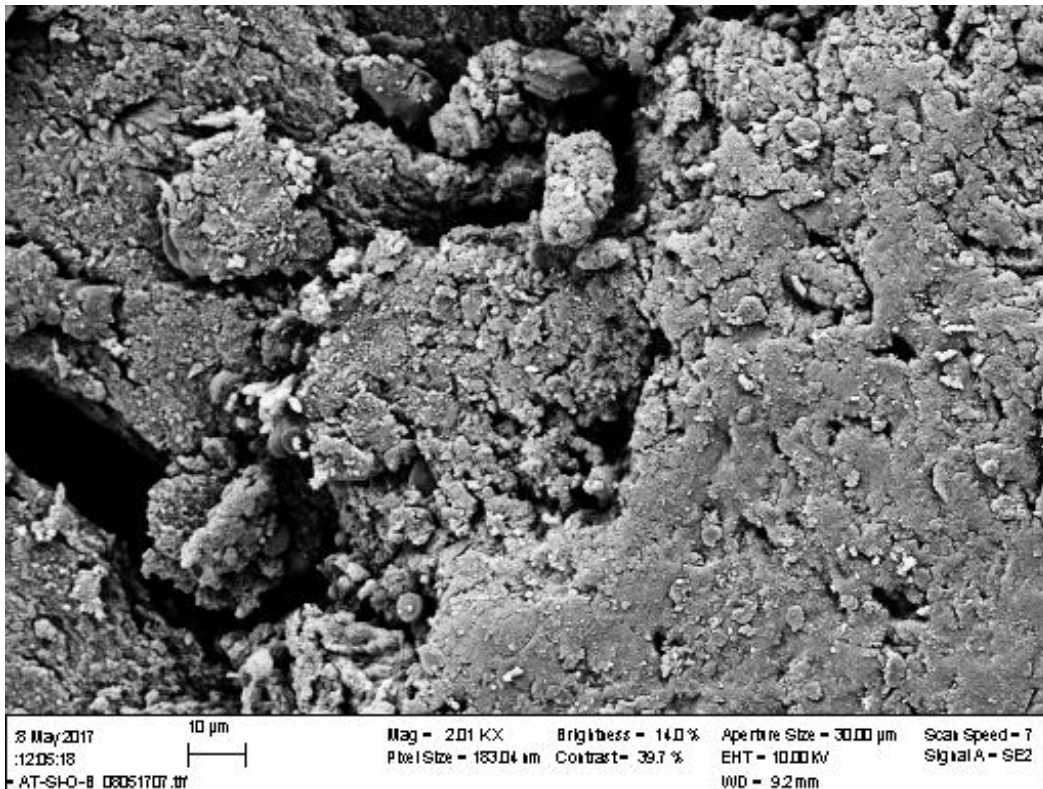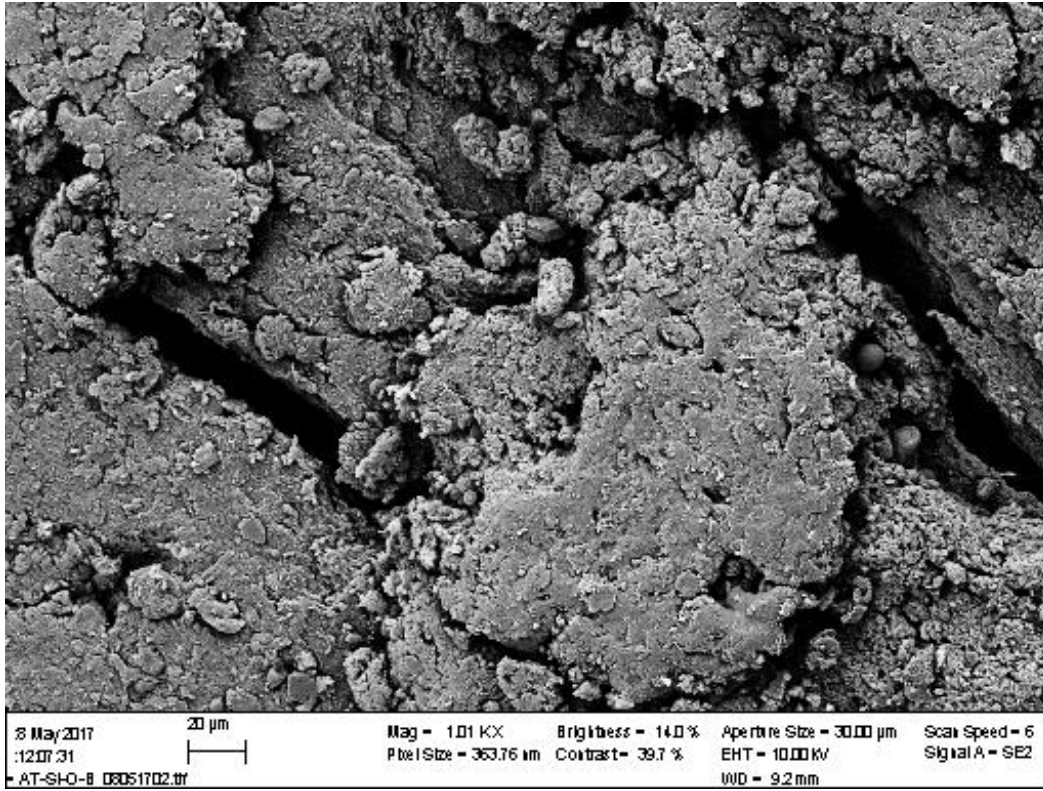
Appendix B: Results from EDS

The EDS of the O-ring rubber and the silicone rubber.

O-ring rubber before acid treatment:
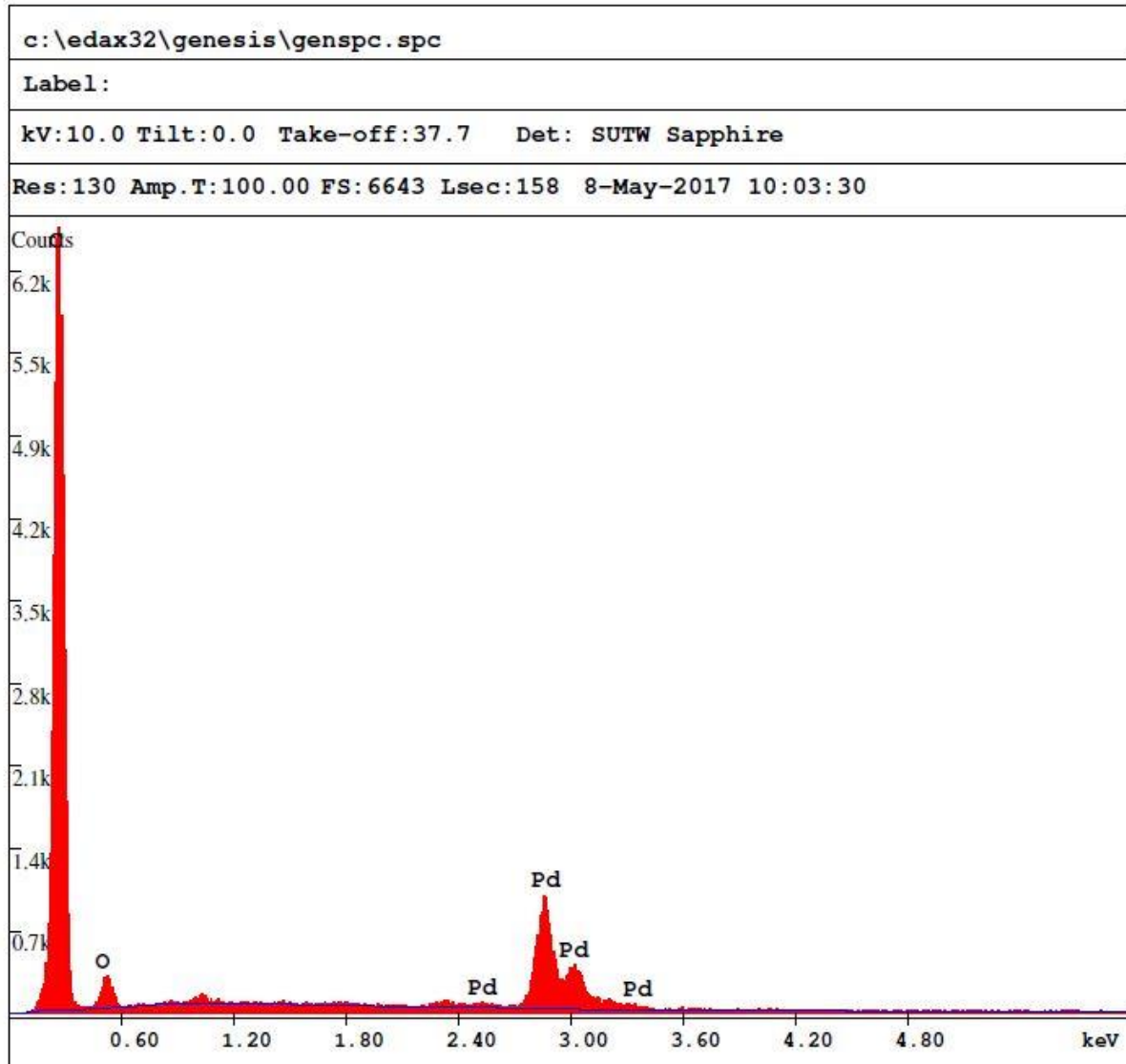
```
c:\edax32\genesis\genspc.spc

Label:

kV:10.0 Tilt:0.0 Take-off:37.7    Det: SUTW Sapphire

Res:130 Amp.T:100.00 FS:6643 Lsec:158  8-May-2017 10:03:30
```



```
EDAX ZAF Quantification (Standardless)
Element Normalized
SEC Table : User   c:\edax32\eds\genuser.sec

Element    Wt %      At %    K-Ratio      Z         A         F
   C K    91.85     93.76    0.8805    1.0018    0.9569    1.0001
   O K     8.15      6.24    0.0271    0.9797    0.3400    1.0000
  Total  100.00    100.00

Element   Net Inte.    Bkgd Inte.    Inte. Error       P/B
   C K     206.28         1.00          0.56         205.57
   O K       9.63         1.90          3.02           5.07
```

O-ring rubber after acid treatment:
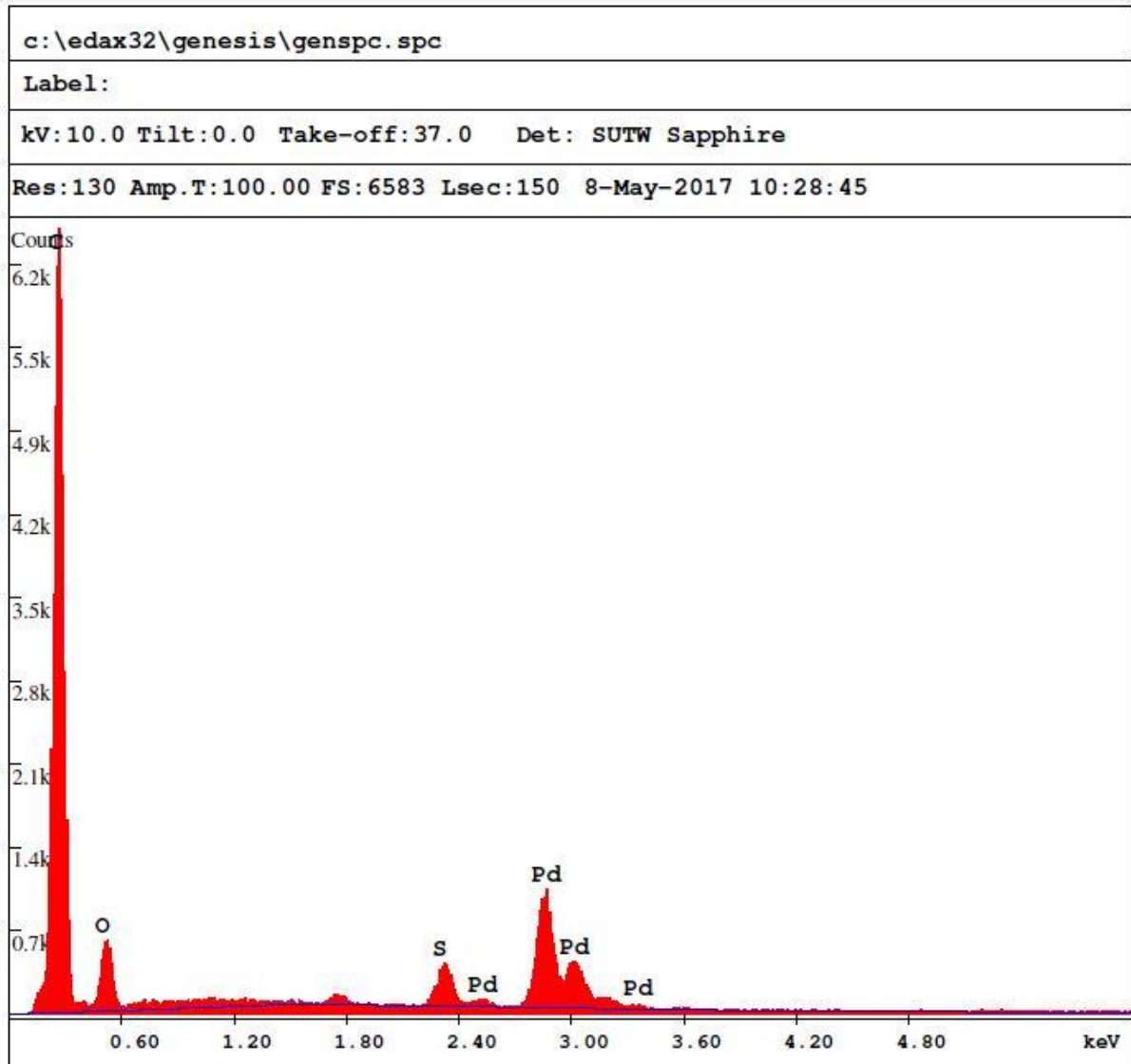

```
c:\edax32\genesis\genspc.spc
Label:
kV:10.0 Tilt:0.0 Take-off:37.0   Det: SUTW Sapphire
Res:130 Amp.T:100.00 FS:6583 Lsec:150  8-May-2017 10:28:45
```

```
EDAX ZAF Quantification (Standardless)
Element Normalized
SEC Table : User  c:\edax32\eds\genuser.sec

Element    Wt %     At %    K-Ratio    Z         A         F
  C K     82.15    88.73    0.4888    1.0090    0.5897    1.0001
  O K      9.97     8.08    0.0335    0.9866    0.3406    1.0000
  S K      7.88     3.19    0.0724    0.9144    1.0047    1.0000
  Total  100.00   100.00

Element   Net Inte.    Bkgd Inte.    Inte. Error      P/B
  C K     211.30         0.48          0.56         442.46
  O K      21.99         0.94          1.81          23.35
  S K      17.39         4.17          2.38           4.18
```

Silicone rubber before acid treatment:
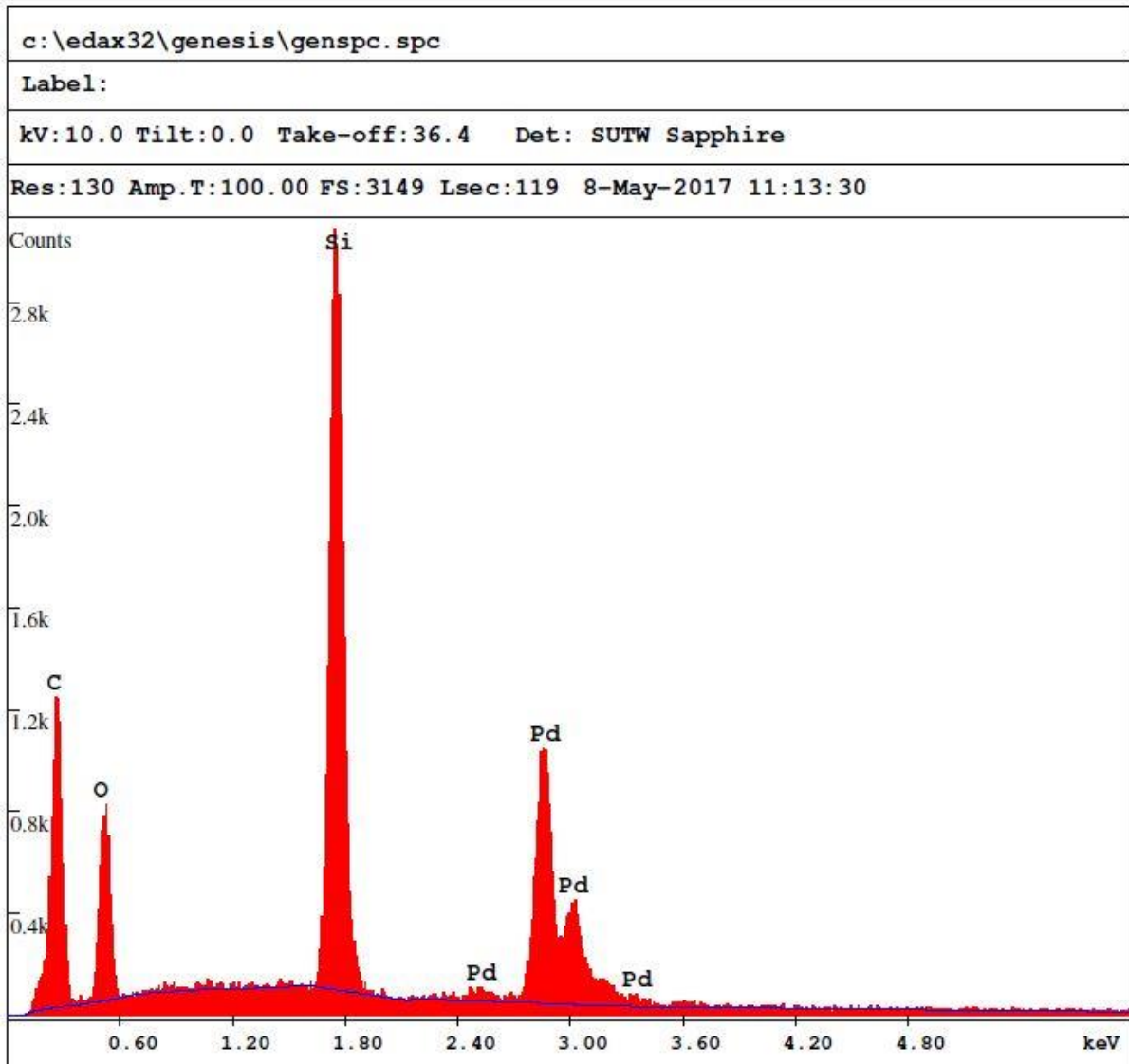
```
c:\edax32\genesis\genspc.spc
Label:
kV:10.0 Tilt:0.0 Take-off:36.4    Det: SUTW Sapphire
Res:130 Amp.T:100.00 FS:3149 Lsec:119  8-May-2017 11:13:30
```



```
EDAX ZAF Quantification (Standardless)
Element Normalized
SEC Table : User  c:\edax32\eds\genuser.sec

Element   Wt %    At %    K-Ratio    Z        A        F
  C K    50.51   65.14    0.1658   1.0284   0.3192   1.0001
  O K    18.18   17.60    0.0735   1.0054   0.4022   1.0002
  SiK    31.31   17.26    0.2890   0.9456   0.9762   1.0000
 Total  100.00  100.00

Element   Net Inte.    Bkgd Inte.    Inte. Error      P/B
  C K     52.02         1.54          1.31          33.87
  O K     35.08         3.34          1.69          10.51
  SiK    176.33         7.59          0.72          23.22
```

Silicone rubber after acid treatment:
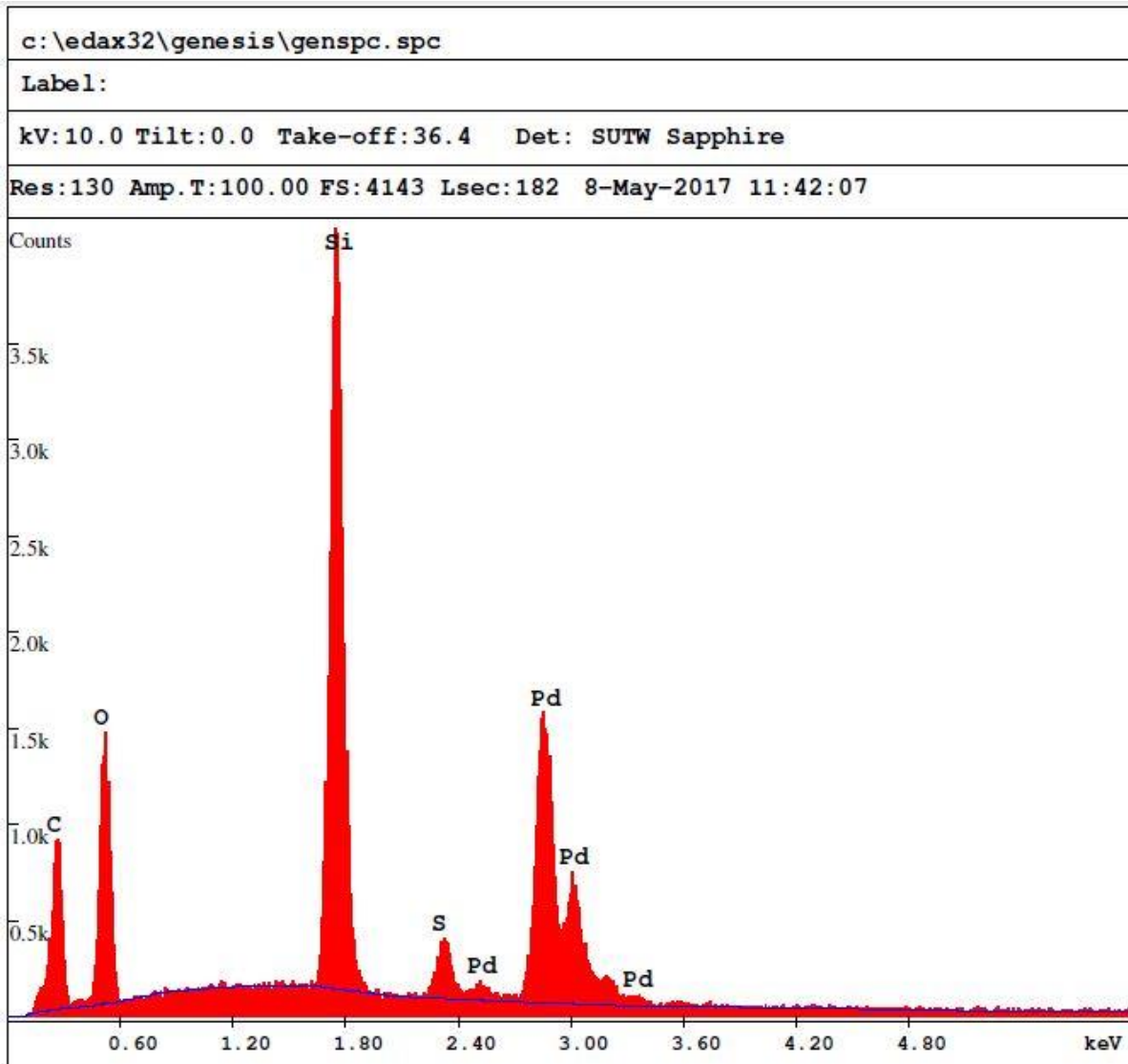

```
c:\edax32\genesis\genspc.spc

Label:

kV:10.0 Tilt:0.0 Take-off:36.4   Det: SUTW Sapphire

Res:130 Amp.T:100.00 FS:4143 Lsec:182  8-May-2017 11:42:07
```

```
EDAX ZAF Quantification (Standardless)
Element Normalized
SEC Table : User  c:\edax32\eds\genuser.sec

Element    Wt %     At %    K-Ratio    Z        A        F
  C K     36.75    51.97    0.0909   1.0382   0.2381   1.0002
  O K     23.02    24.43    0.0977   1.0148   0.4184   1.0002
  SiK     30.48    18.43    0.2832   0.9551   0.9704   1.0028
  S K      9.75     5.17    0.0853   0.9419   0.9284   1.0000
 Total   100.00   100.00

Element   Net Inte.    Bkgd Inte.    Inte. Error      P/B
  C K      25.03         1.17          1.55         21.48
  O K      40.98         2.48          1.22         16.53
  SiK     151.87         7.14          0.63         21.28
  S K      13.11         5.11          2.73          2.57
```

Appendix C: Results from Casing – Cement bond strength test

Force vs Time from the Casing – Cement bond strength test.

Some specimens had zero bond strength, there is no graph shown for these.

CC-I-4

CC-I-5

CC-I-6

CC-I-7

CC-I-8

CC-I-9

CC-II-1

CC-II-2

CC-II-7

CC-II-8

CC-II-9

CC-II-10

CC-II-11

CC-II-12

CC-II-14

CC-III-4

CC-III-5

CC-III-7

CC-III-8

CC-III-9
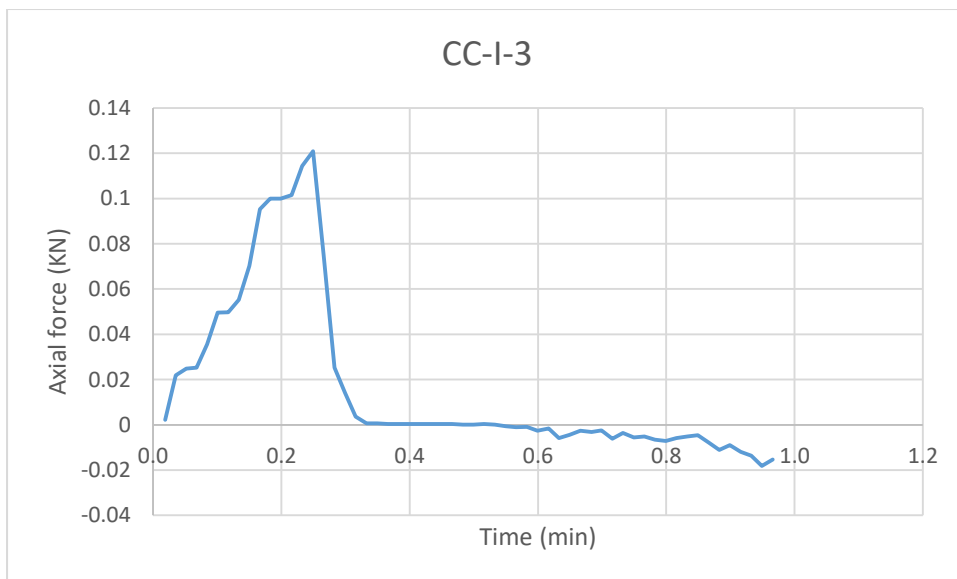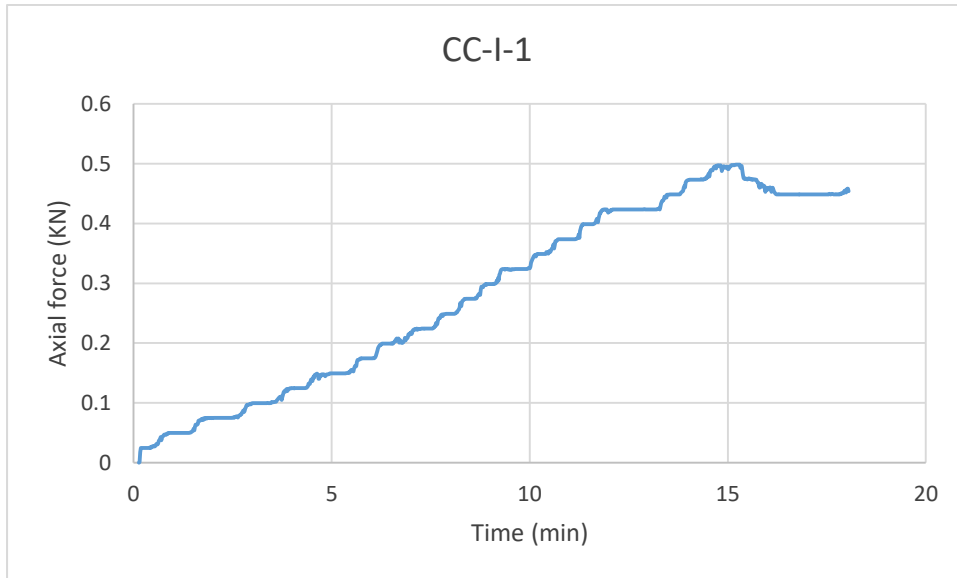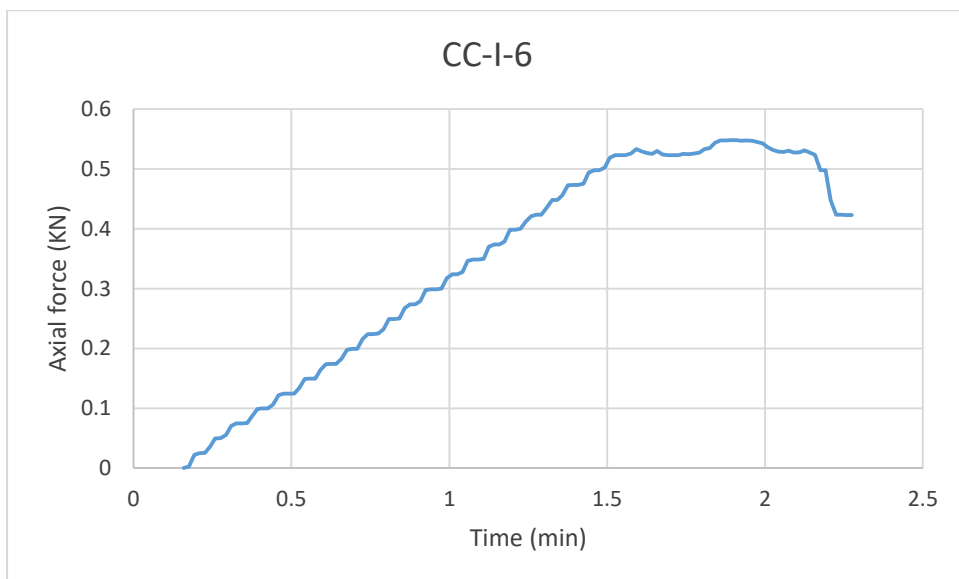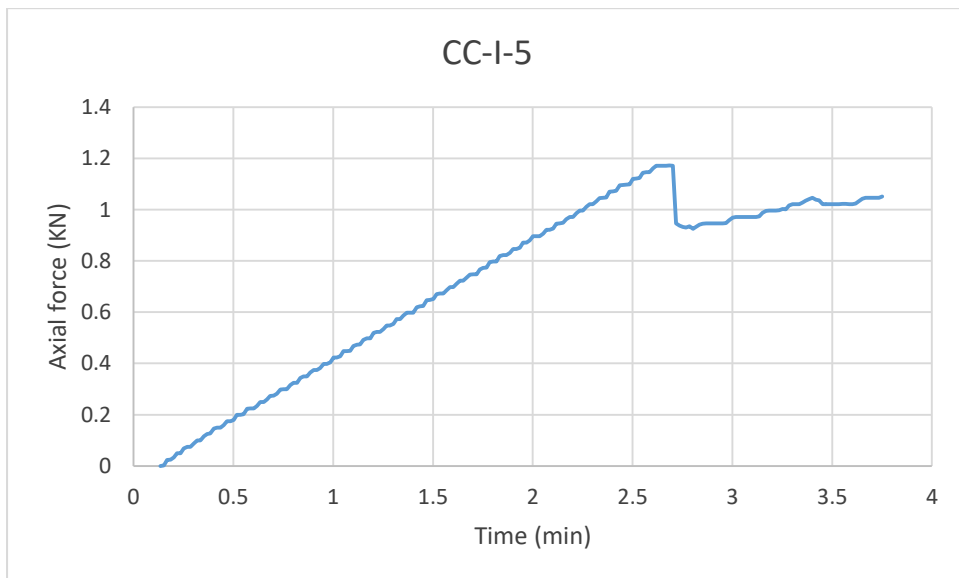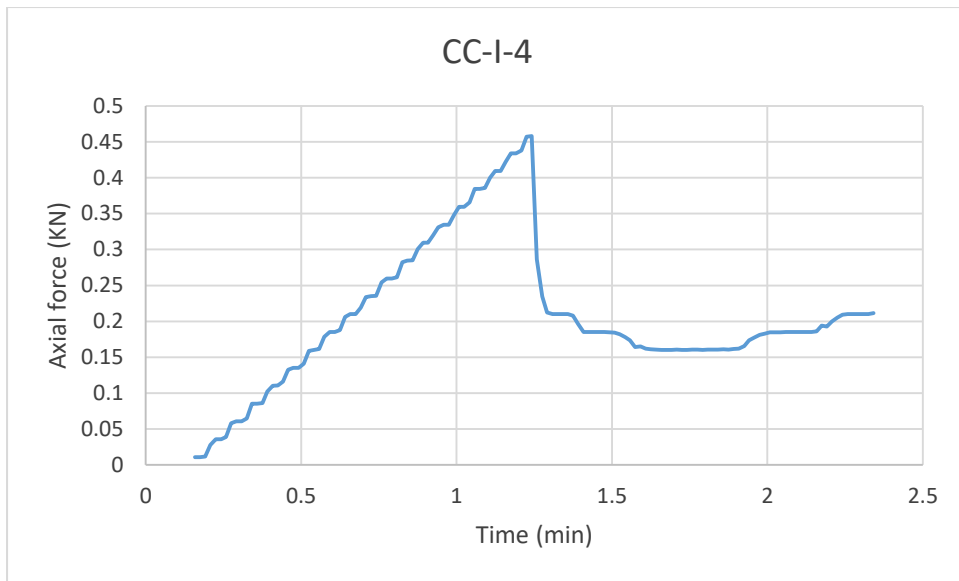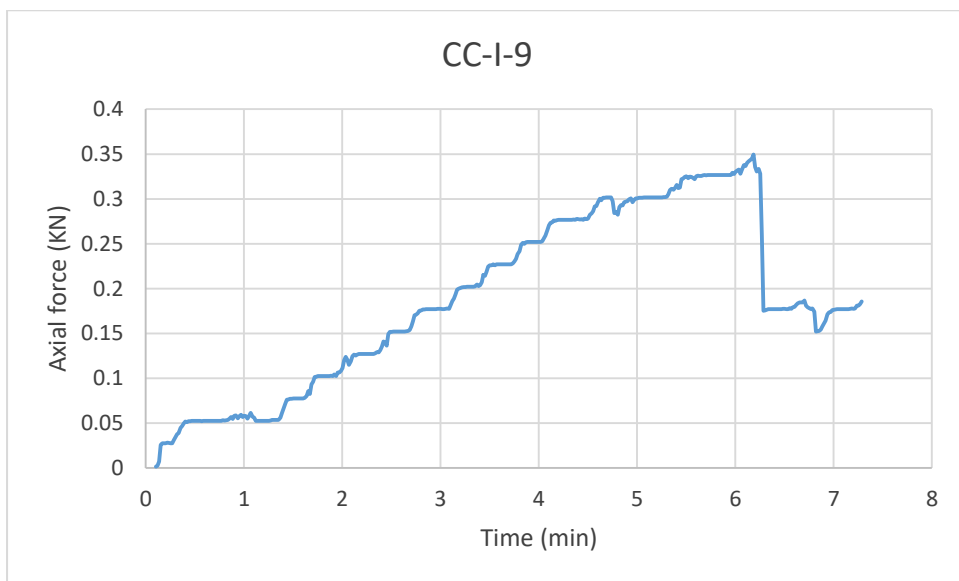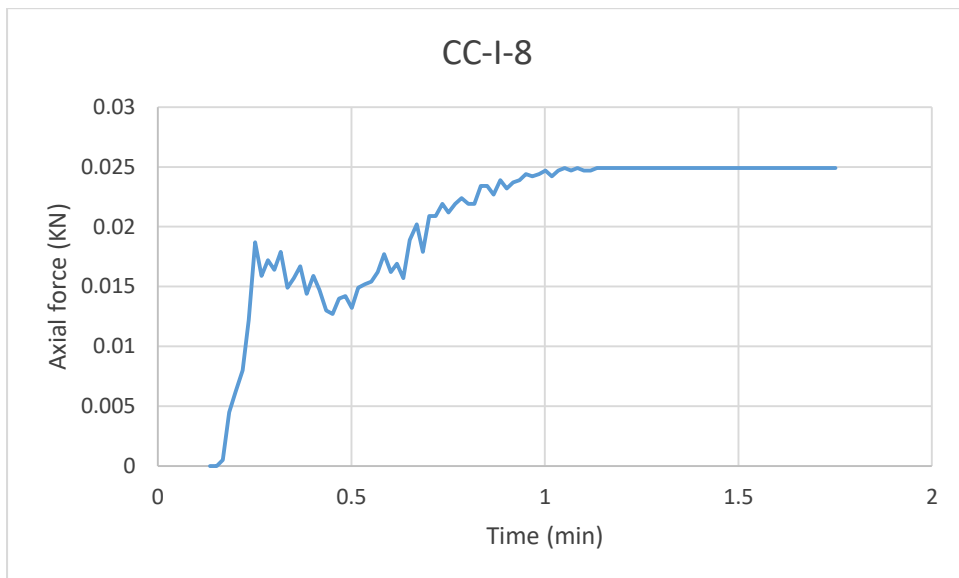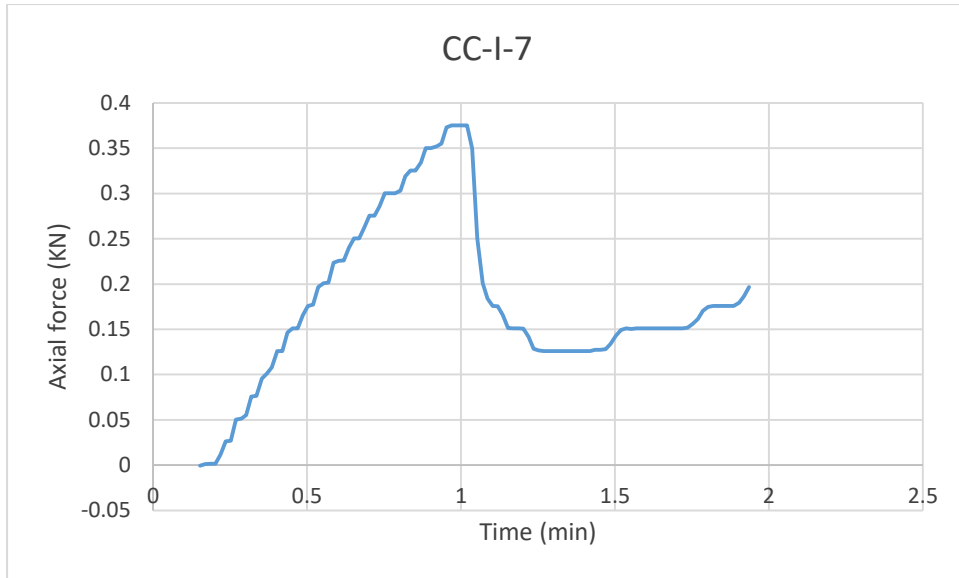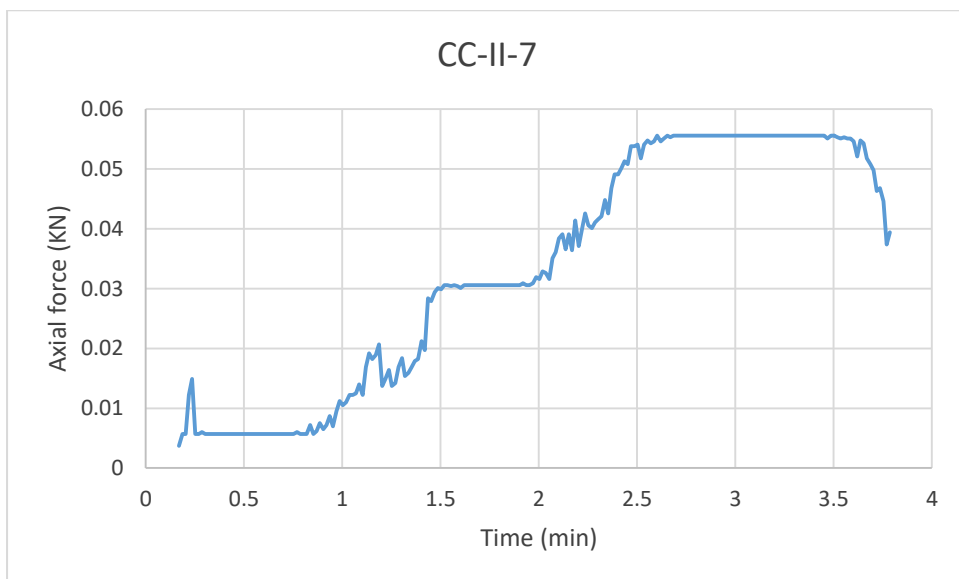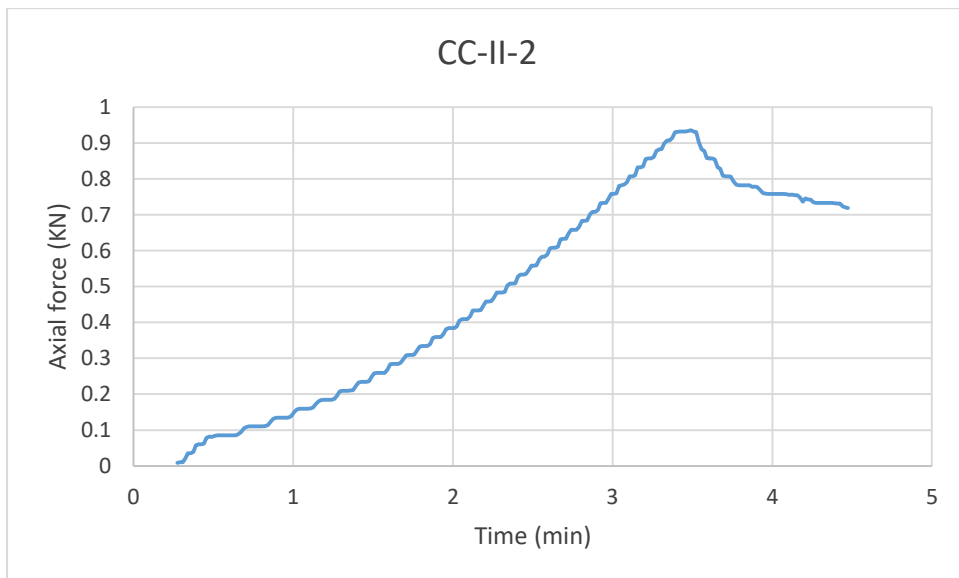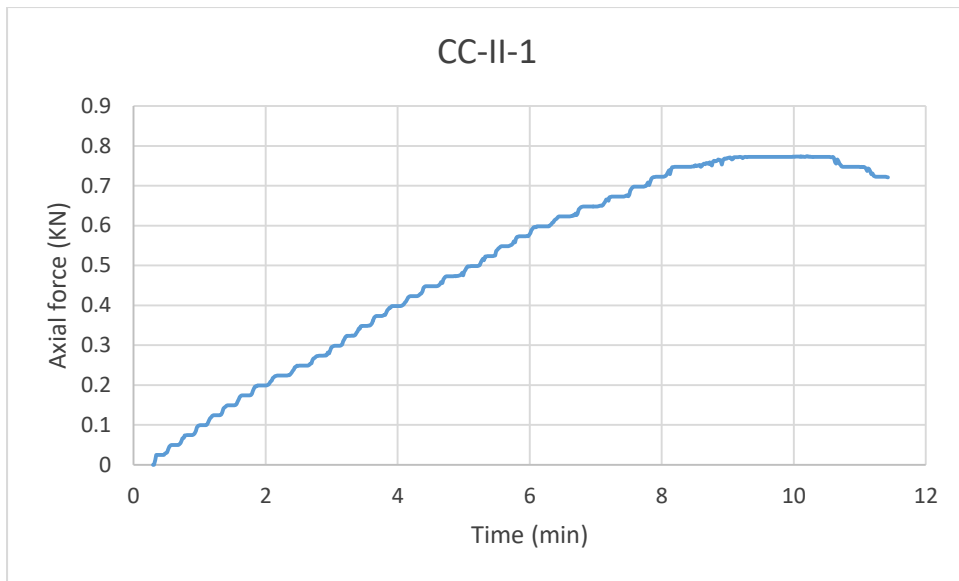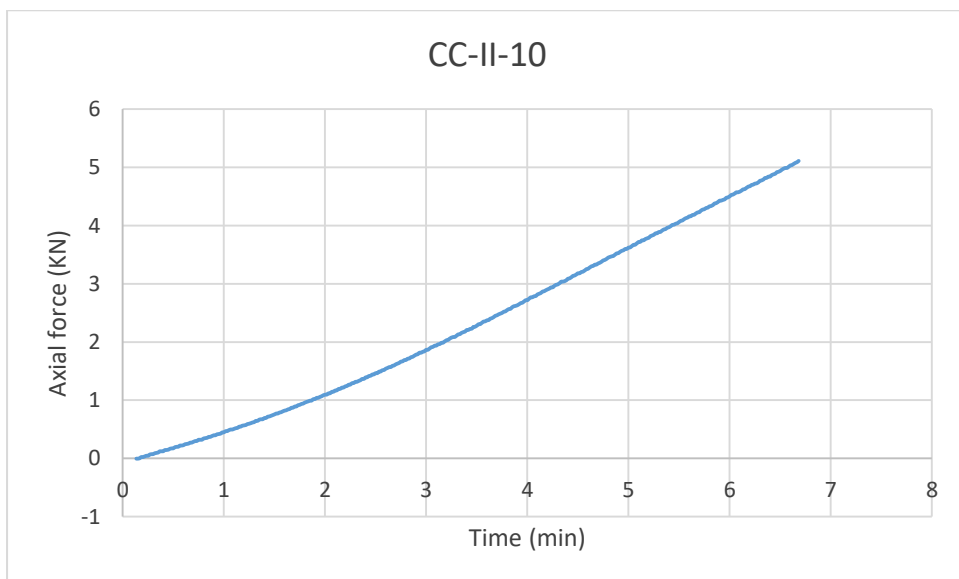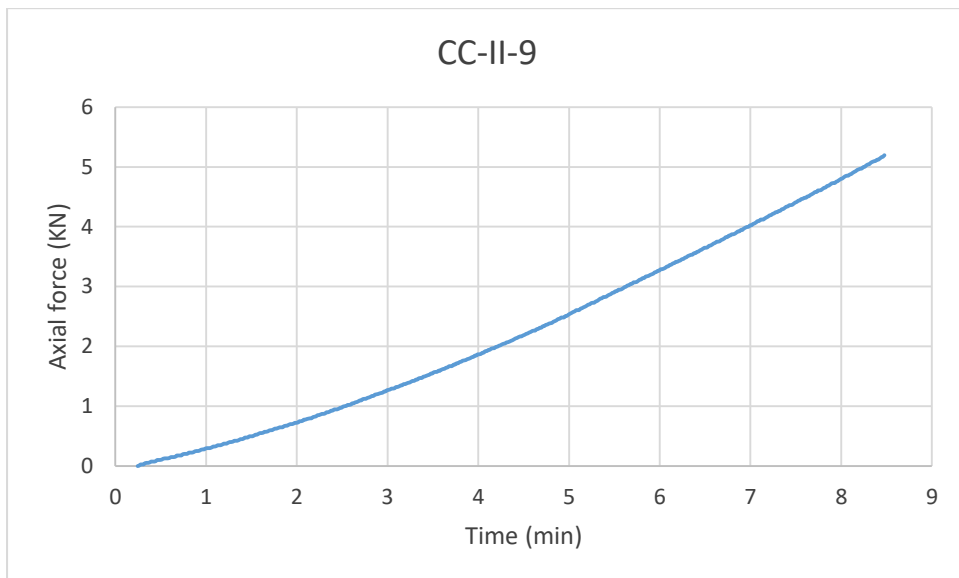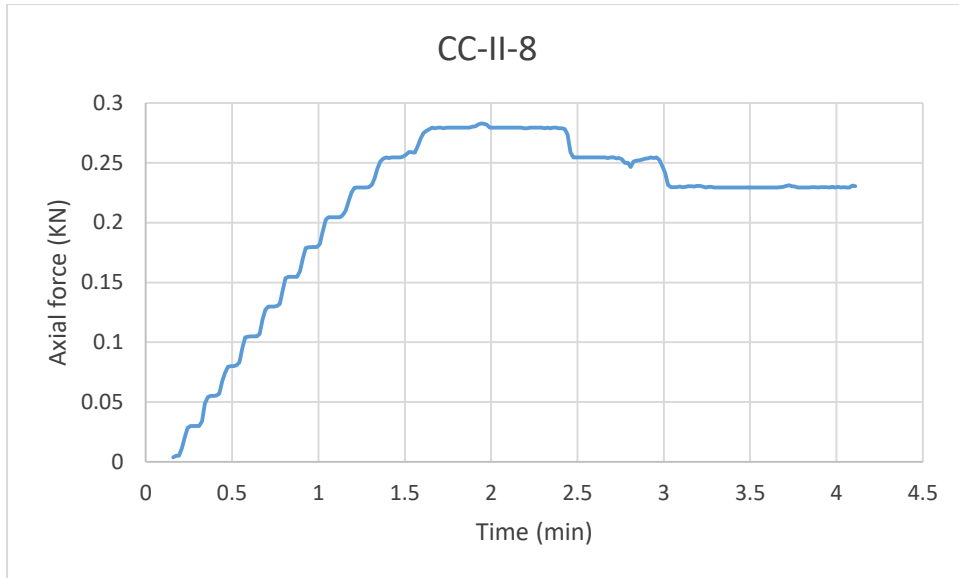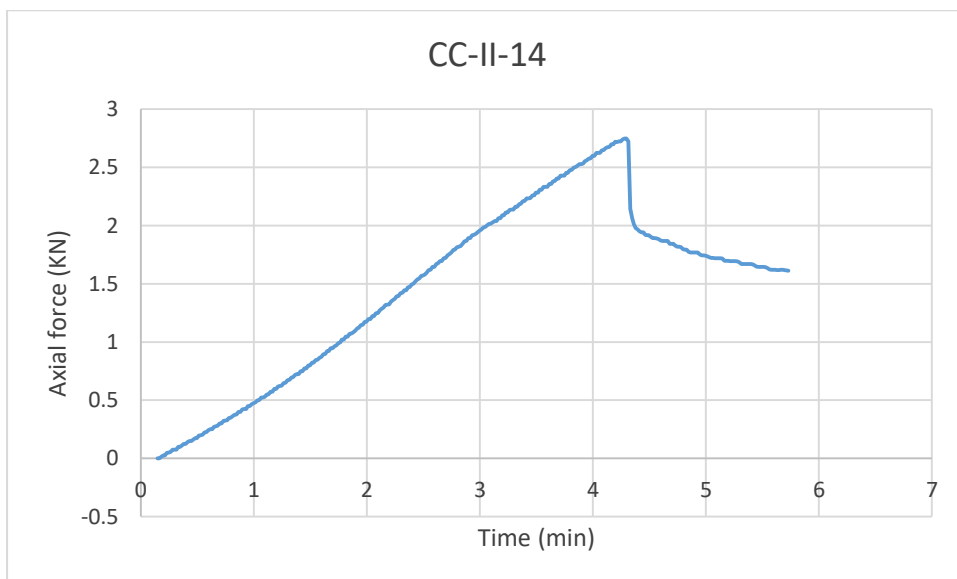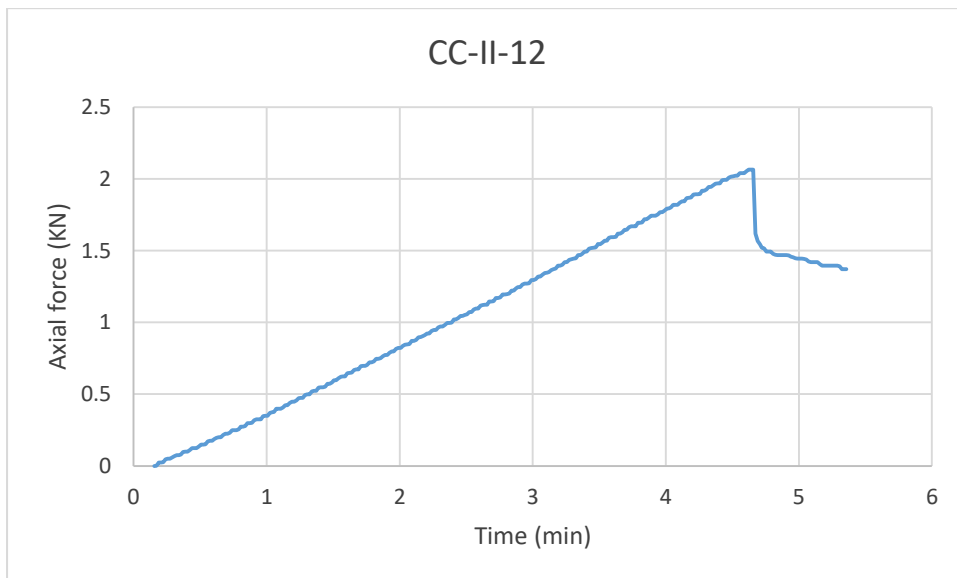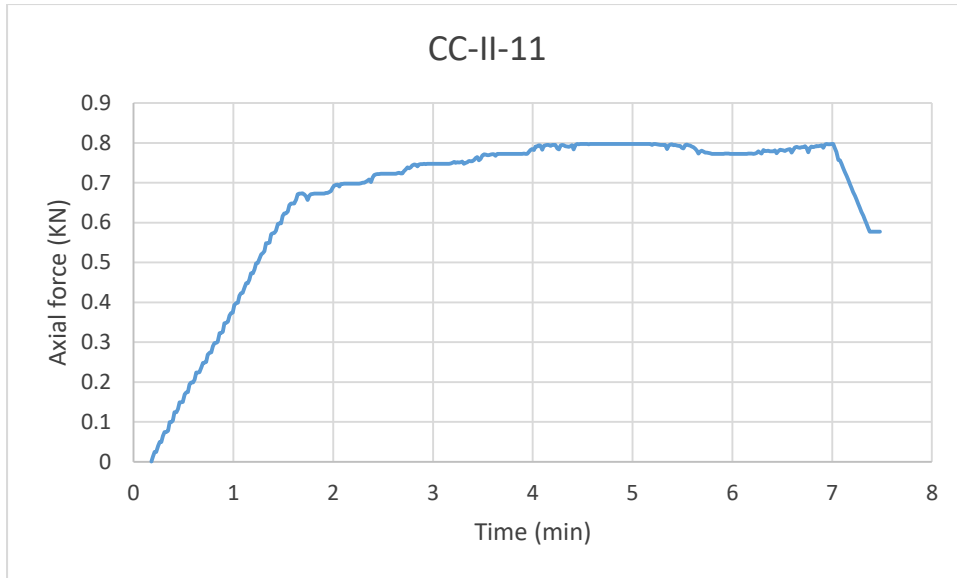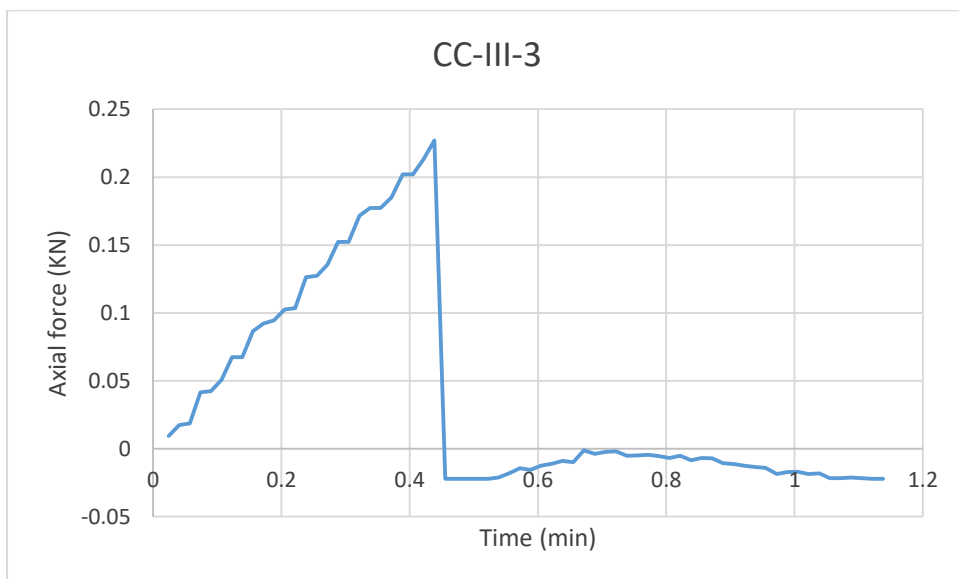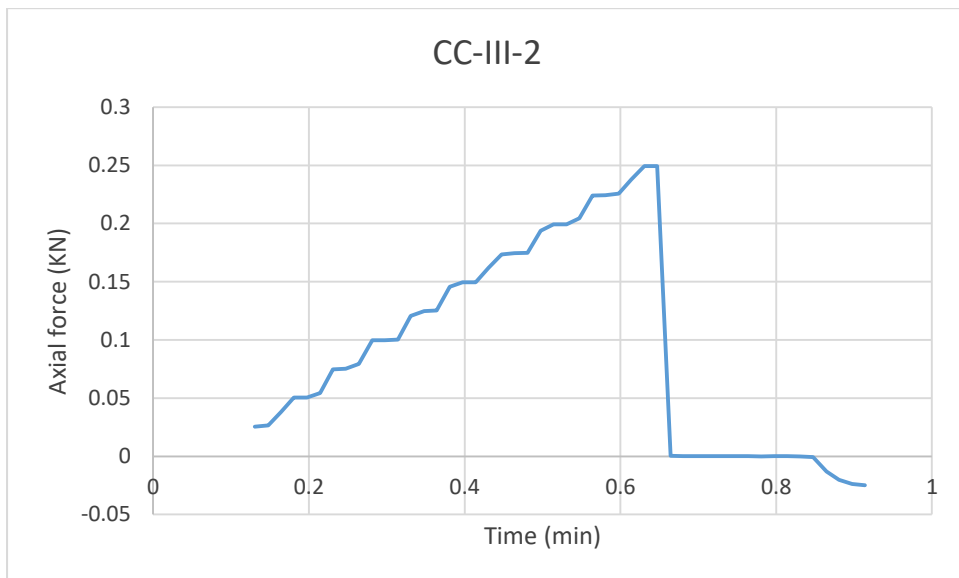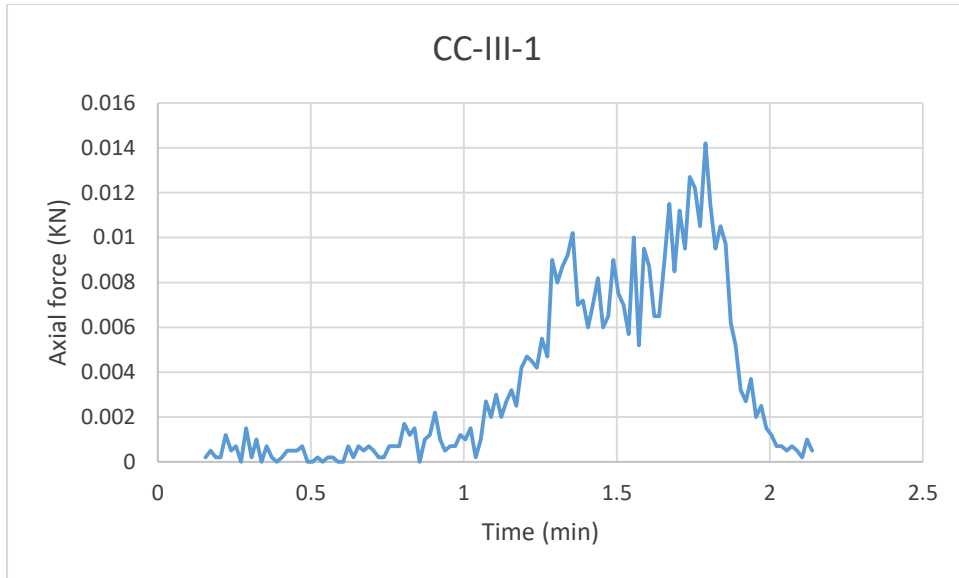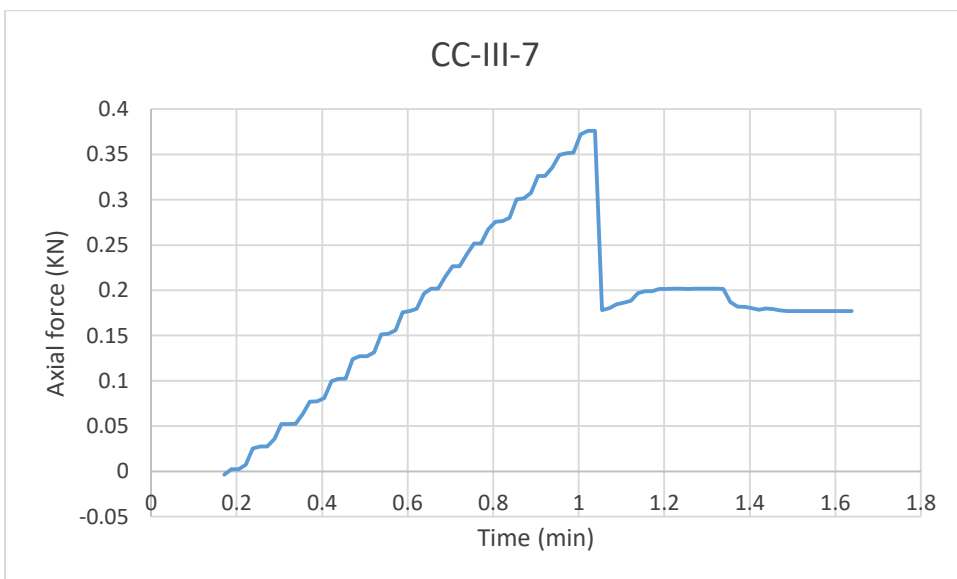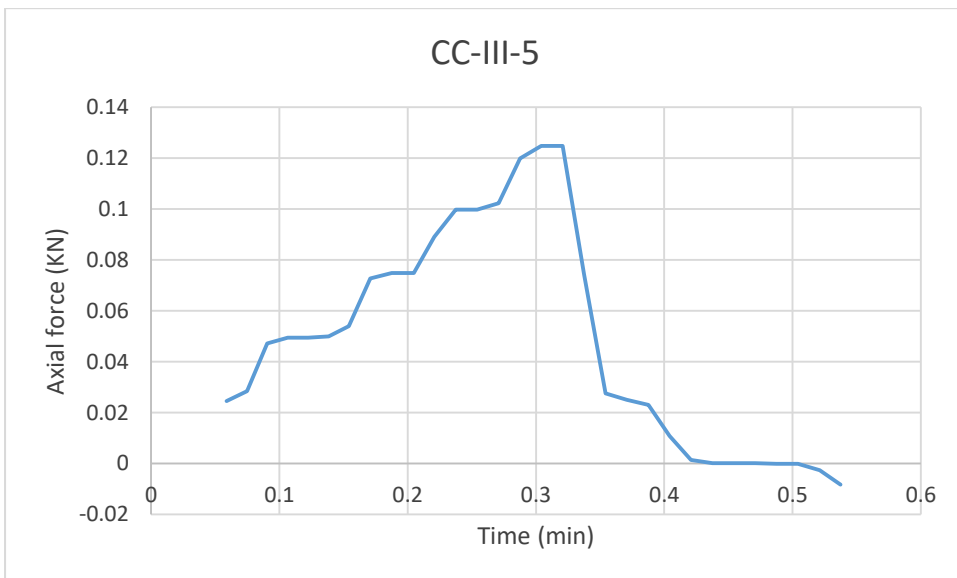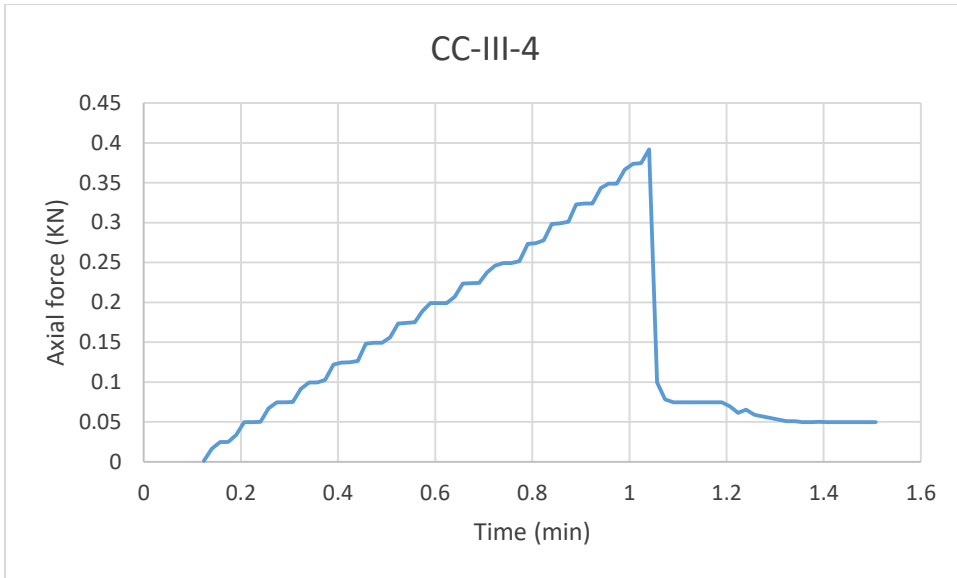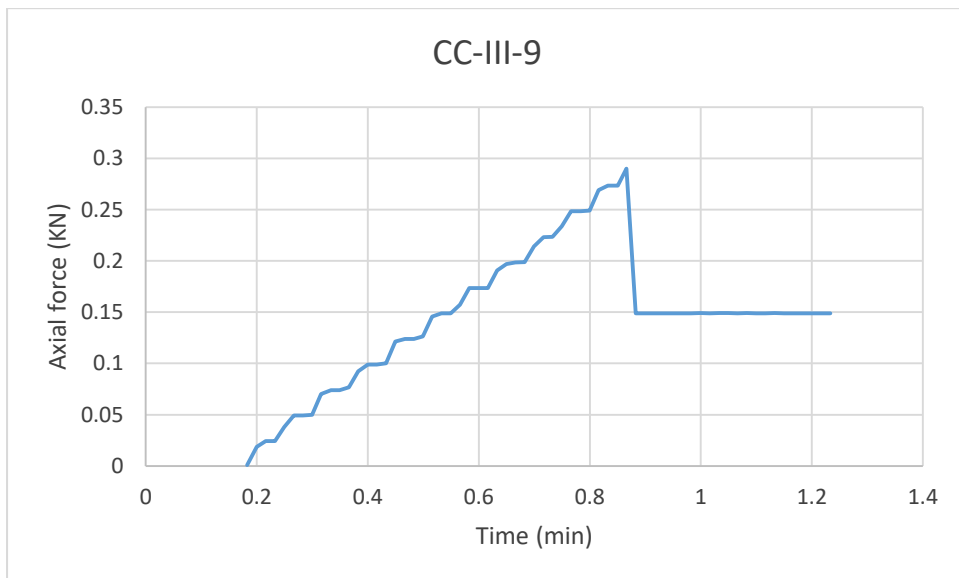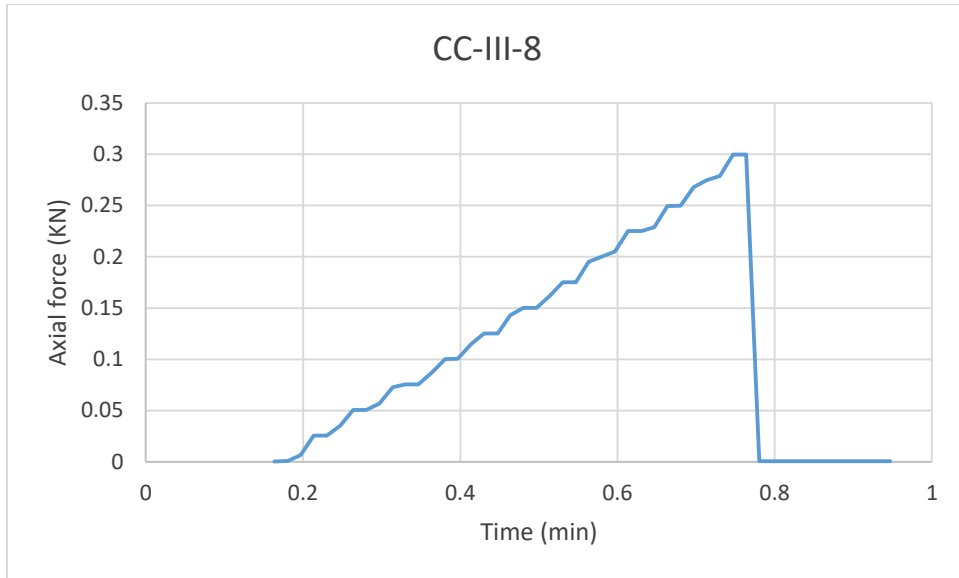
Appendix D: Results from the destructive UCS test

Force vs Deformation from the destructive UCS test of Cement Core Plugs.

CC-3

CC-4

CC-5

CC-6

CC-7

CC-8
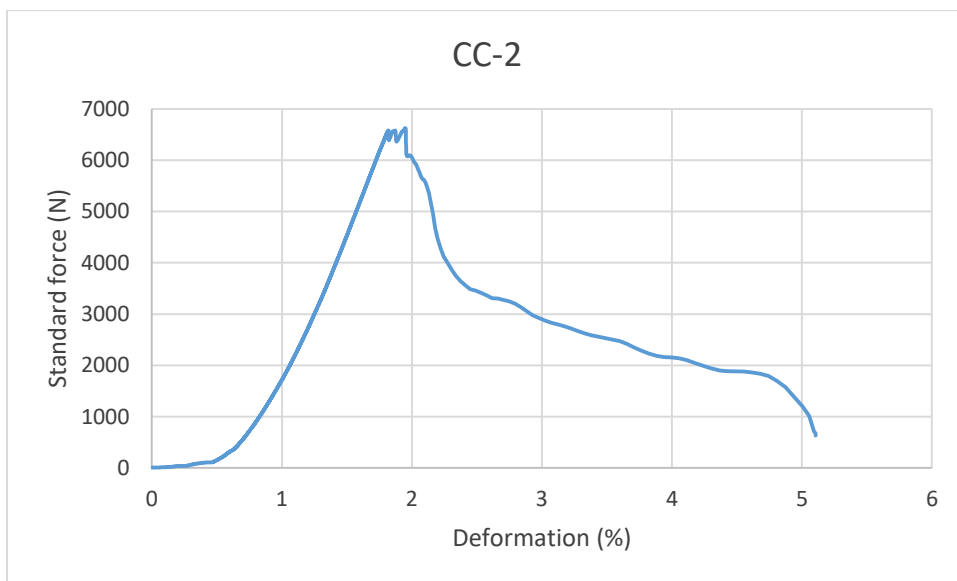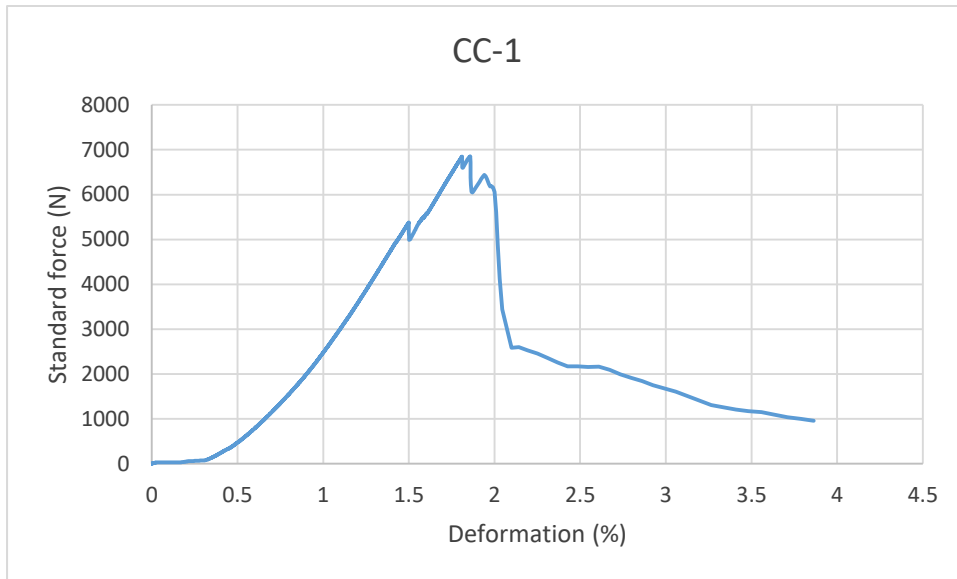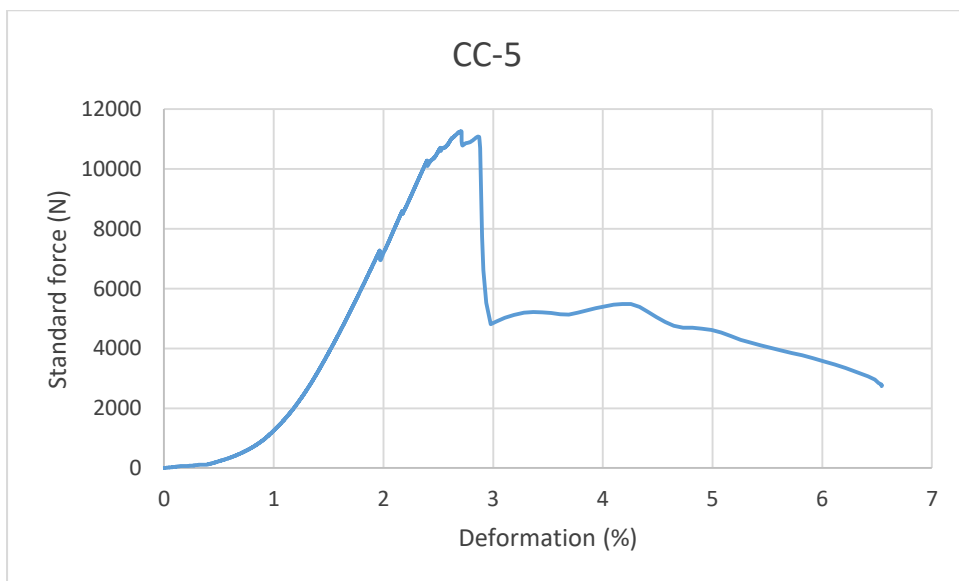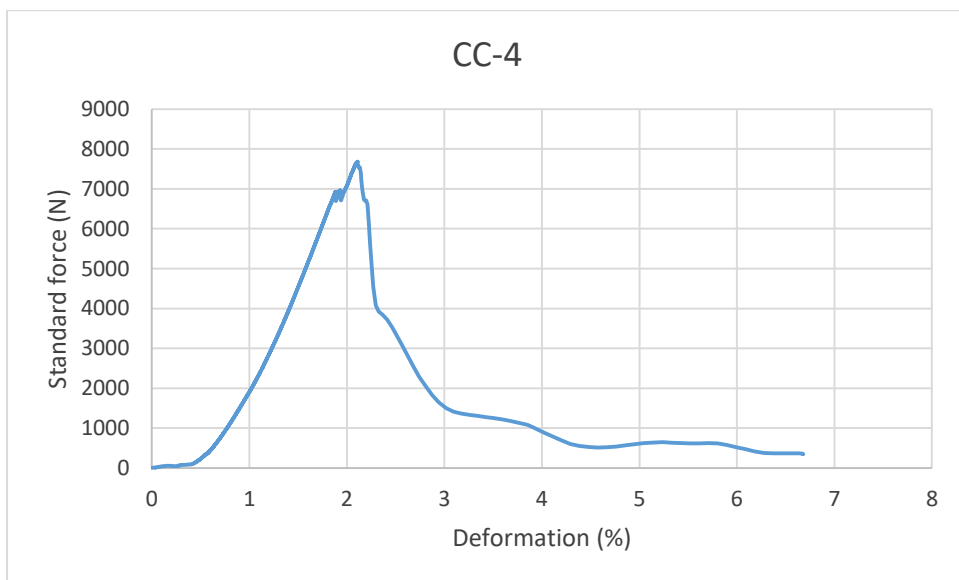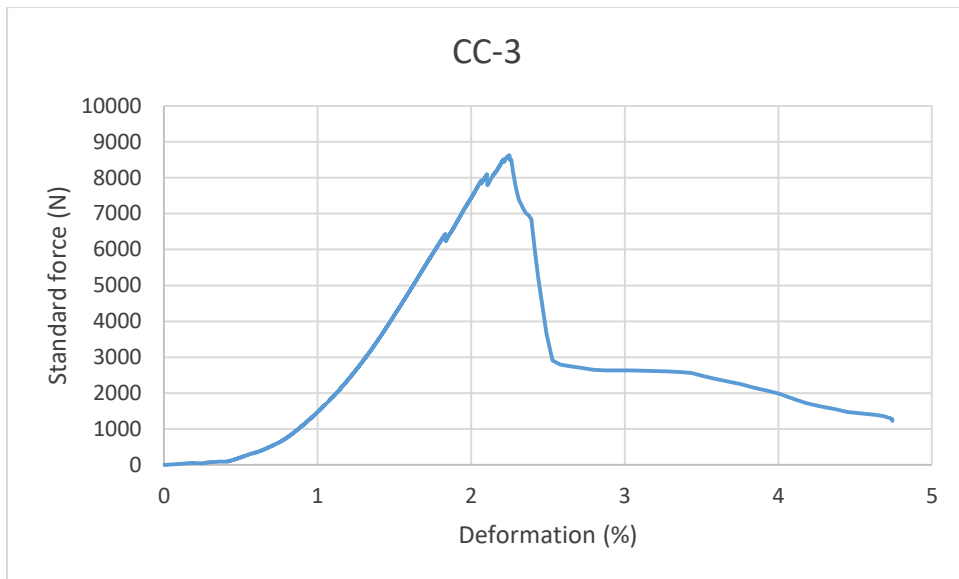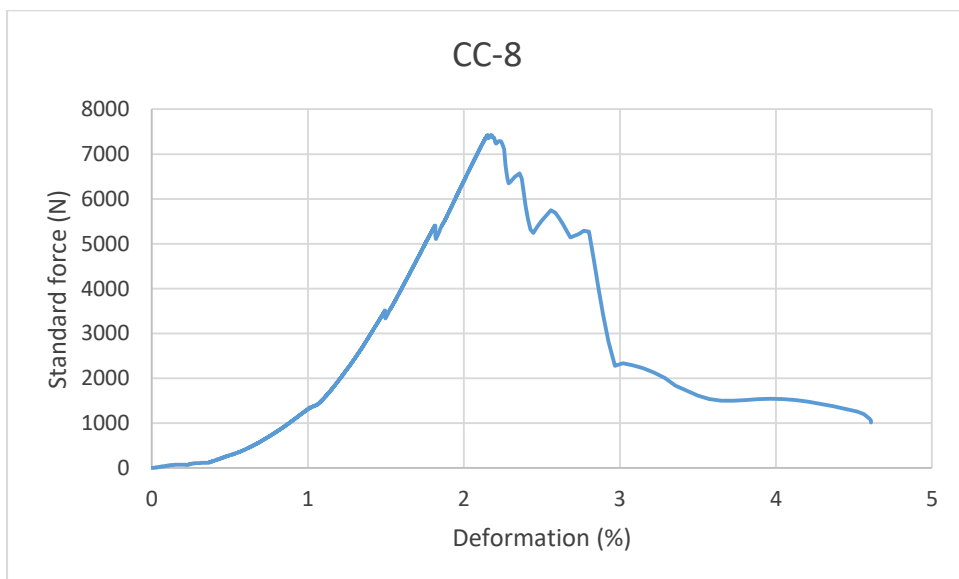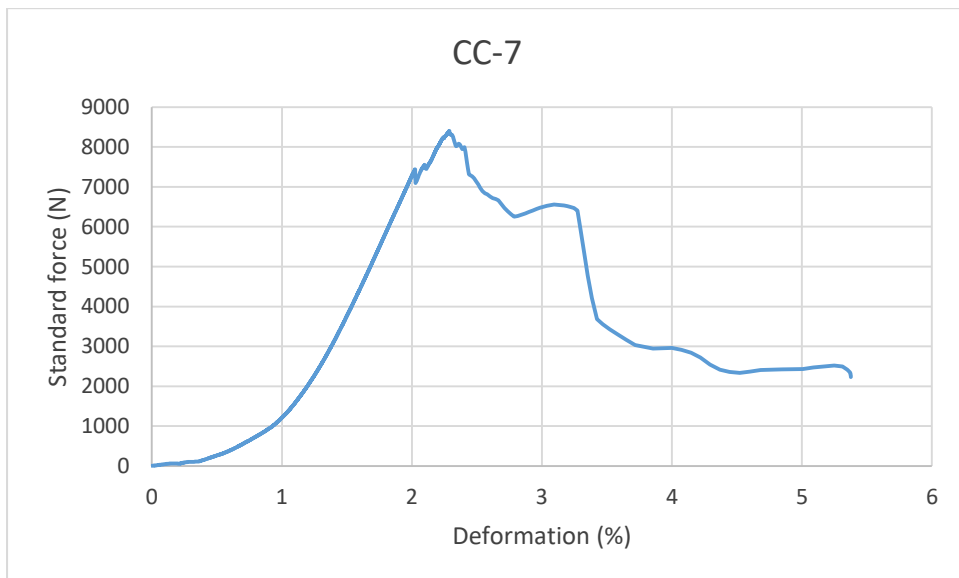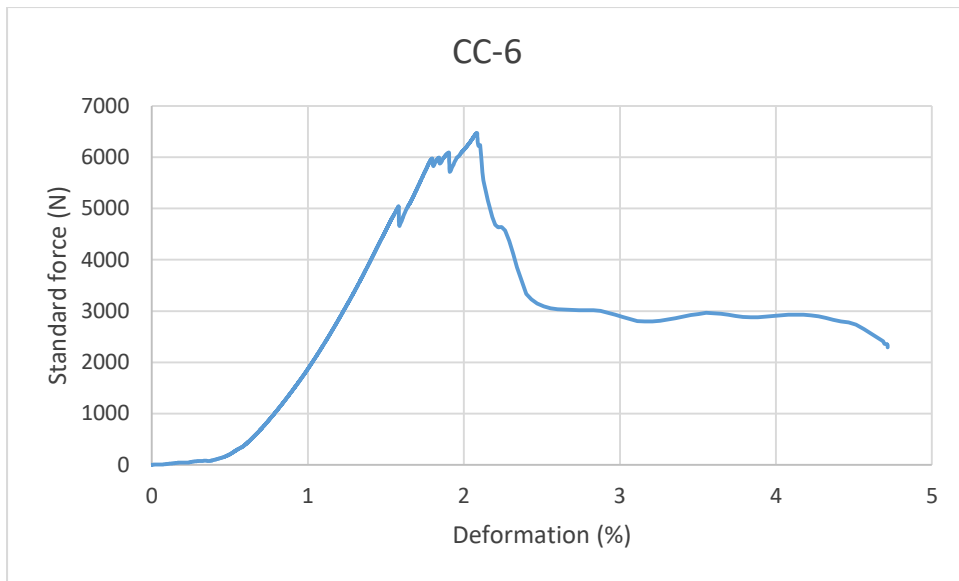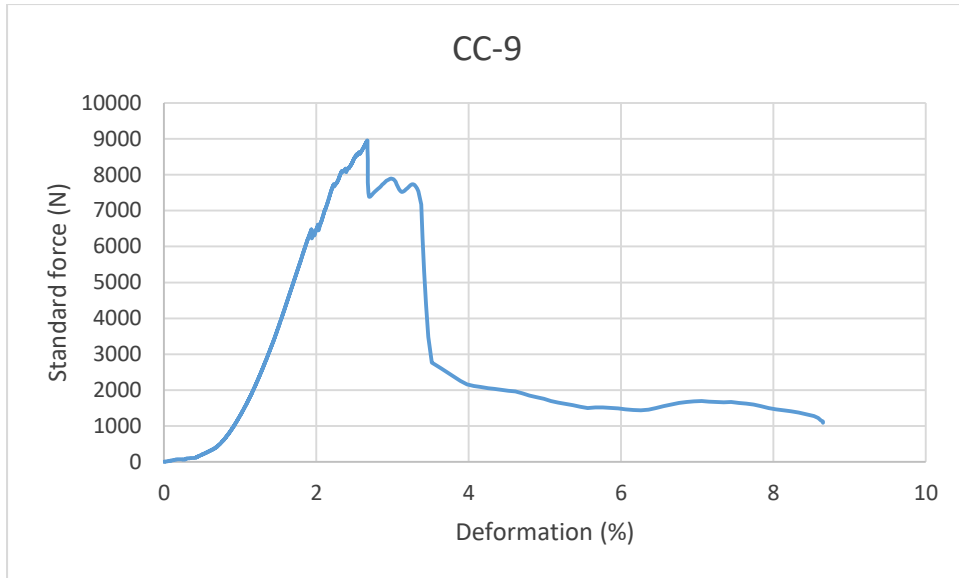
Appendix E: Results from Formation – Cement –Casing bond test

Force vs Deformation from the Formation – Cement – Casing bond test.
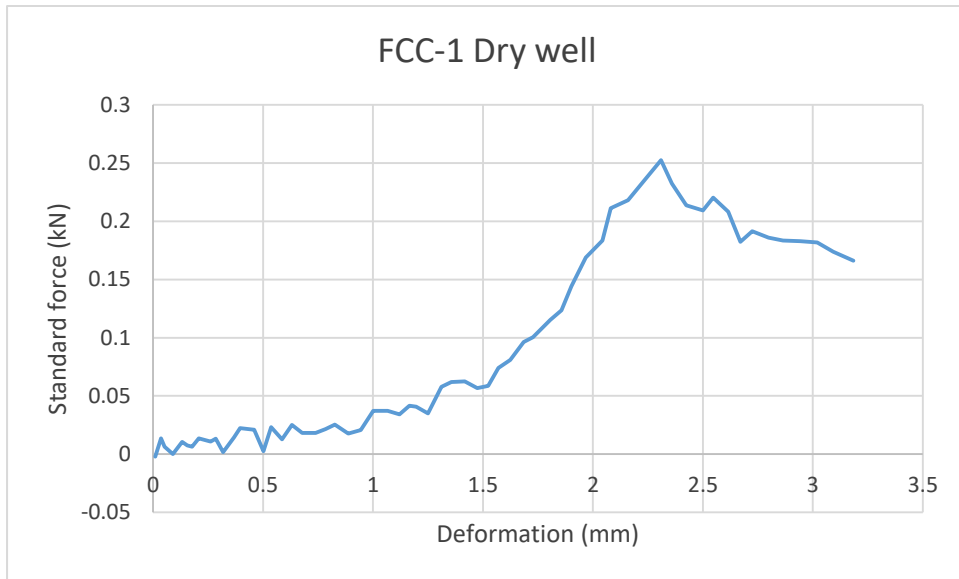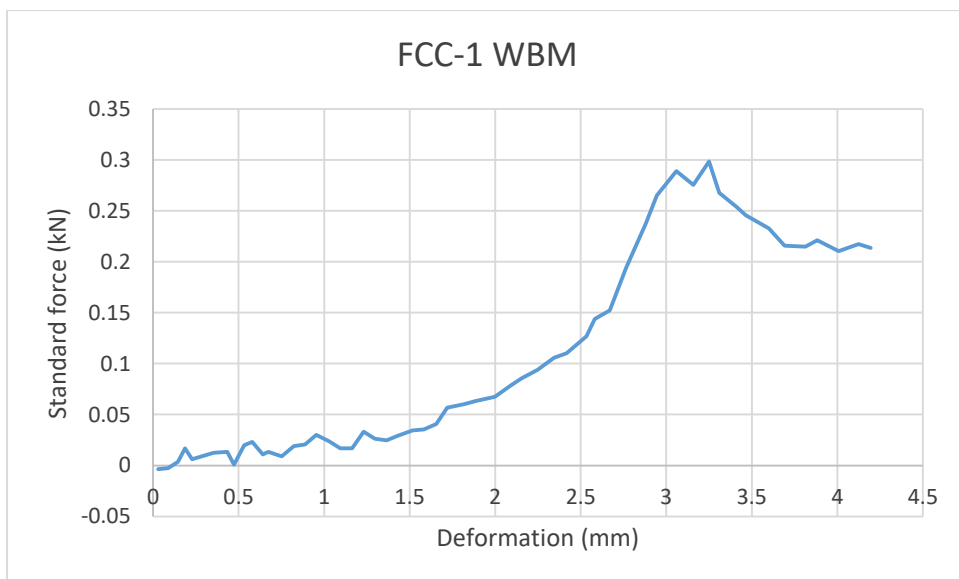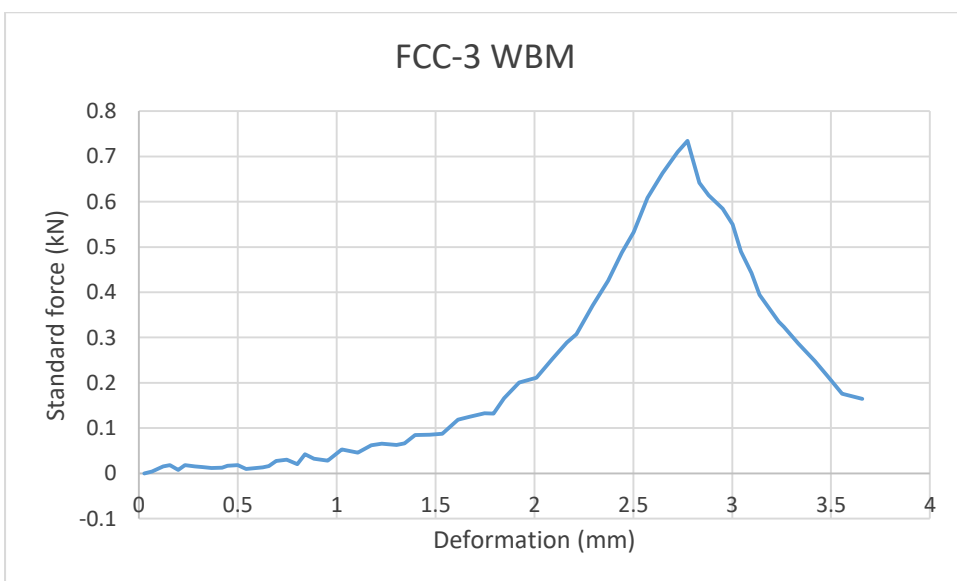

Weak point: Cement – Casing interface.
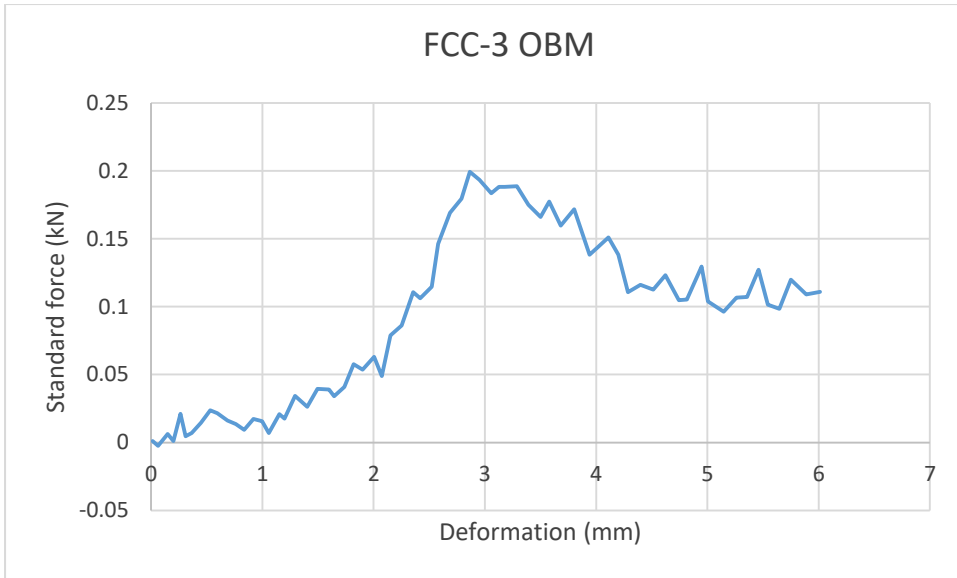

Weak point: Cement – Casing interface.
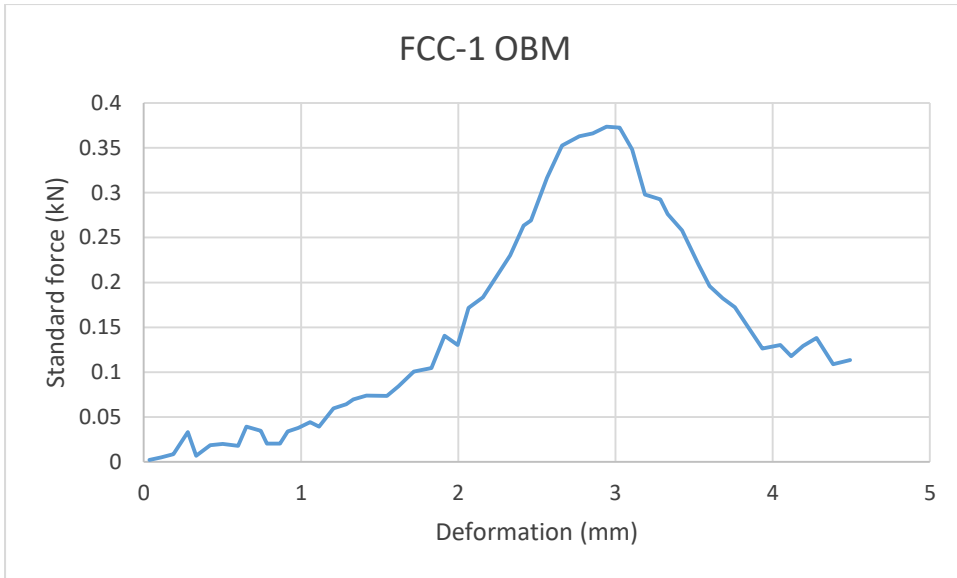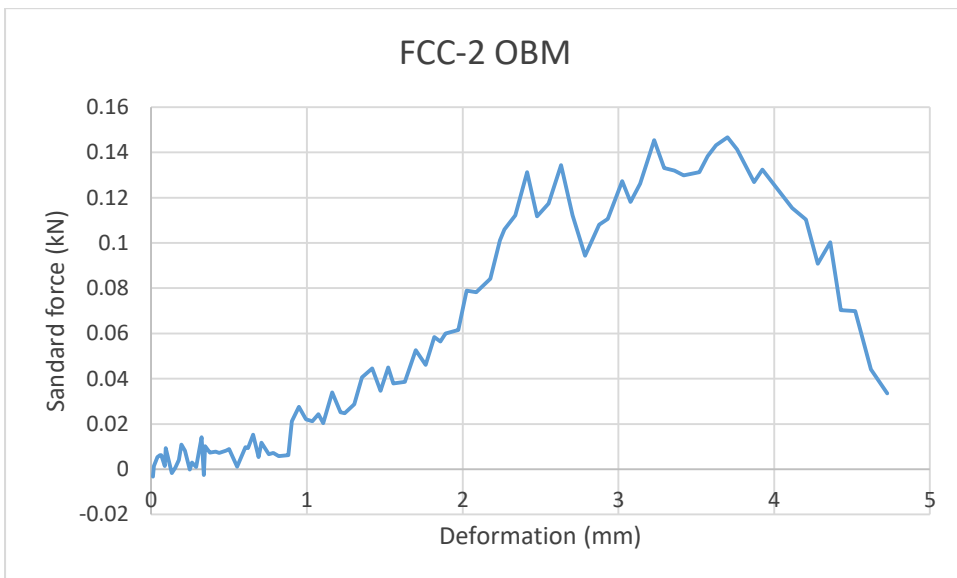
FCC-1 OBM

Weak point: Formation – Cement interface.

FCC-2 OBM
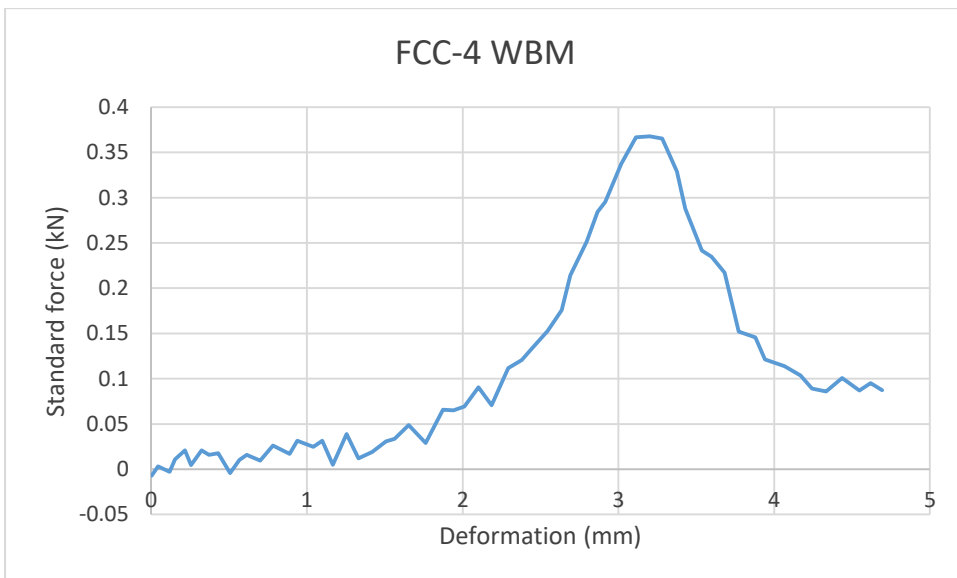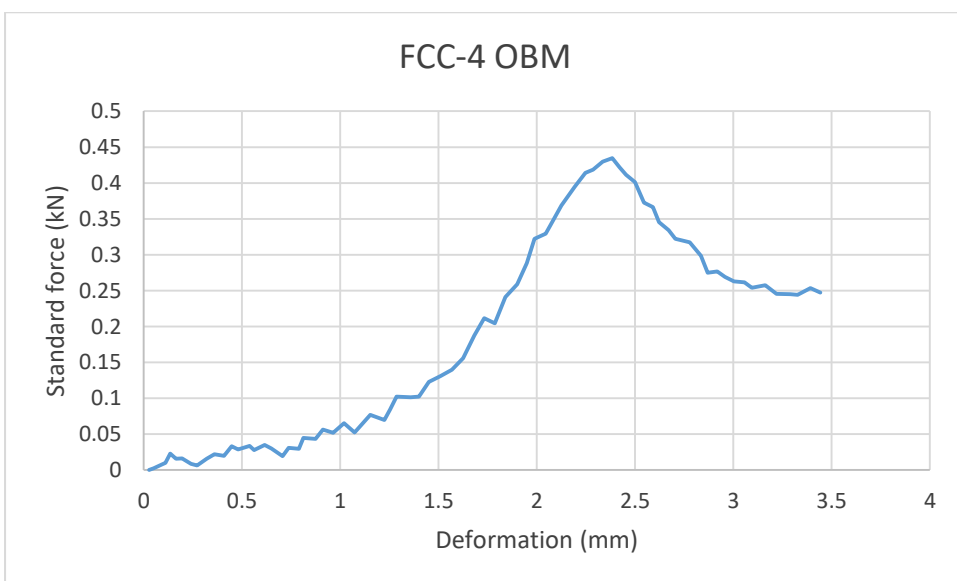
Weak point: Formation – Cement interface.

FCC-3 WBM

Weak point: Formation – Cement interface.

FCC-3 OBM

Weak point:

Formation –

Cement interface.

FCC-4 WBM

Weak point:

Formation –

Cement interface.
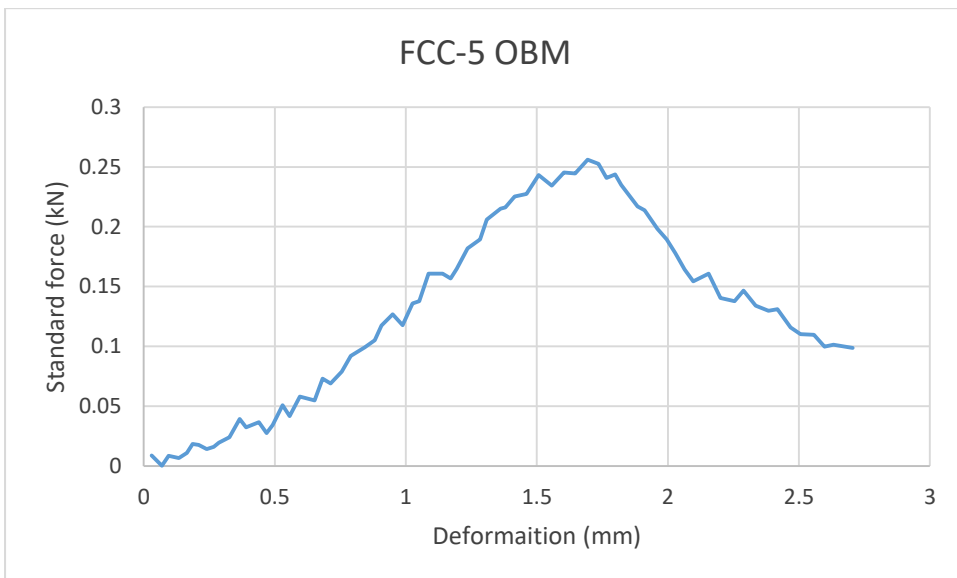
FCC-4 OBM

Weak point:

Formation –

Cement interface.

FCC-5 WBM
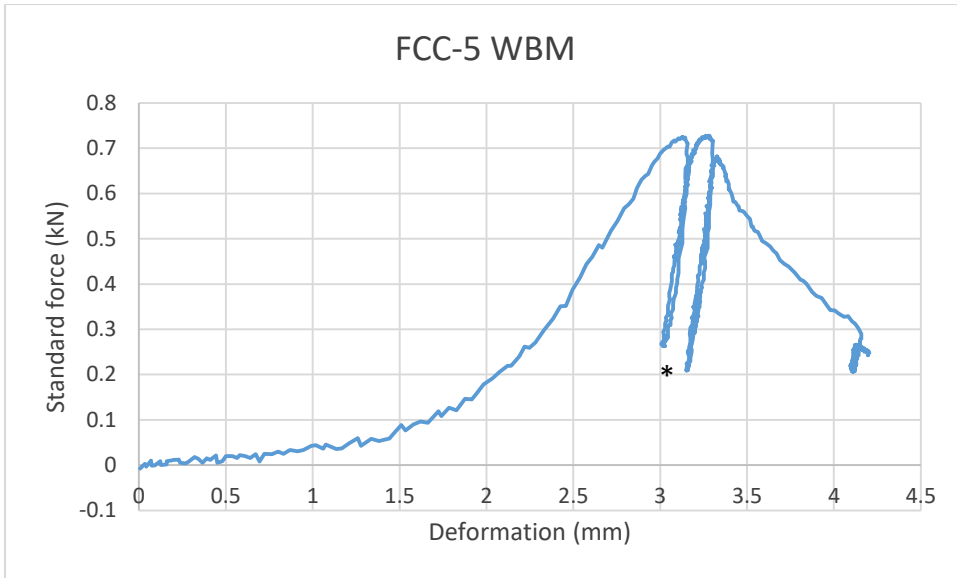
Weak point:
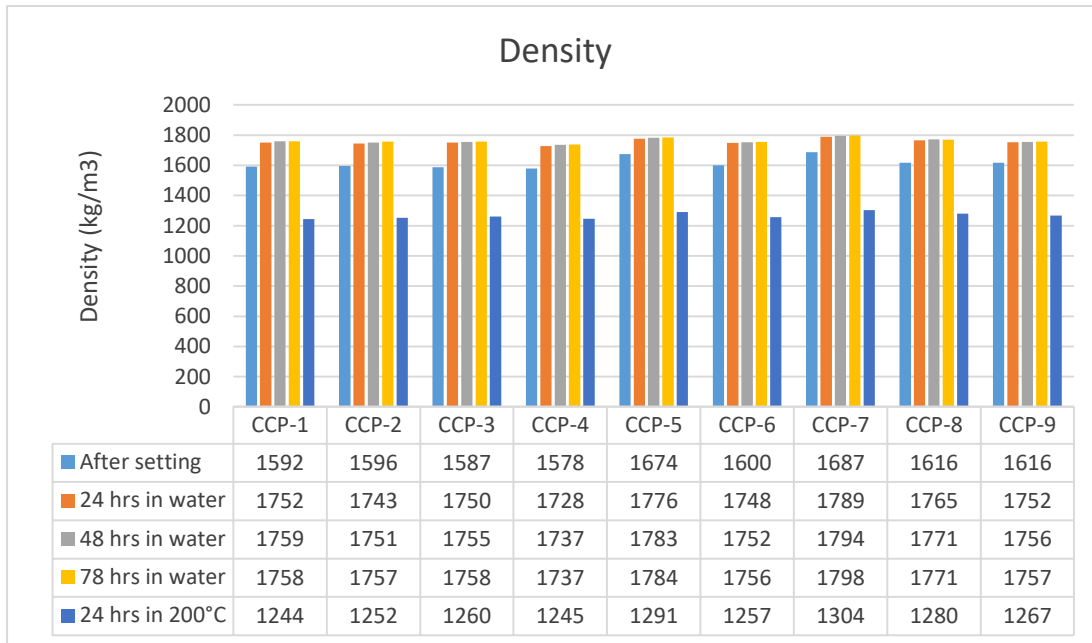
Formation –

Cement interface.

*Comment:

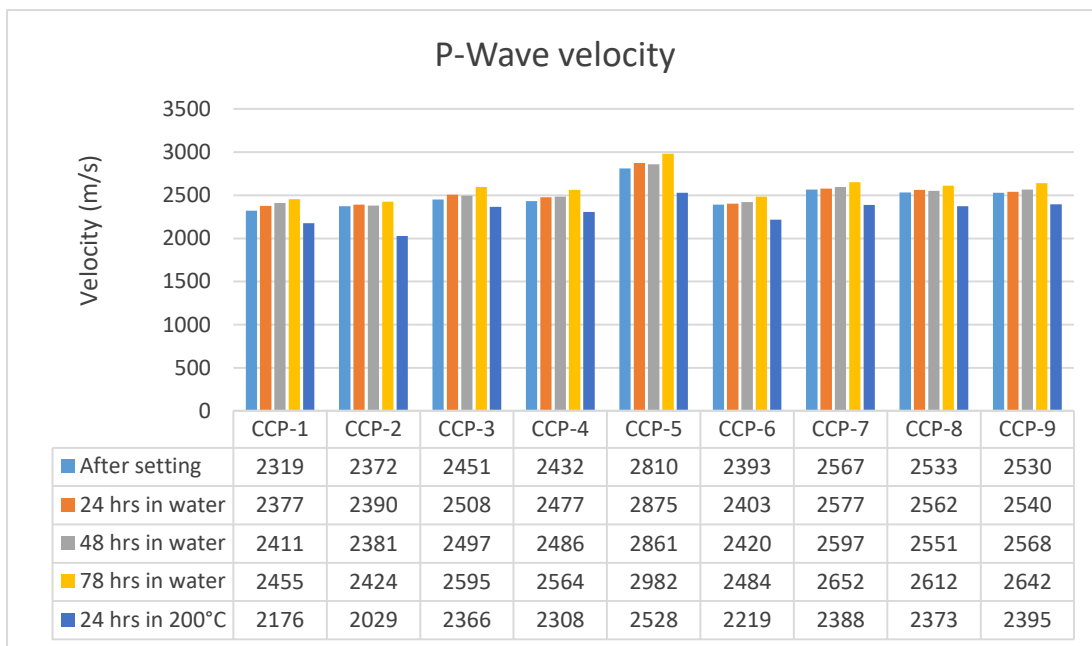The test was accidentally stopped before failure, but then started again.

FCC-5 OBM

Weak point:

Formation –

Cement interface.

Appendix F: Additional data for Cement Core Plugs

Density:

Density

	CCP-1	CCP-2	CCP-3	CCP-4	CCP-5	CCP-6	CCP-7	CCP-8	CCP-9
After setting	1592	1596	1587	1578	1674	1600	1687	1616	1616
24 hrs in water	1752	1743	1750	1728	1776	1748	1789	1765	1752
48 hrs in water	1759	1751	1755	1737	1783	1752	1794	1771	1756
78 hrs in water	1758	1757	1758	1737	1784	1756	1798	1771	1757
24 hrs in 200°C	1244	1252	1260	1245	1291	1257	1304	1280	1267

P-wave velocity:

P-Wave velocity

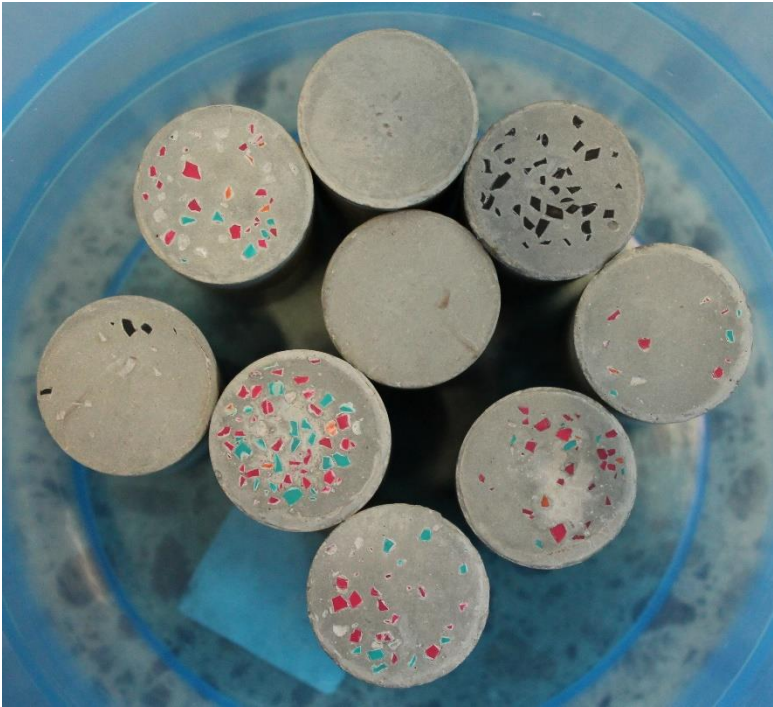|	CCP-1	CCP-2	CCP-3	CCP-4	CCP-5	CCP-6	CCP-7	CCP-8	CCP-9
After setting	2319	2372	2451	2432	2810	2393	2567	2533	2530
24 hrs in water	2377	2390	2508	2477	2875	2403	2577	2562	2540
48 hrs in water	2411	2381	2497	2486	2861	2420	2597	2551	2568
78 hrs in water	2455	2424	2595	2564	2982	2484	2652	2612	2642
24 hrs in 200°C	2176	2029	2366	2308	2528	2219	2388	2373	2395

Appendix G: Additional pictures of Cement Core plugs

Cement core plugs before destructive test:

Top of the core plugs

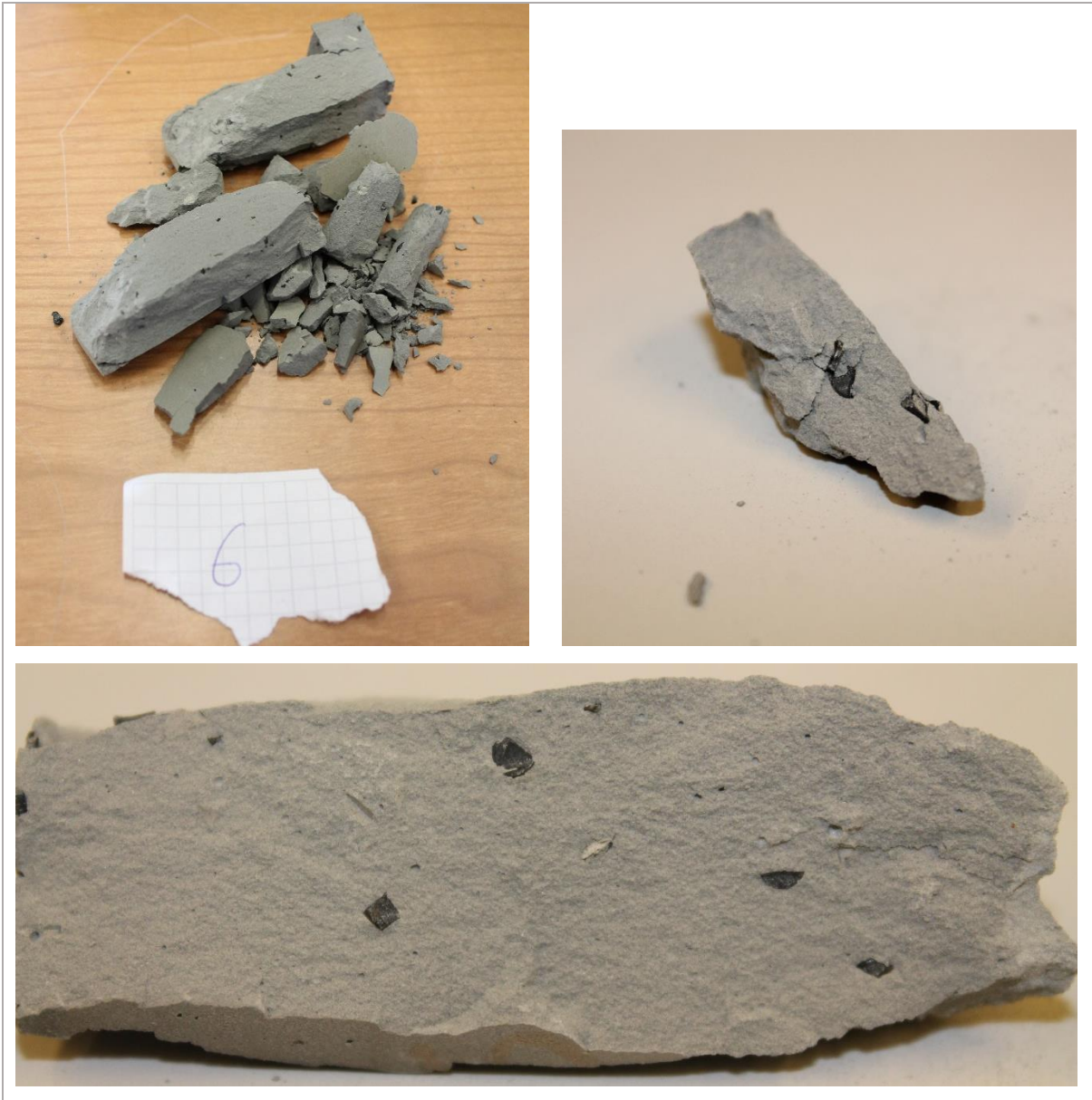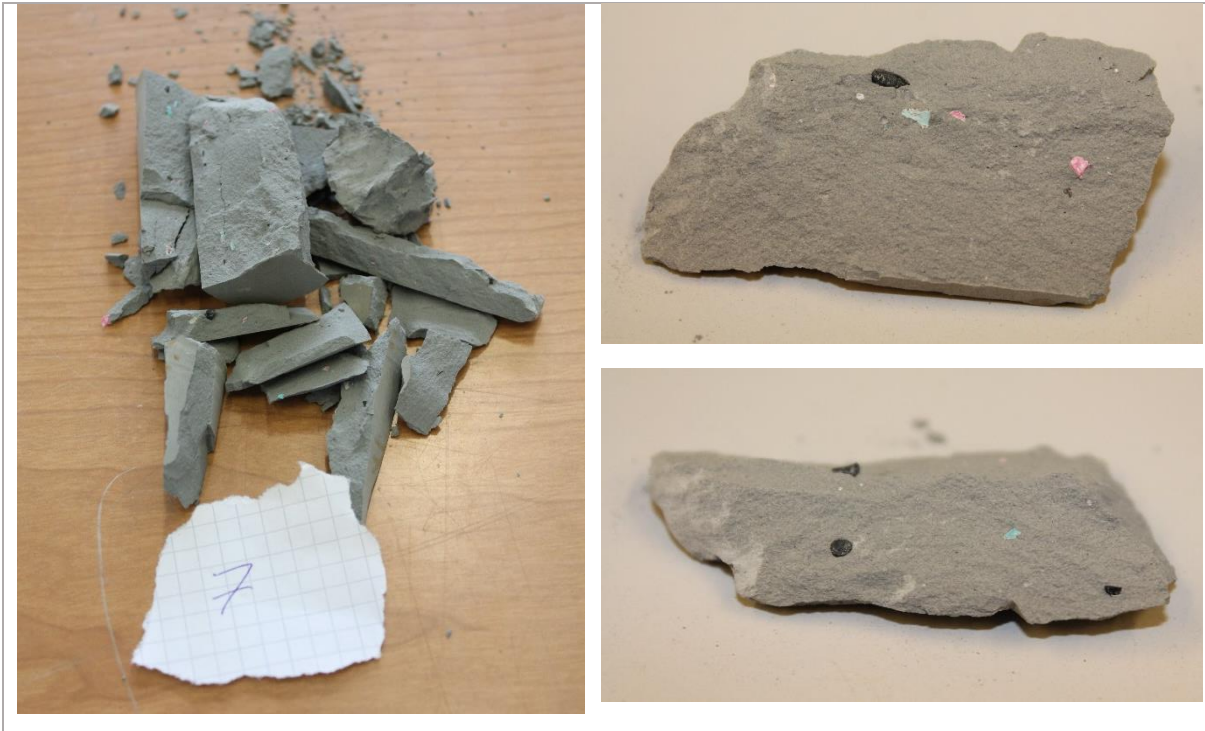**Cement core plugs after destructive test:**

CCP-2

CCP-3

Cement core plugs after destructive test:

CCP-4

CCP-5

CCP-6

CCP-7

CCP-8

CCP-9

Appendix H: Additional pictures of Formation – Cement – Casing

Preparation of FCC:

Drilled holes in a concrete block (FCC-1)

Mud applied on the borehole wall (FCC-1)

Cement poured between formation wall and casing (FCC-1)

The set cement (FCC-1)

Concrete block containing (from left): FCC-1 dry, FCC-1 WBM and FCC-1 OBM:

After setting, front

After setting, bottom

After heating in 200°C for 24 hours, top
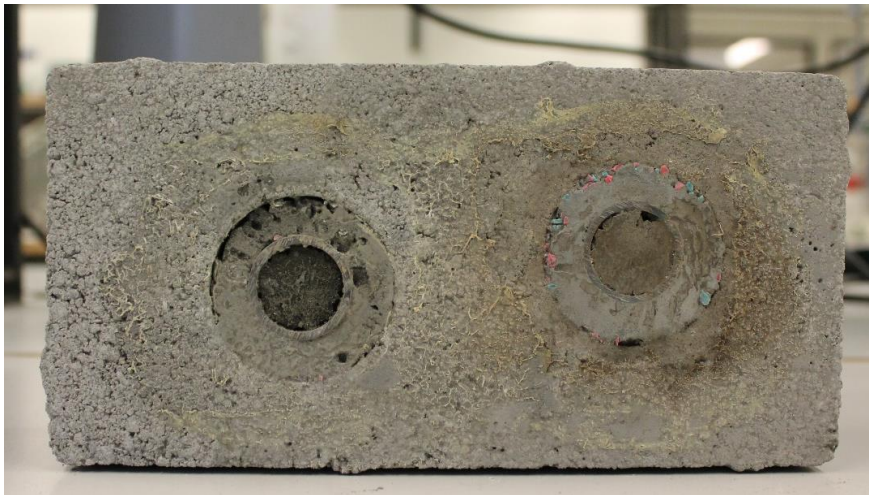

After heating in 200°C for 24 hours, bottom
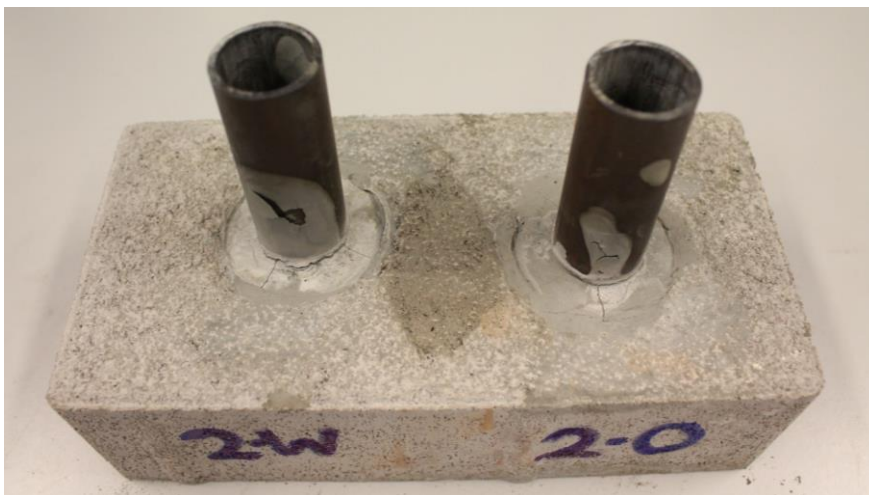

After bond strength test

Concrete block containing (from left): FCC-2 WBM and FCC-2 OBM:

After setting, top

After setting, bottom

After heating in 200°C for 24 hours, top

After heating in 200°C for 24 hours, bottom

After bond strength test

Concrete block containing (from left): FCC-3 WBM, FCC-3 OBM and FCC-4 WBM:

After setting, top

After setting, bottom
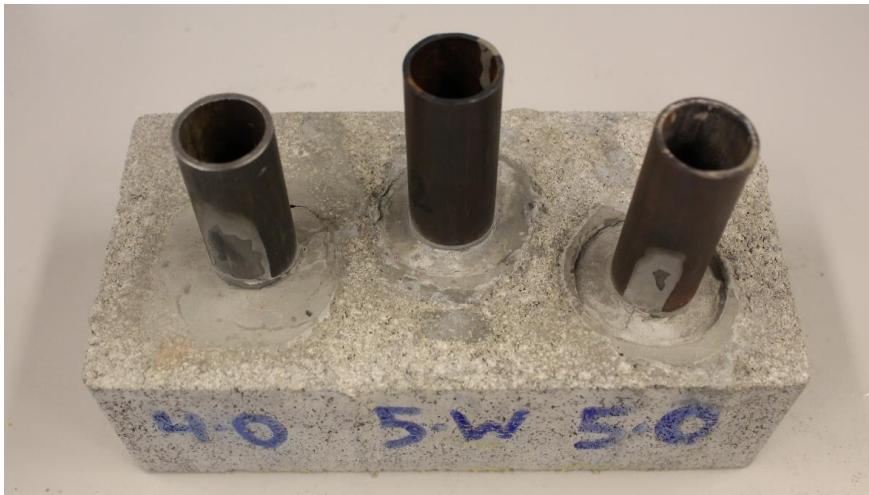

After heating in 200°C for 24 hours, top

After heating in 200°C for 24 hours, bottom

After bond strength test

Concrete block containing (from left): FCC-4 OBM, FCC-5 WBM and FCC-5 OBM:

After setting, top

After setting, bottom

After heating in 200°C for 24 hours, top

After heating in 200°C for 24 hours, bottom

After bond strength test

Appendix I: Heating of rubber

O-ring rubber and silicone rubber was heated in 200°C for 24 hours.

Untreated O-ring rubber before heating

Untreated O-ring rubber after heating

Acid treated O-ring rubber before heating

Acid treated O-ring rubber after heating

Untreated silicone rubber before heating

Untreated silicone rubber after heating

Acid treated silicone rubber before heating

Acid treated silicone rubber after heating